Imaging Atmospheric Cherenkov Telescopes

An introduction into ground-based gamma-ray astronomy

Gernot Maier

VHE Astronomy - Crab Nebula

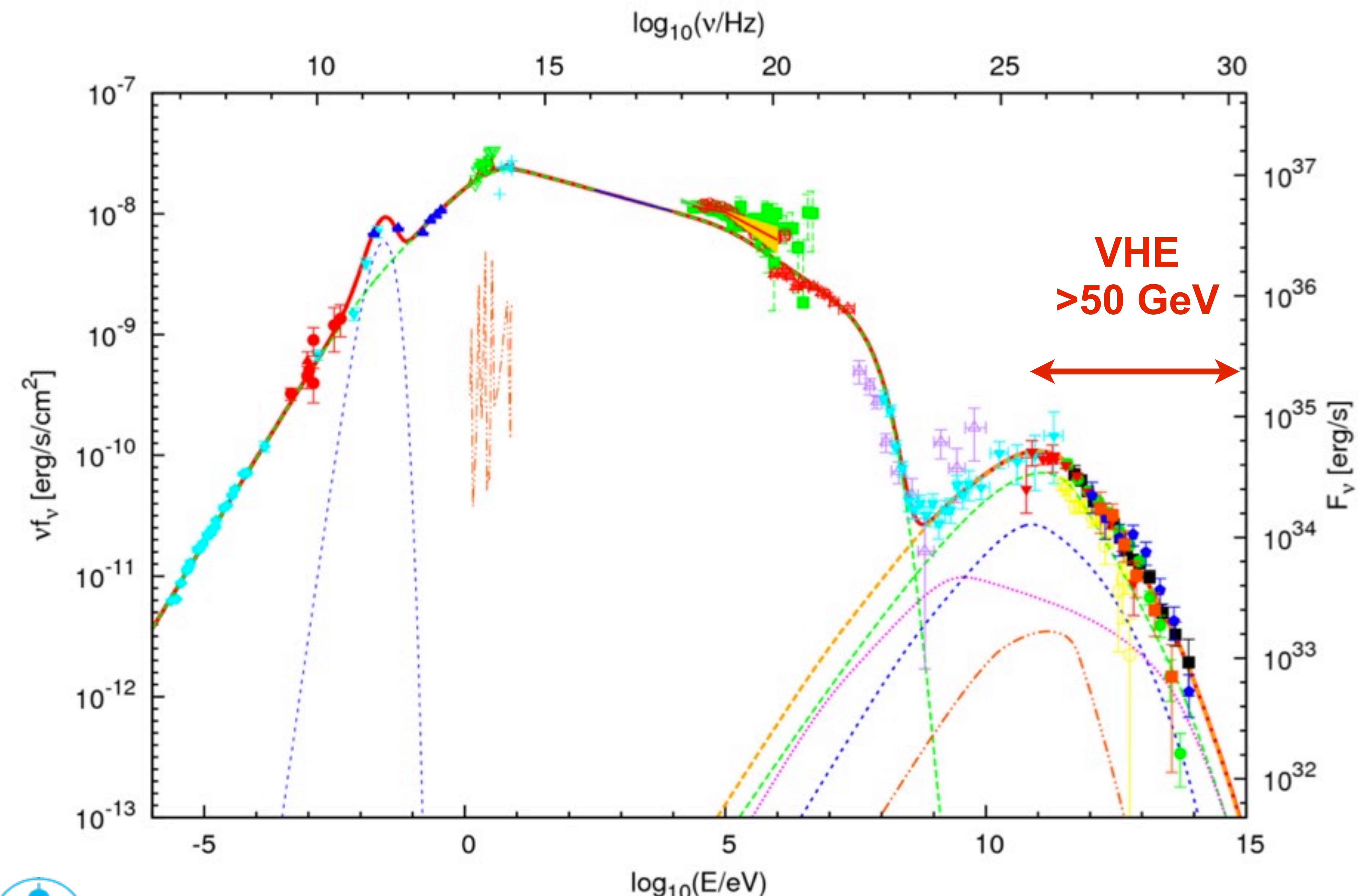

VHE Astronomy - Crab Nebula

Crab Nebula among the strongest sources:
>1 TeV: 7 photon/m²/y

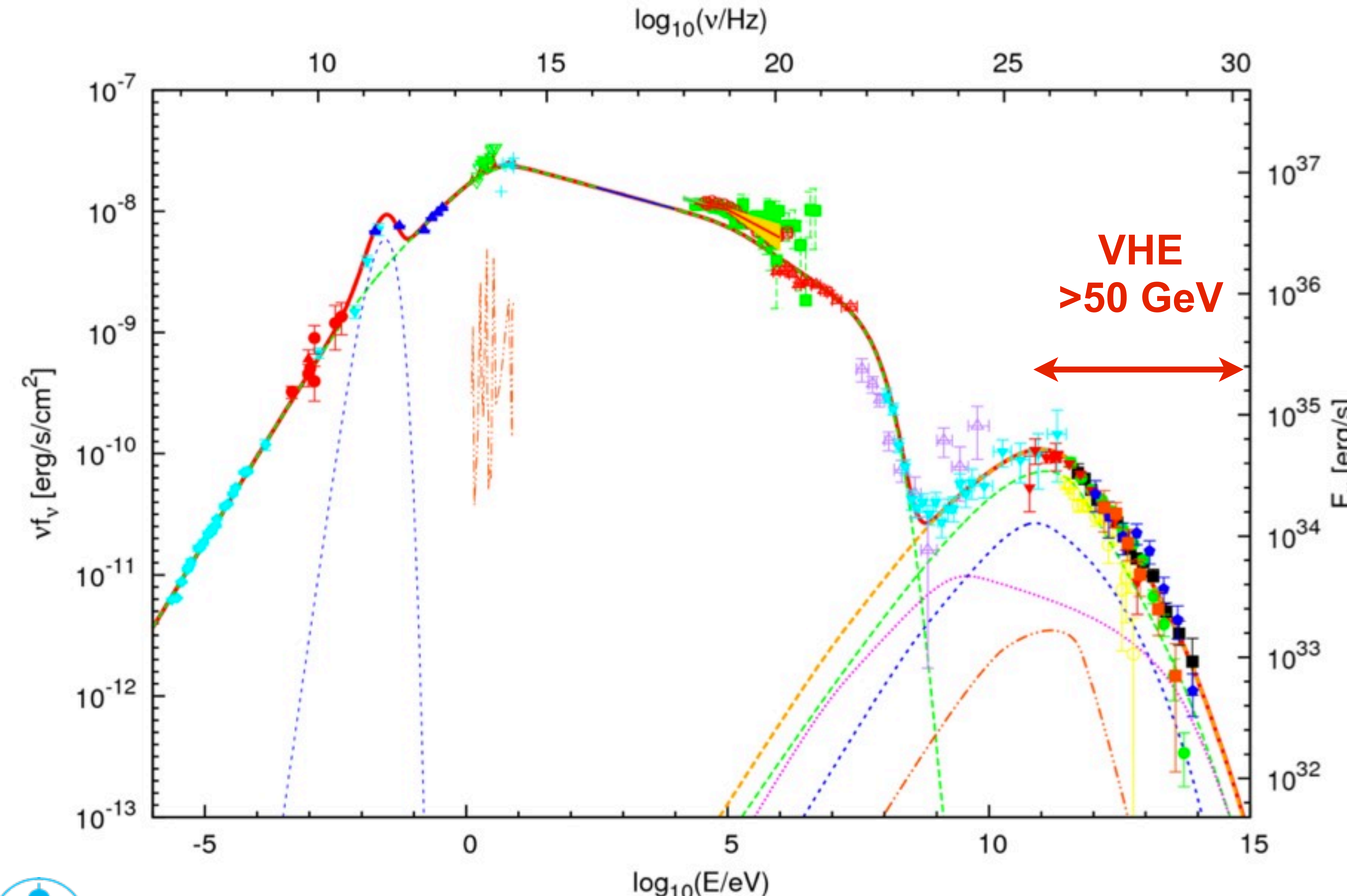

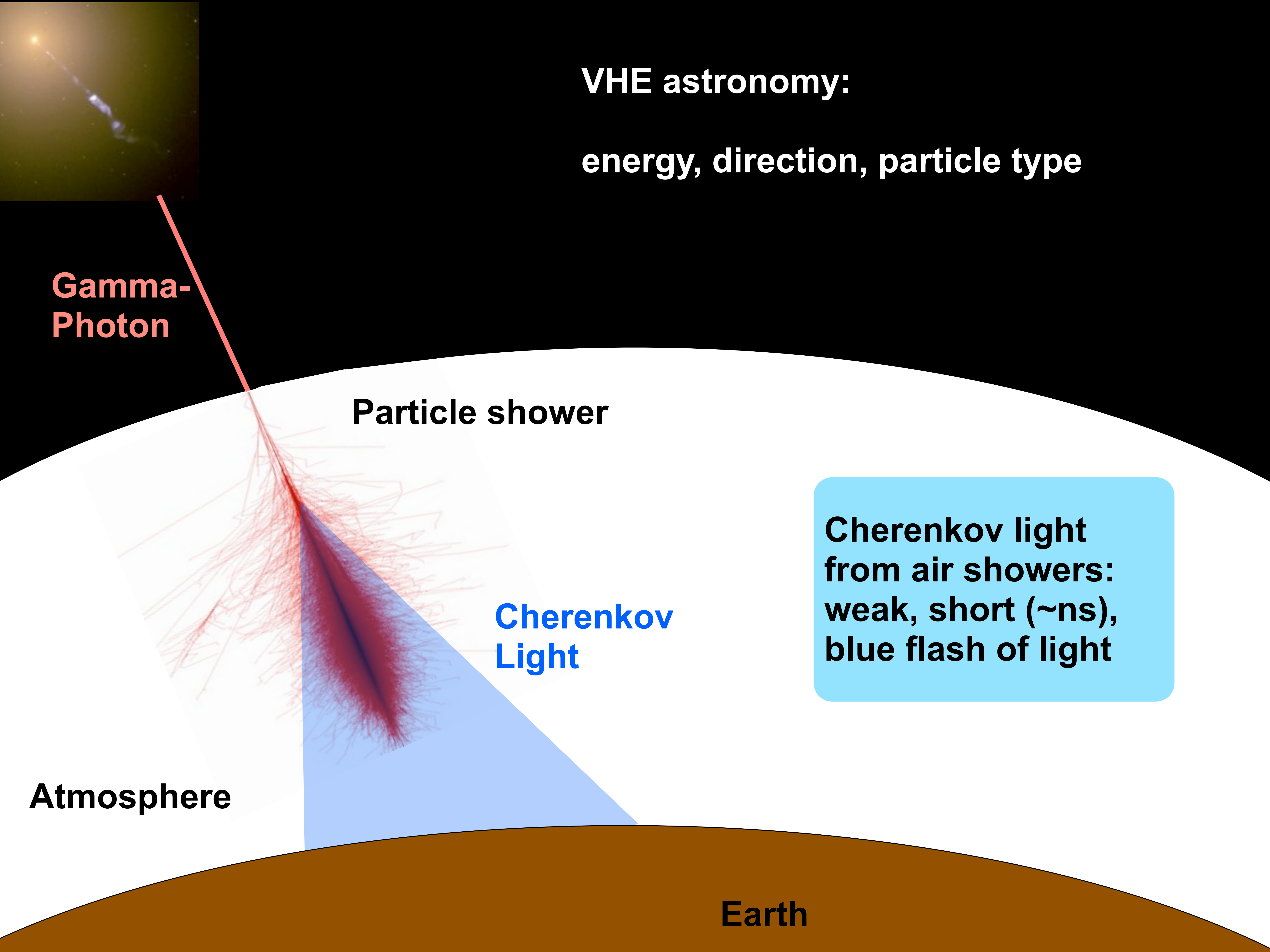

VHE astronomy:
energy, direction, particle type
Gamma-Photon
Particle shower
Cherenkov light from air showers: weak, short (~ns), blue flash of light
Cherenkov Light
Atmosphere
Earth

Photon absorption - Energy loss of electrons/positrons

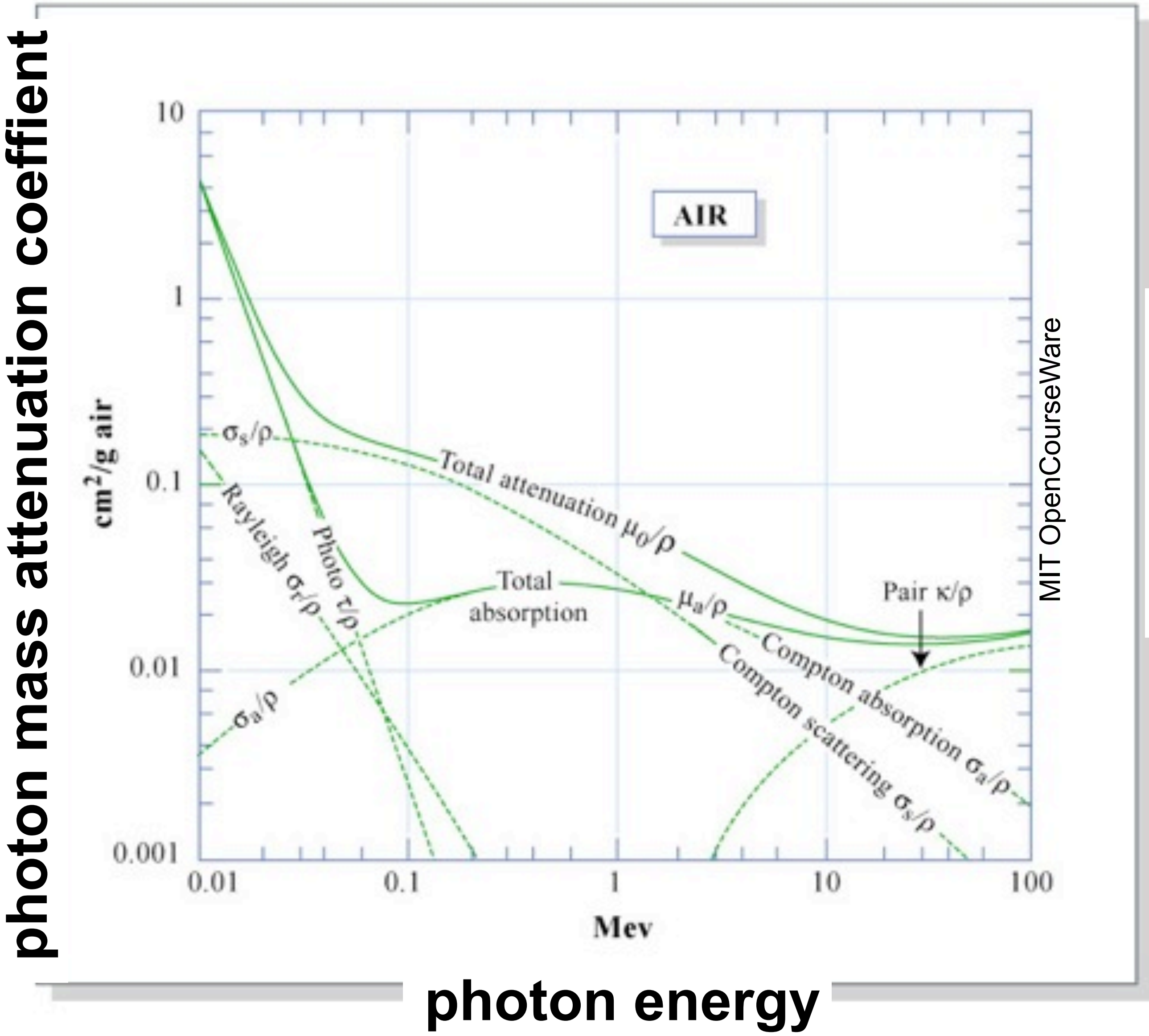

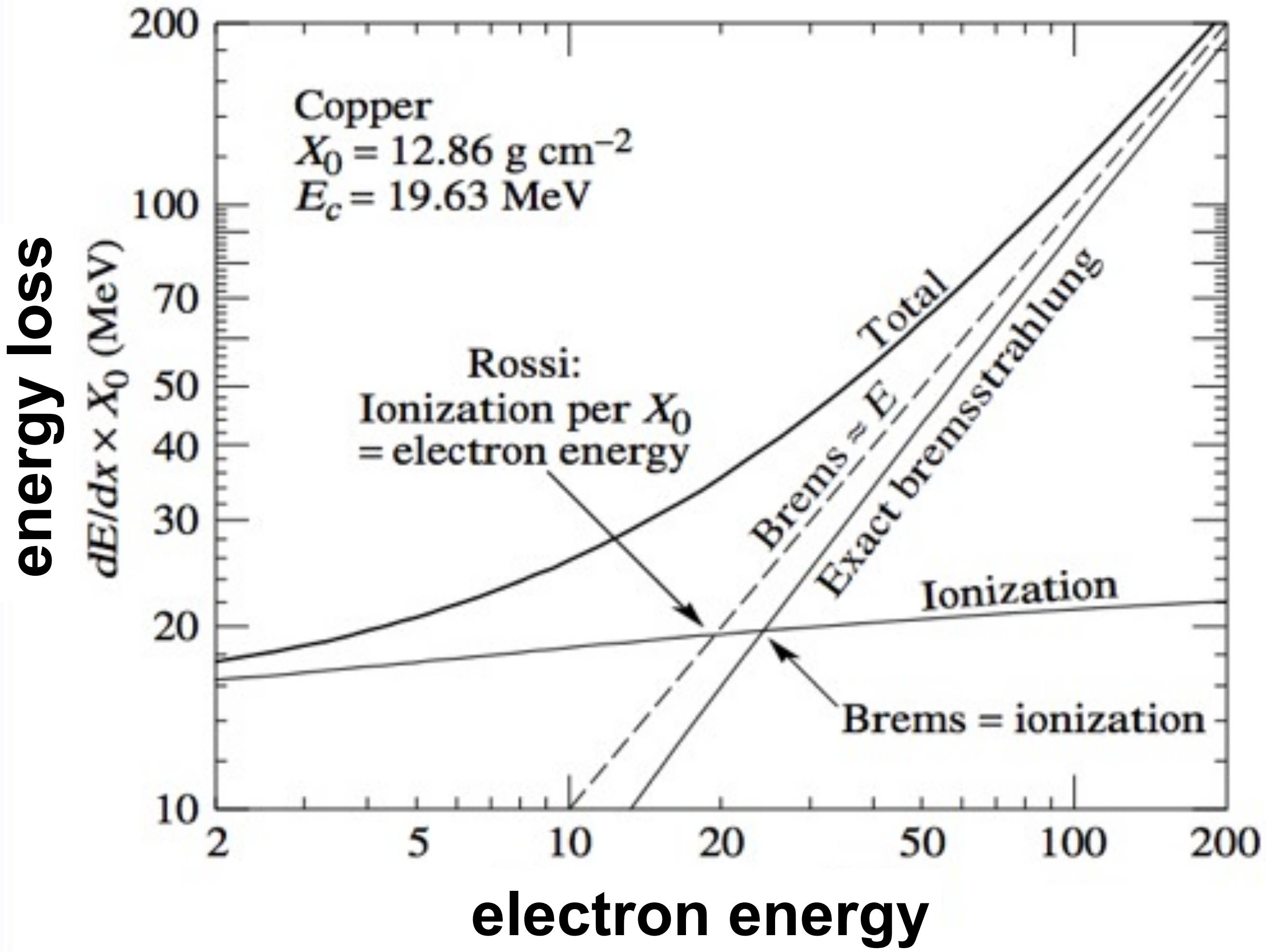

radiation length:

mean distance over which a high-energy electron losses all but 1/e of its energy by Bremsstrahlung

7/9 of mean free path for pair production by high-energy photon

$$X_0 = \frac{716.4 \text{ g cm}^{-2} A}{Z(Z+1)\ln(287/\sqrt{Z})}$$

in air: $X_0 = 37.15 \text{ g/cm}^2$

Extensive Air Showers: Heitler model

Stanev 2010

electron energy drops < 84 MeV: ionization losses dominate; end of cascade

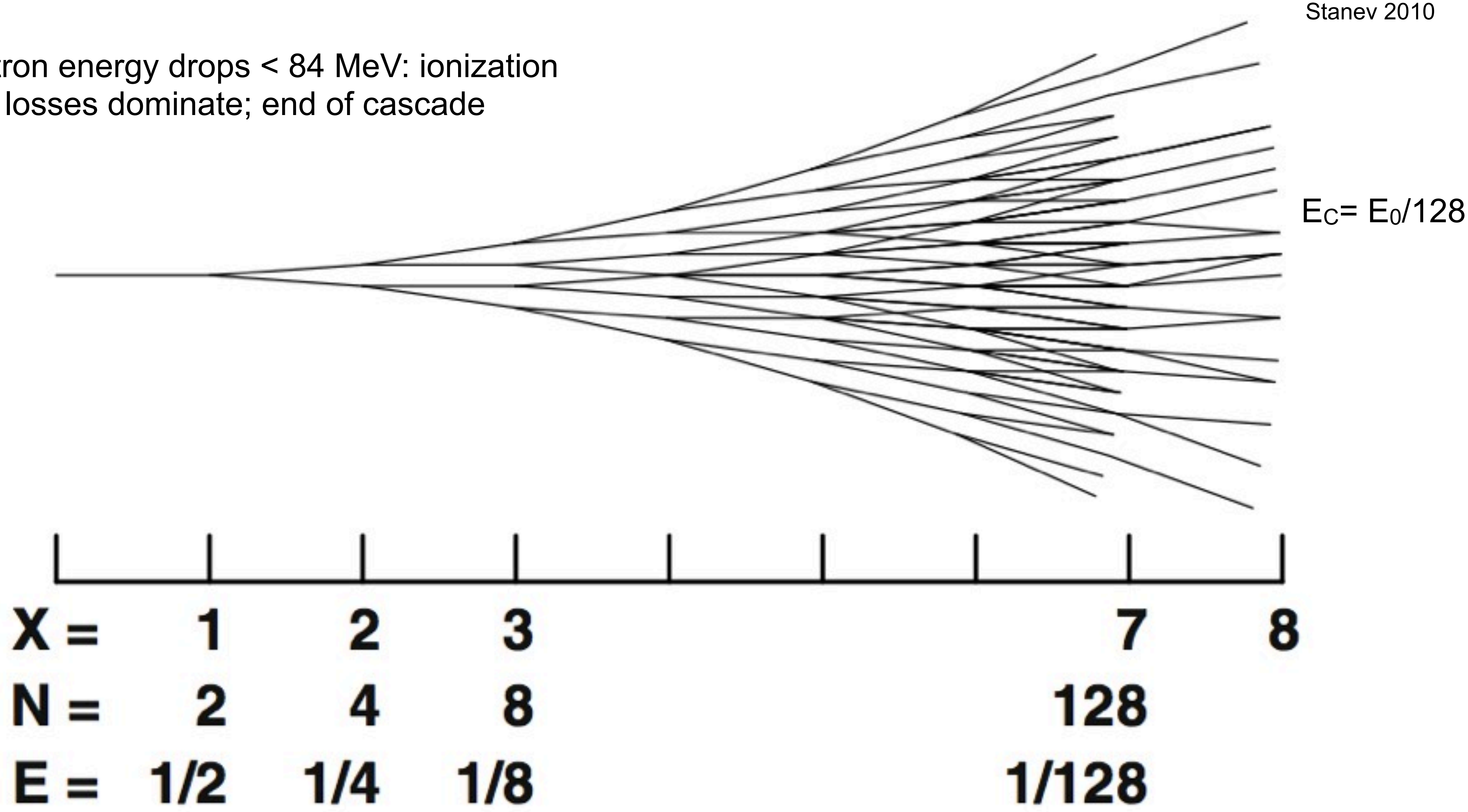

$$N(X) = 2^{X/\lambda} \qquad E(X) = \frac{E_0}{N(X)}$$

Longitudinal distributions

$$N_{max} = N(X_{max}) = \frac{E_0}{E_C} \propto E_0$$

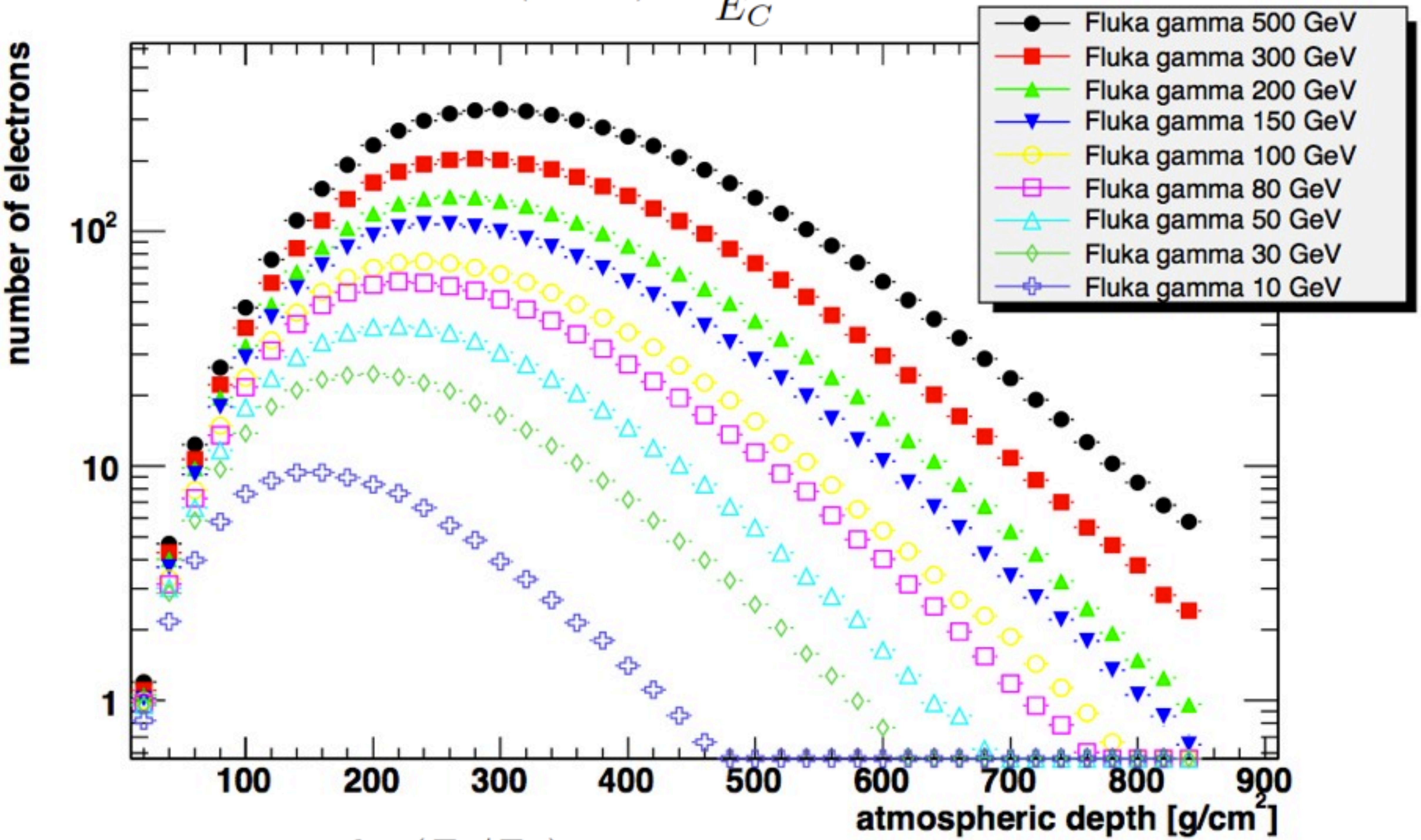

$$X_{max} = \lambda \frac{\log(E_0/E_C)}{\log 2} \propto \log(E_0)$$

Multiple Coulomb Scattering

projected scatter angle: distribution with Gaussian width:

$$\theta_0 = \frac{13.6\text{ MeV}}{\beta c p} z \sqrt{x/X_0}\left[1 + 0.038 \ln(x/X_0)\right]$$

p, βc, and z are the momentum, velocity, and charge number of the incident particle, and x/X_0 is the thickness of the scattering medium in radiation lengths

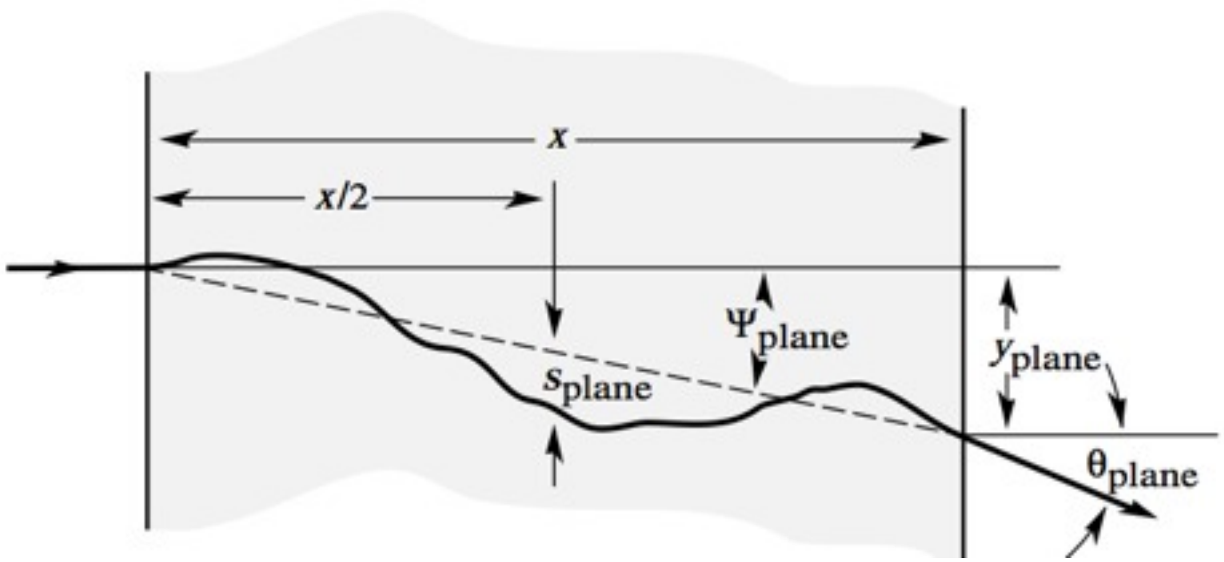

15.7 MeV electrons passing through two thin gold foils

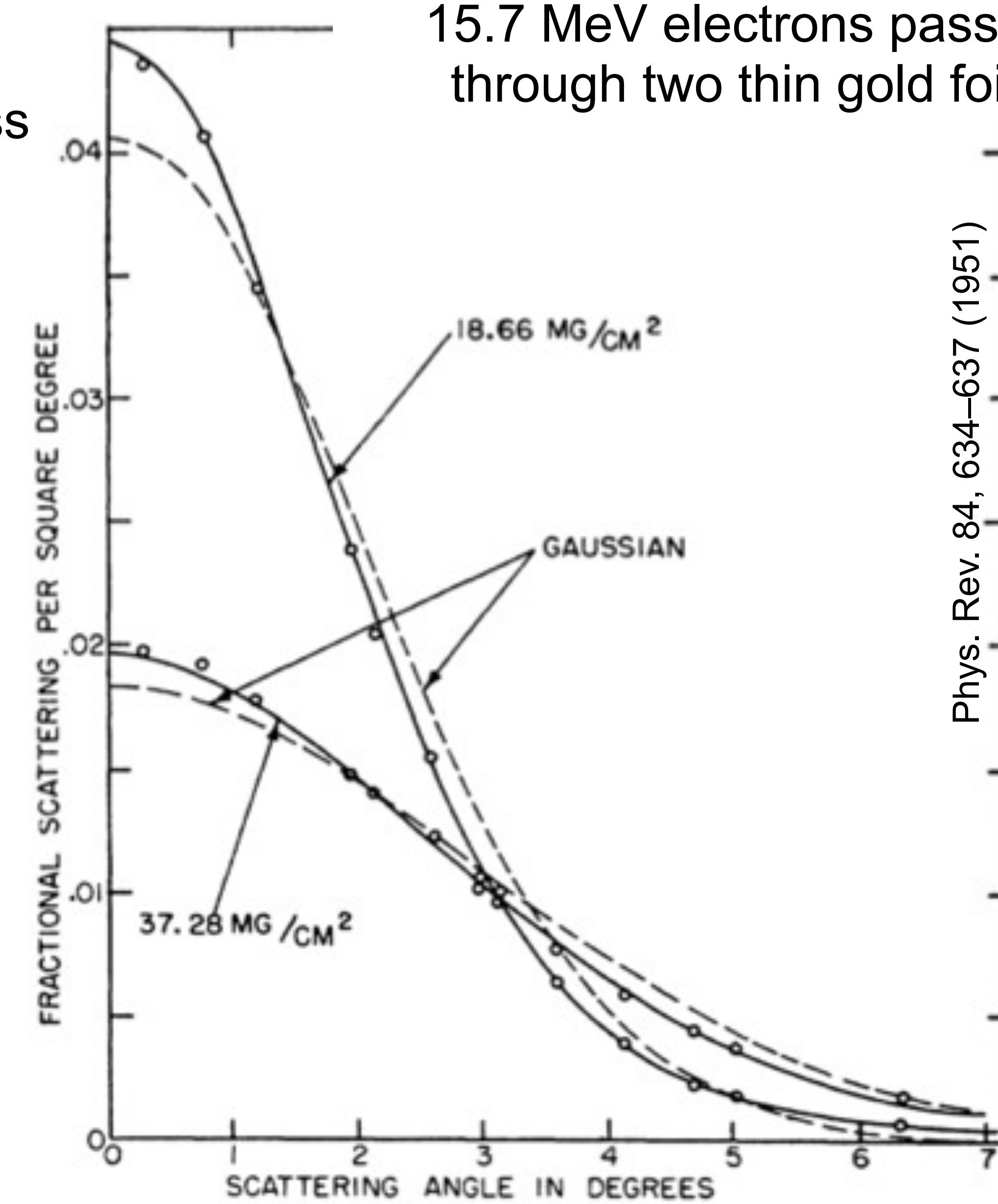

Phys. Rev. 84, 634–637 (1951)

detailed description: Molière theory

Lateral distribution

Lateral distribution

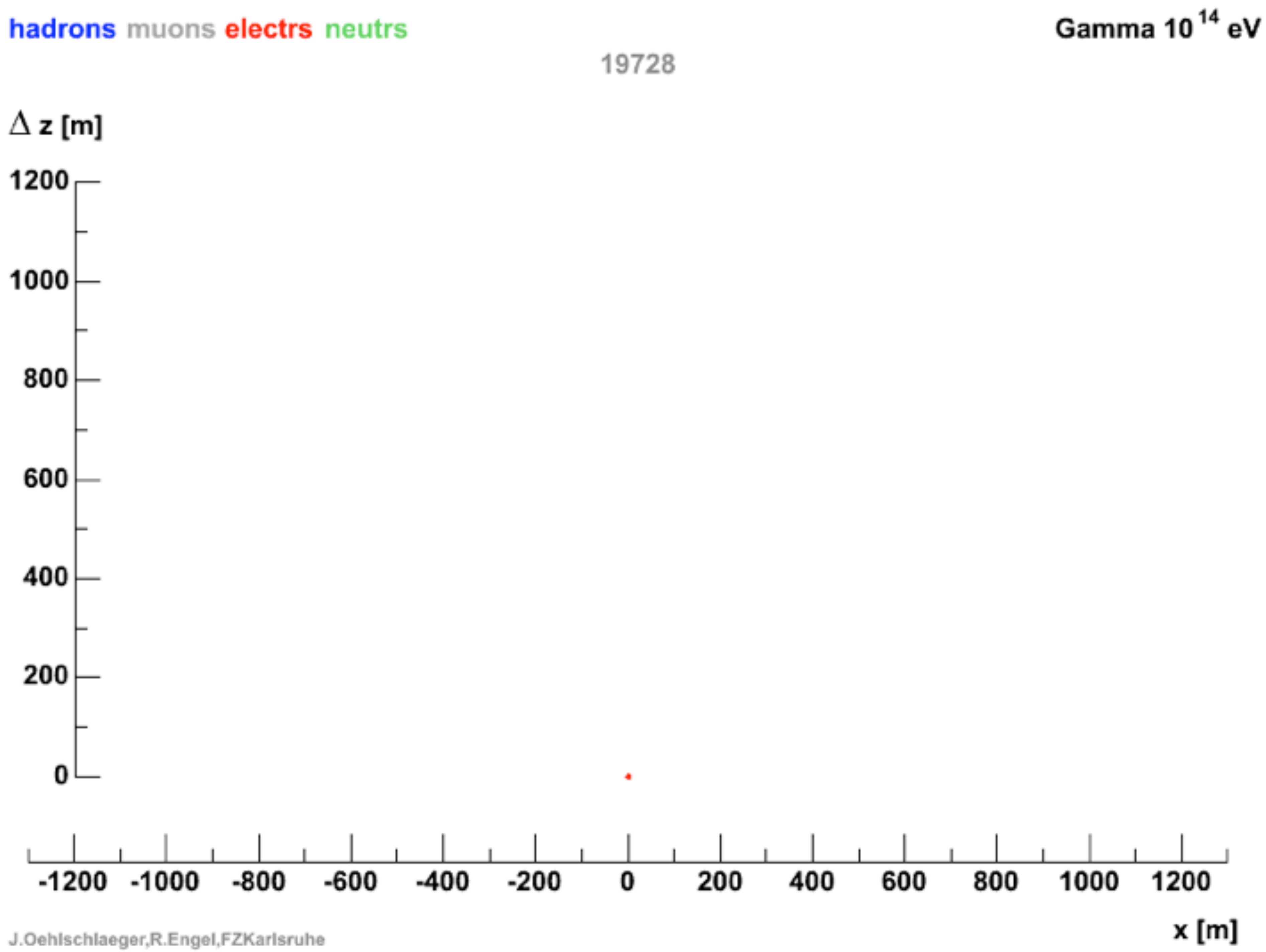

Cherenkov Radiation

emitted when velocity *v* of charged particle exceeds local speed of light:

$$nv/c = n\beta > 1$$

(n = local refractive index)

Pavel Alekseyevich Cherenkov (Nobel price1958)

light is emitted along a cone with half opening angle θ:

$$\cos\theta = 1 / (\beta n)$$

number of Cherenkov photons per path length x:

$$\frac{d^2N}{dx d\lambda} = \frac{2\pi\alpha z^2}{\lambda^2}\left(1 - \frac{1}{\beta^2 n^2(\lambda)}\right)$$

Density - refractive Index

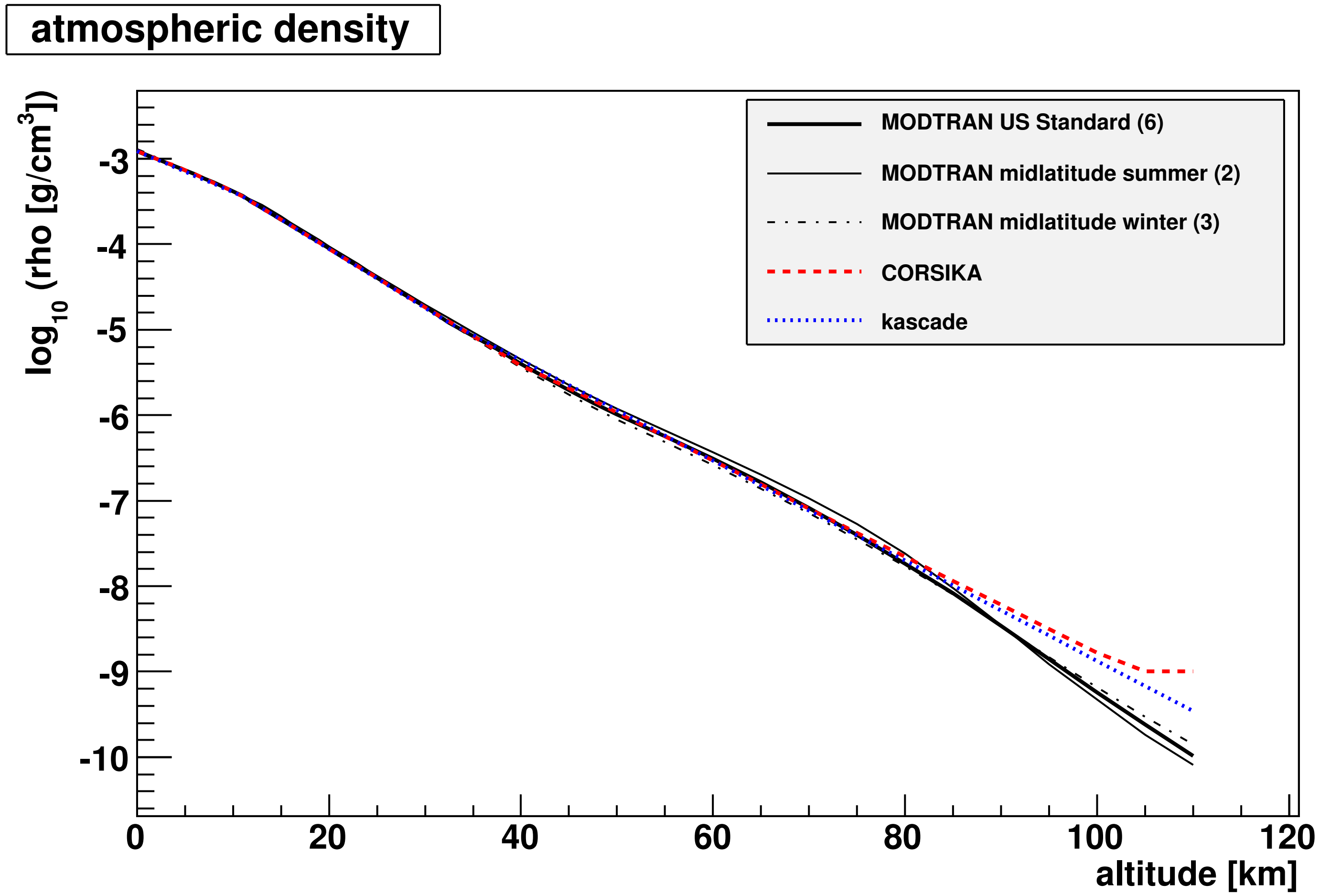

Density - refractive Index

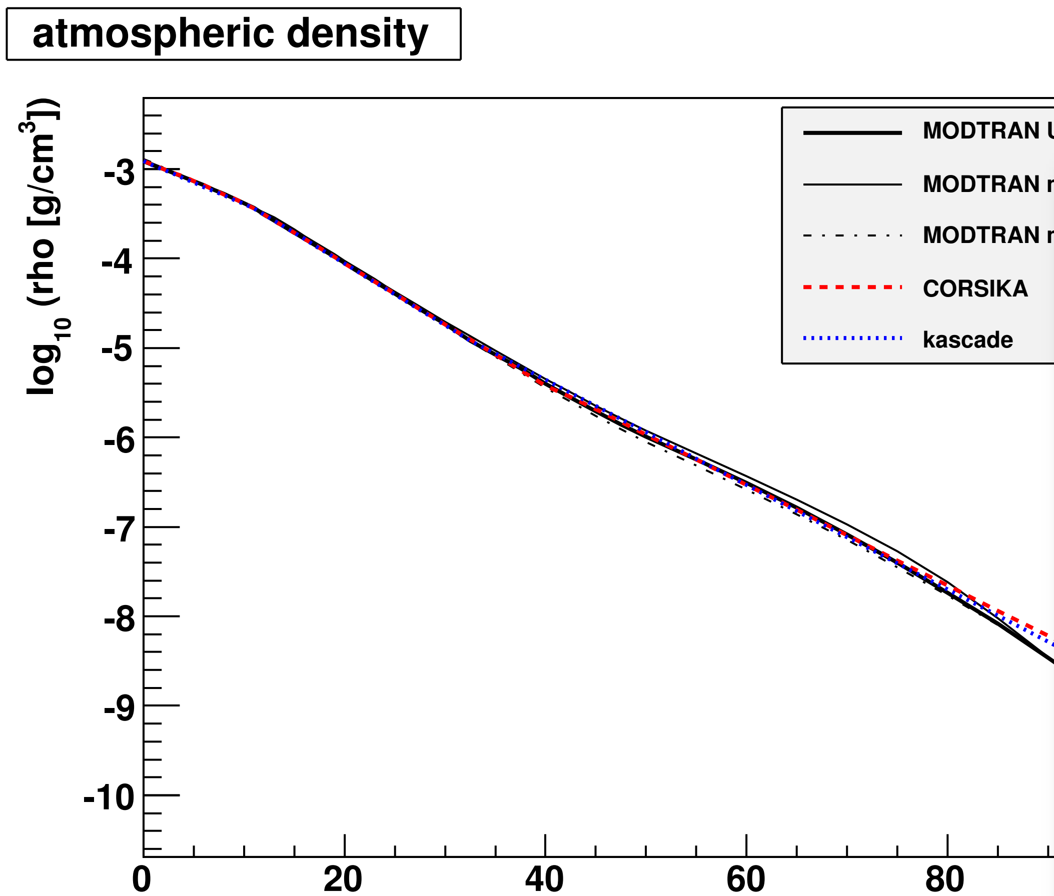

refractive index in air
scales with density

$$n = 1 + 0.000283\ \rho(h)/\rho(0)$$

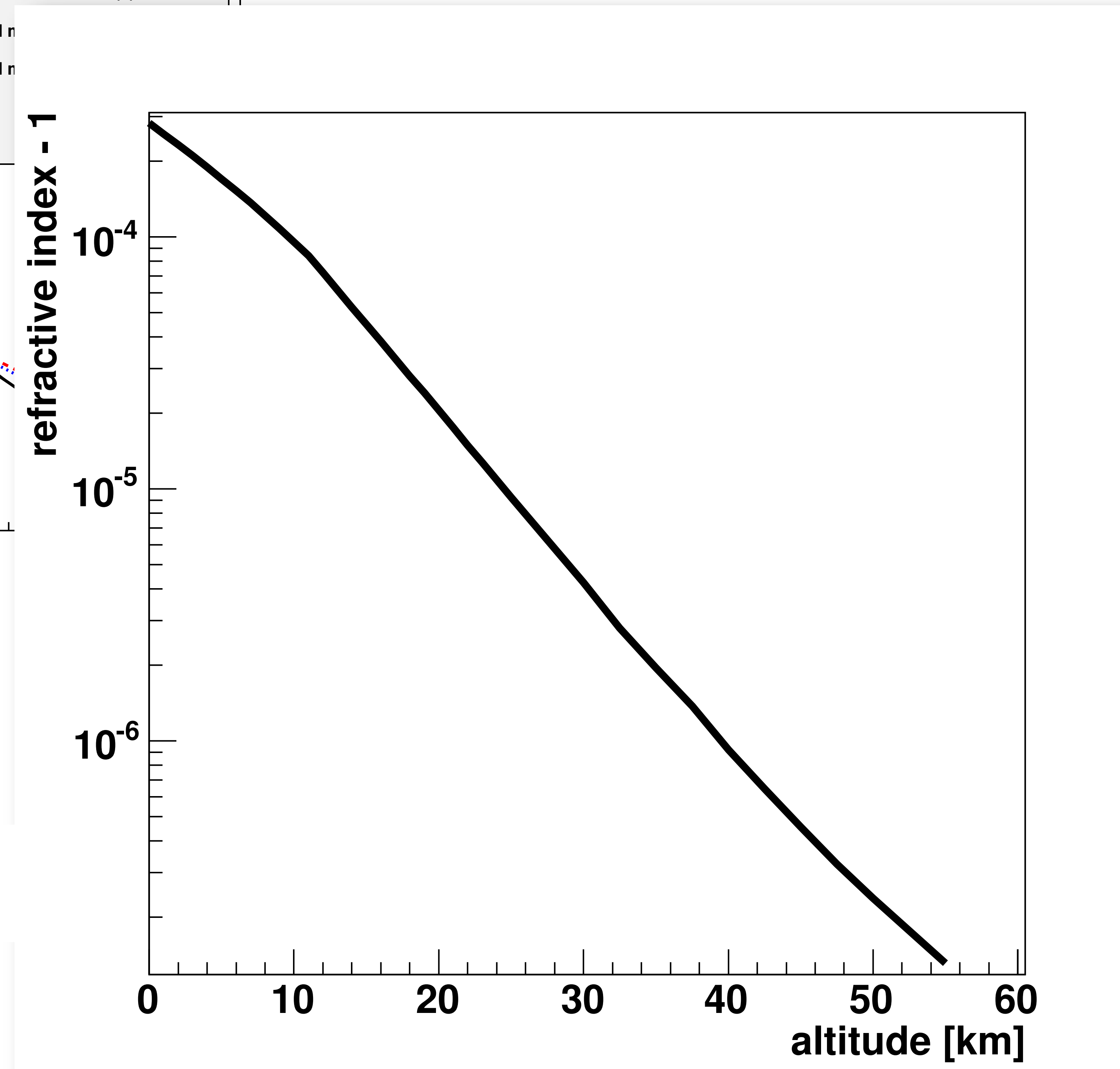

Cherenkov radiation: emission angle

light is emitted along a cone with half opening angle θ:

$$\cos\theta = 1 / (\beta n)$$

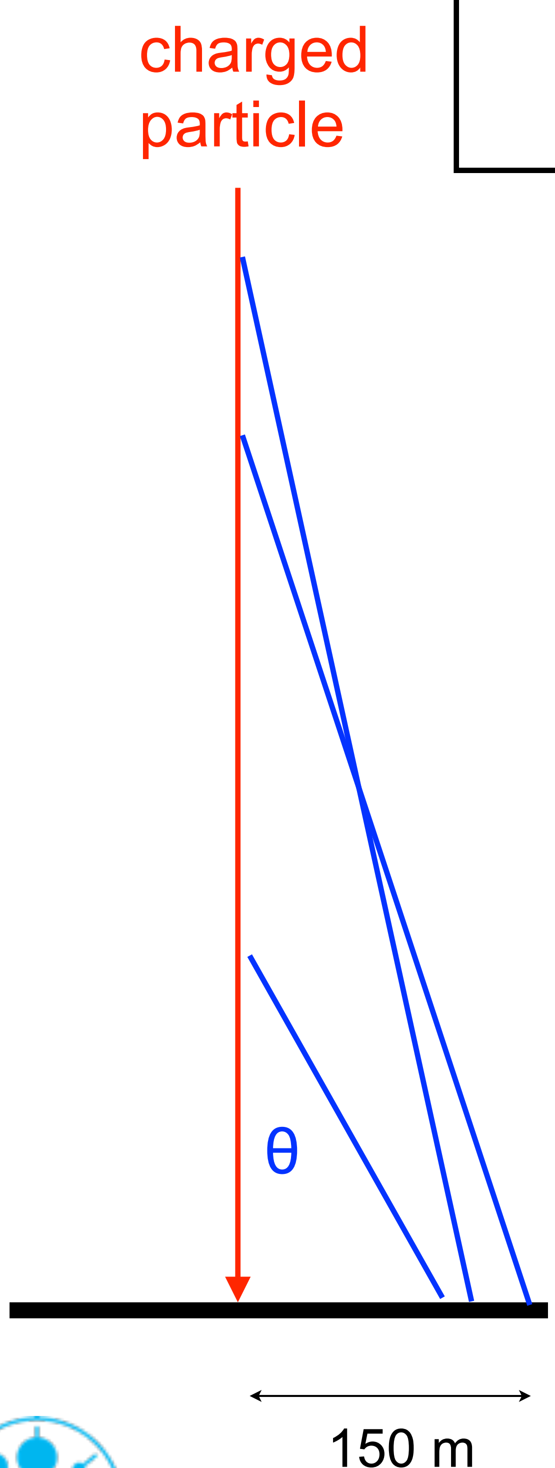

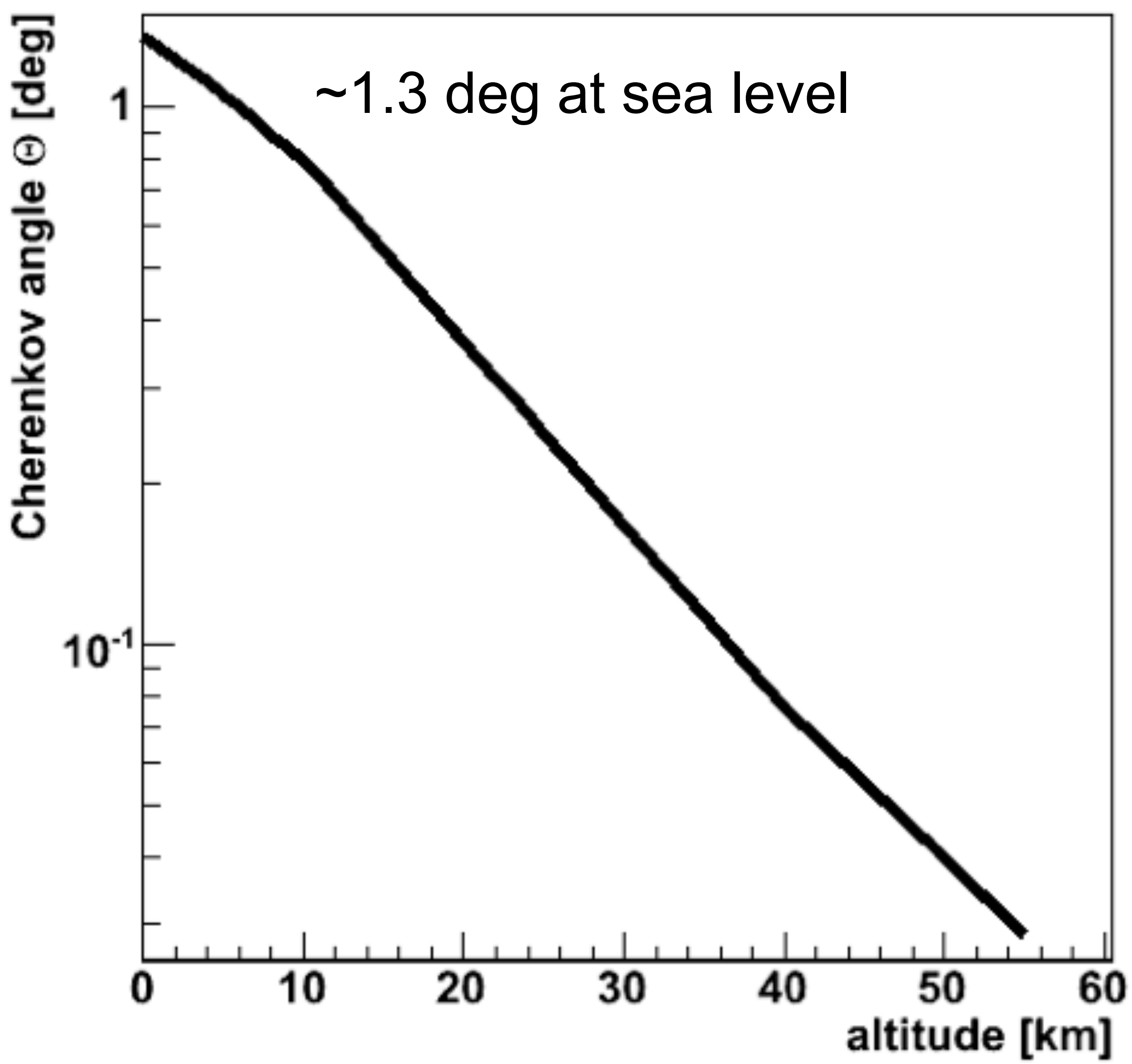

Cherenkov radiation: emission angle

light is emitted along a cone with half opening angle θ:

$$\cos\theta = 1 / (\beta n)$$

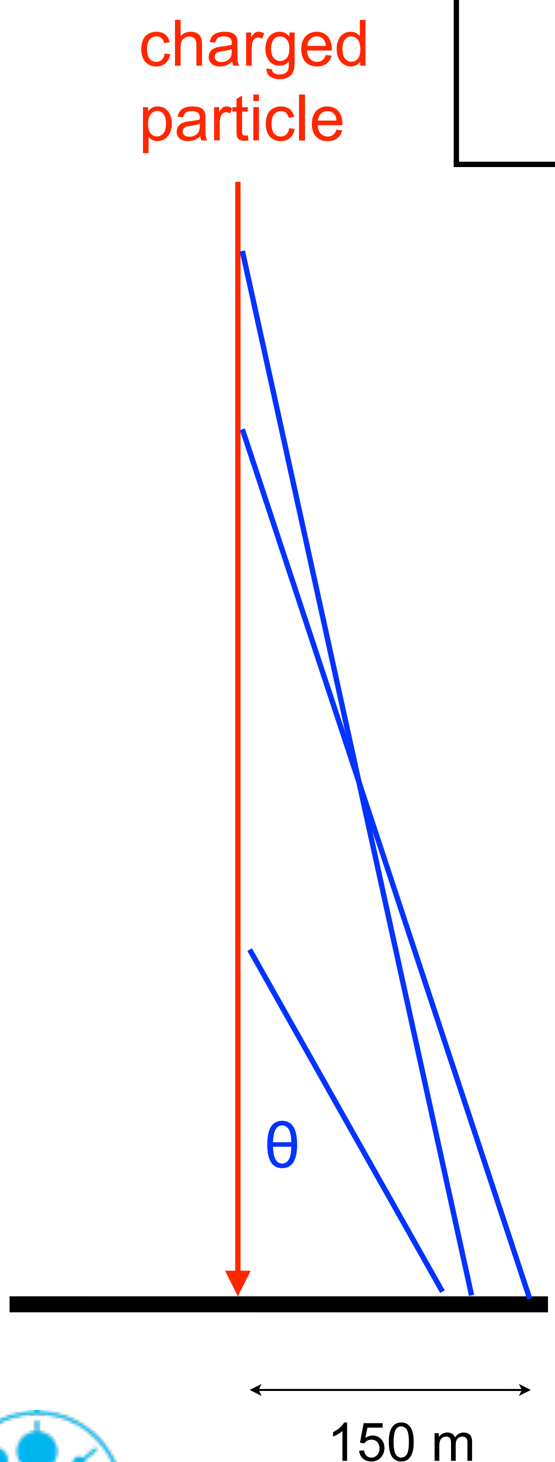

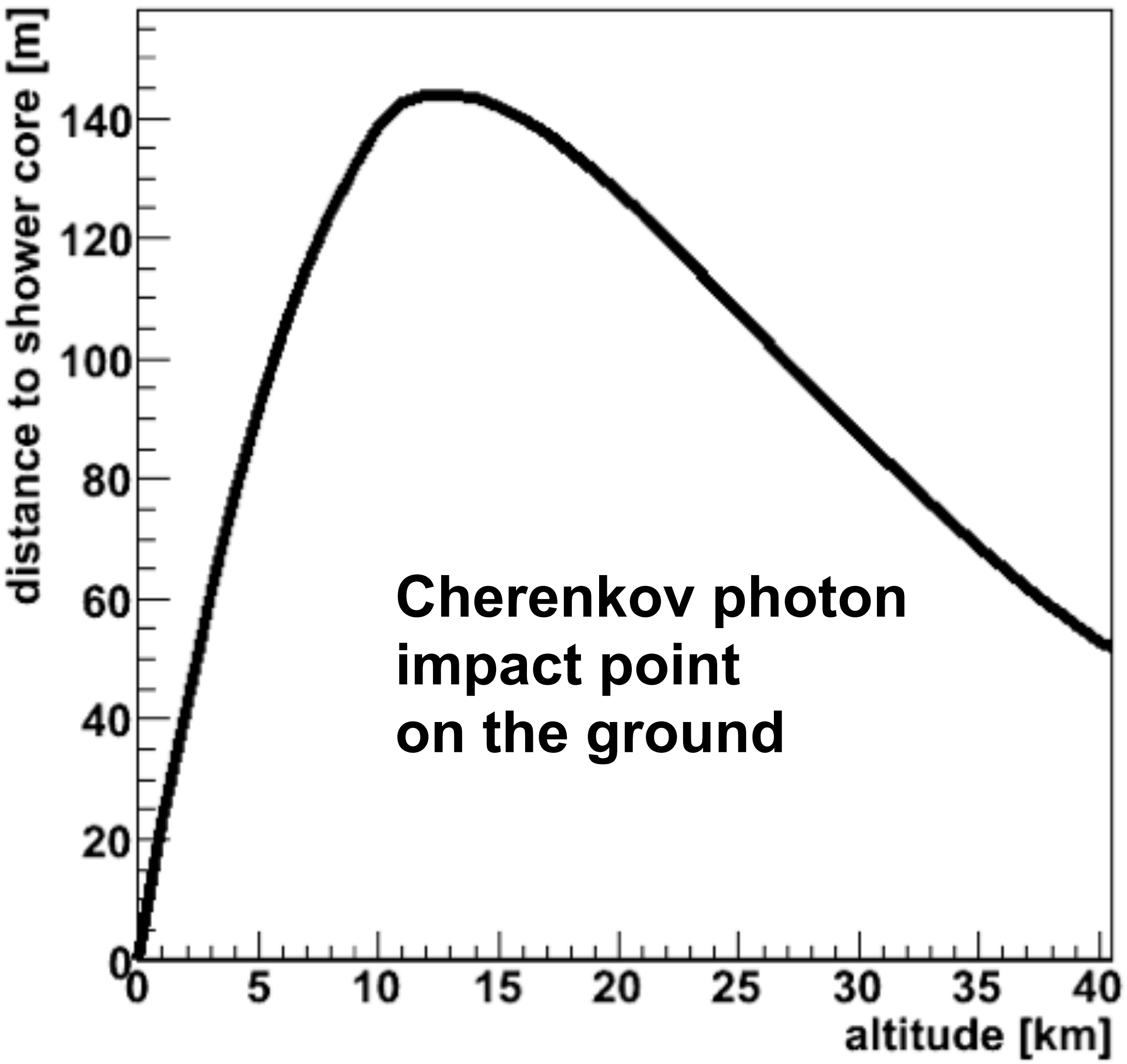

Lateral distribution of Cherenkov photons on the ground

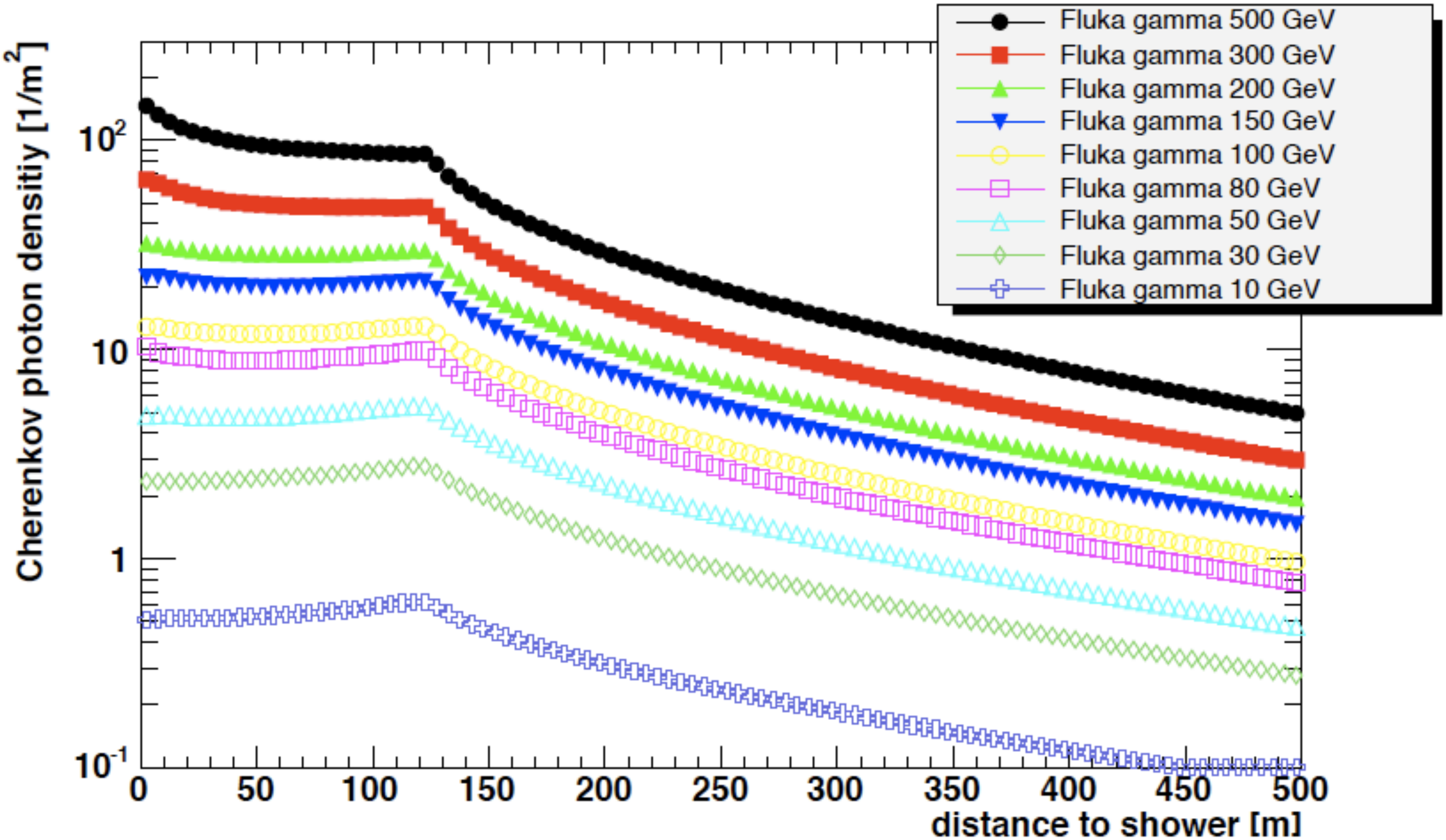

typical mirror area: 100 m^2

Lateral distribution of Cherenkov photons on the ground

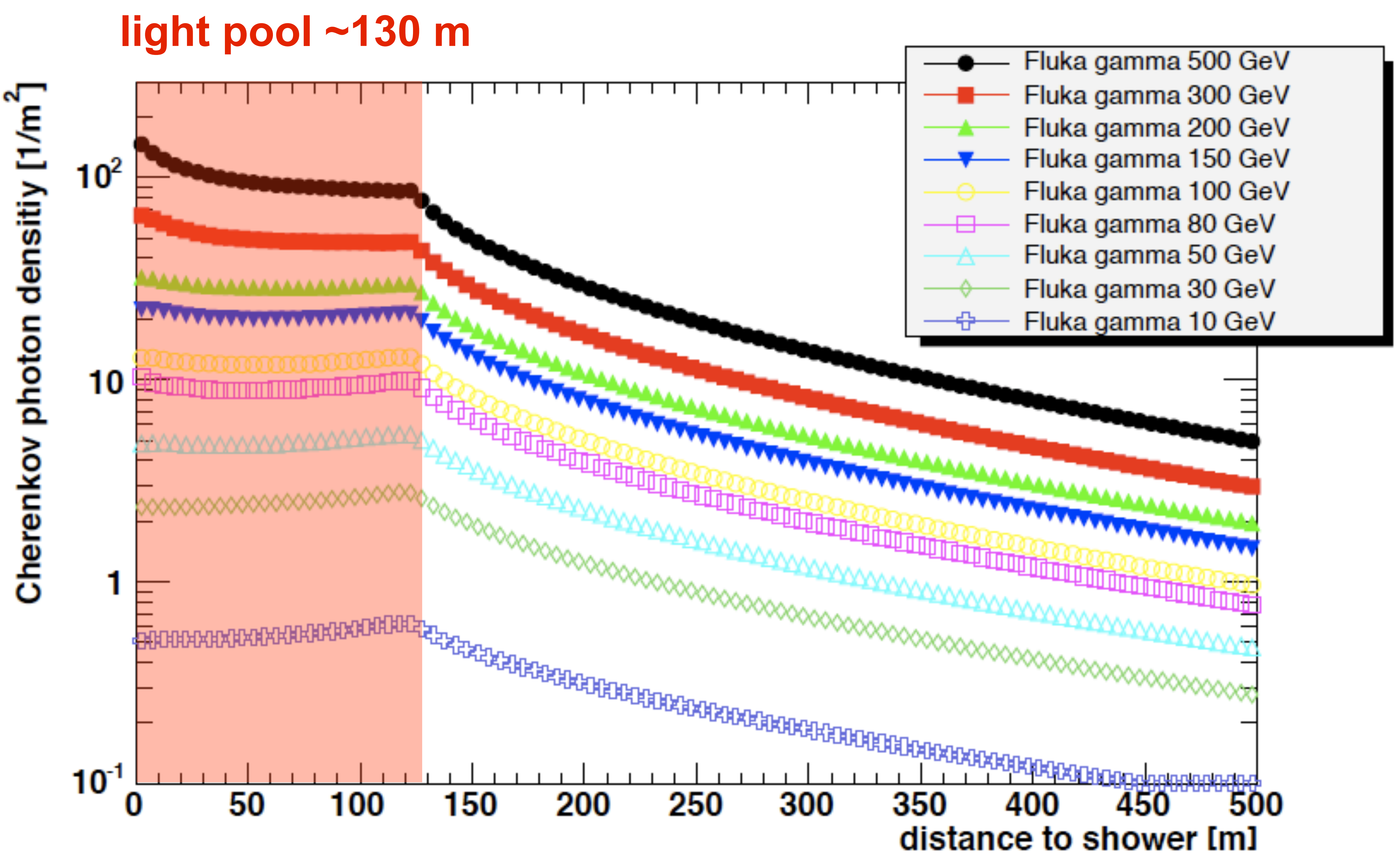

typical mirror area: 100 m²

Lateral distribution of Cherenkov photons on the ground

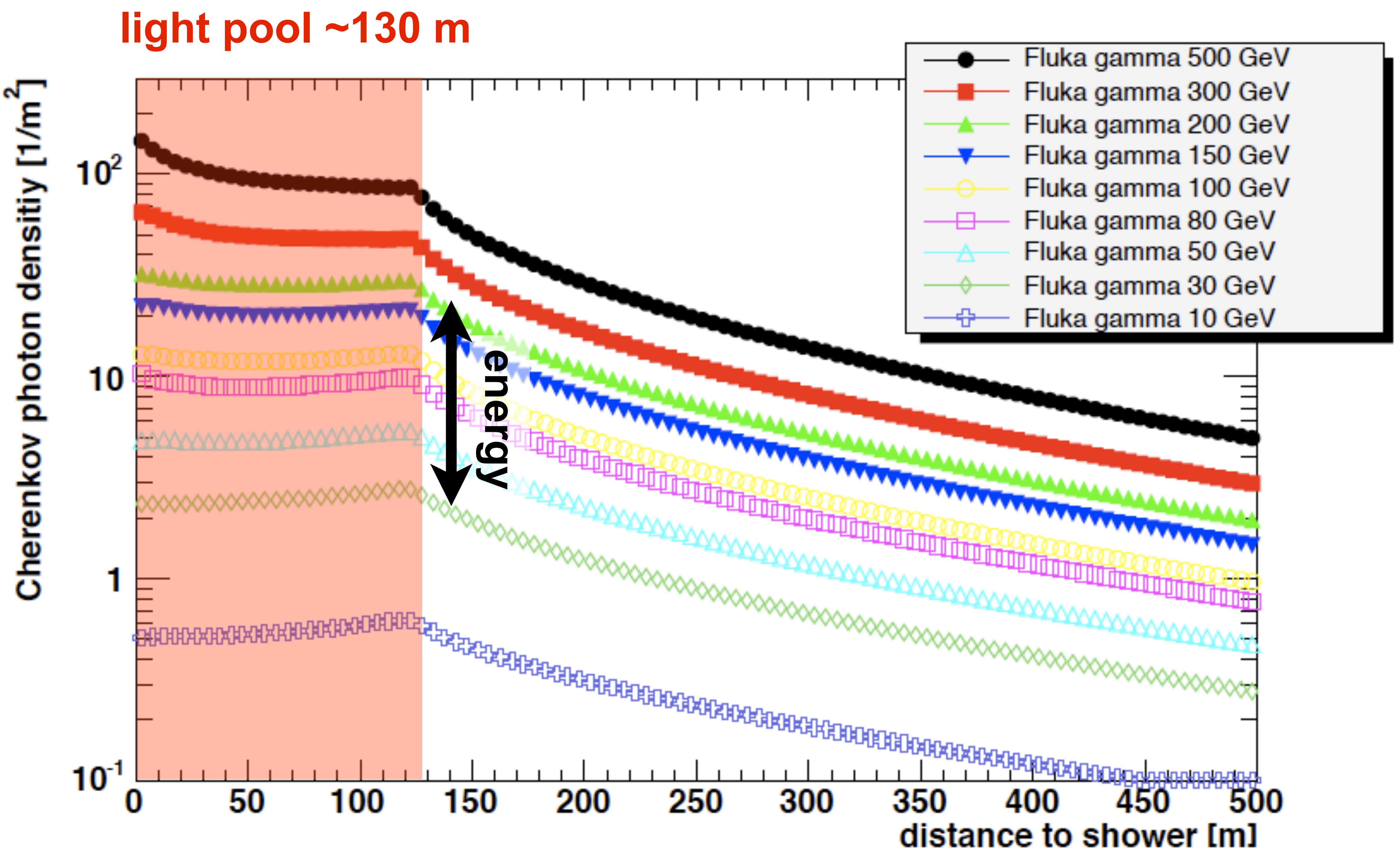

typical mirror area: 100 m²

Particle lateral distributions

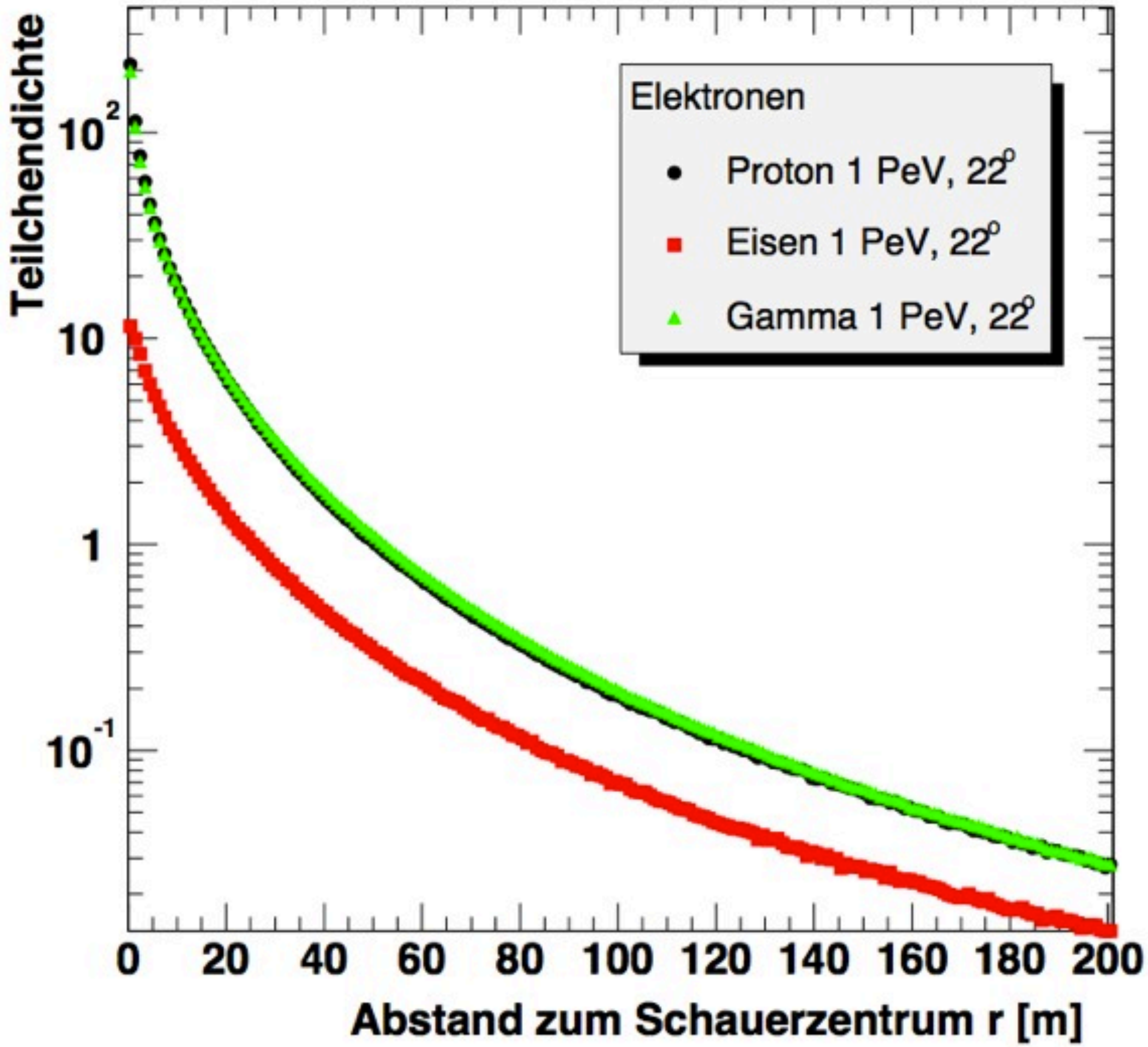

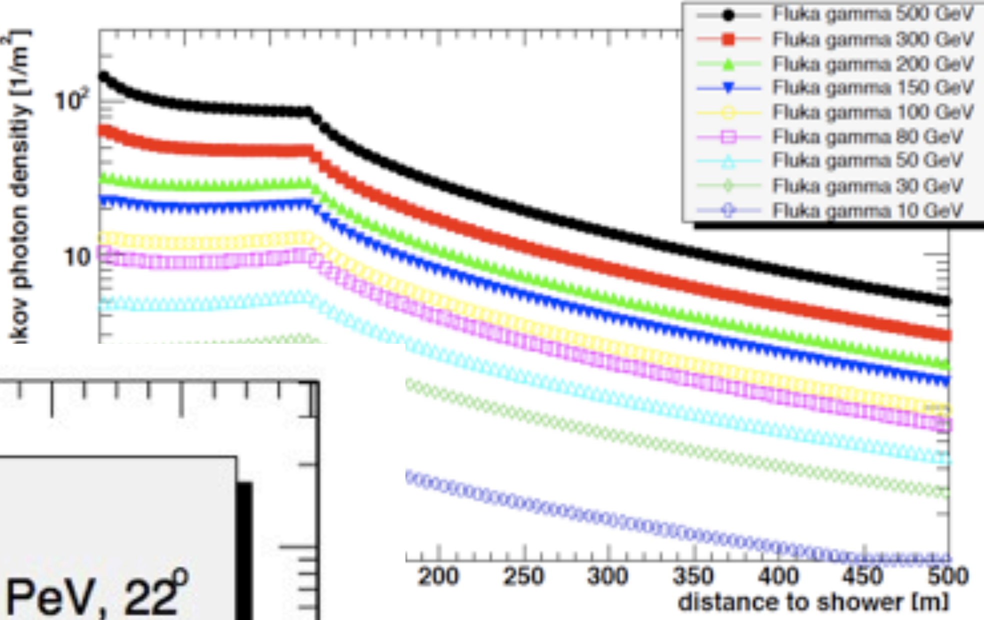

KASCADE air shower array

VERITAS

Cherenkov photon arrival times

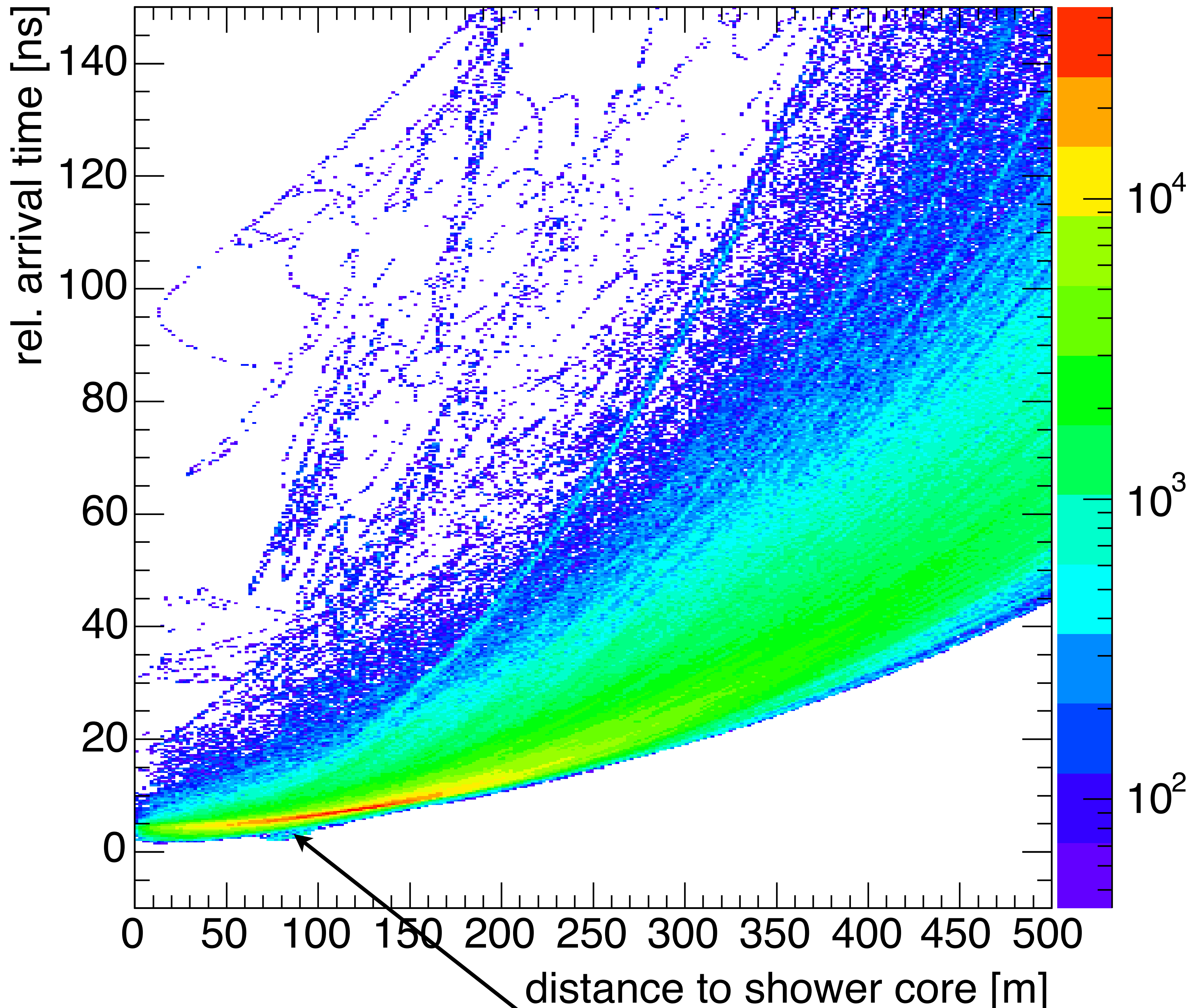

most light arrives within few ns

Shower fluctuations

randomly selected showers with 80 GeV primary photon energy

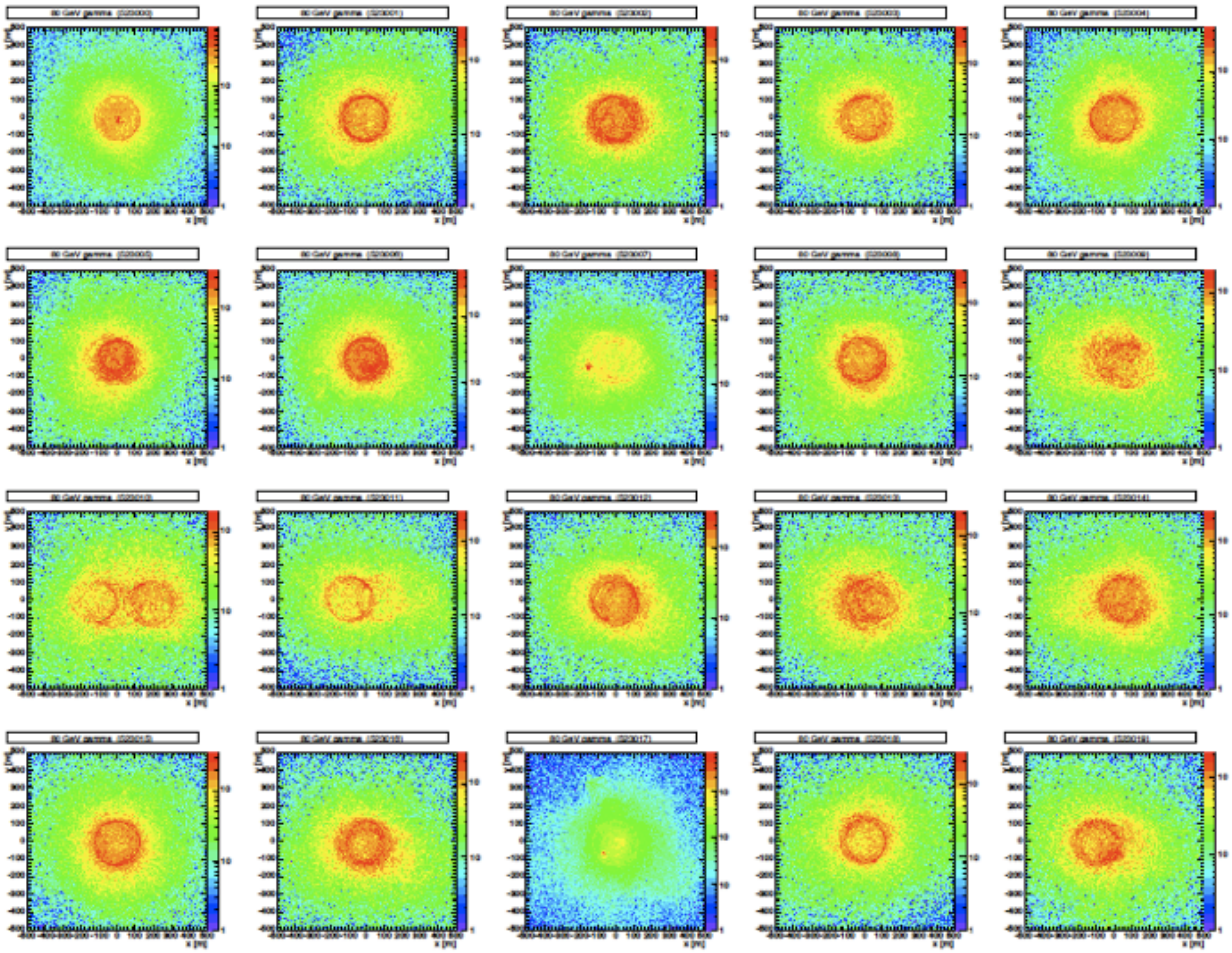

Shower fluctuations

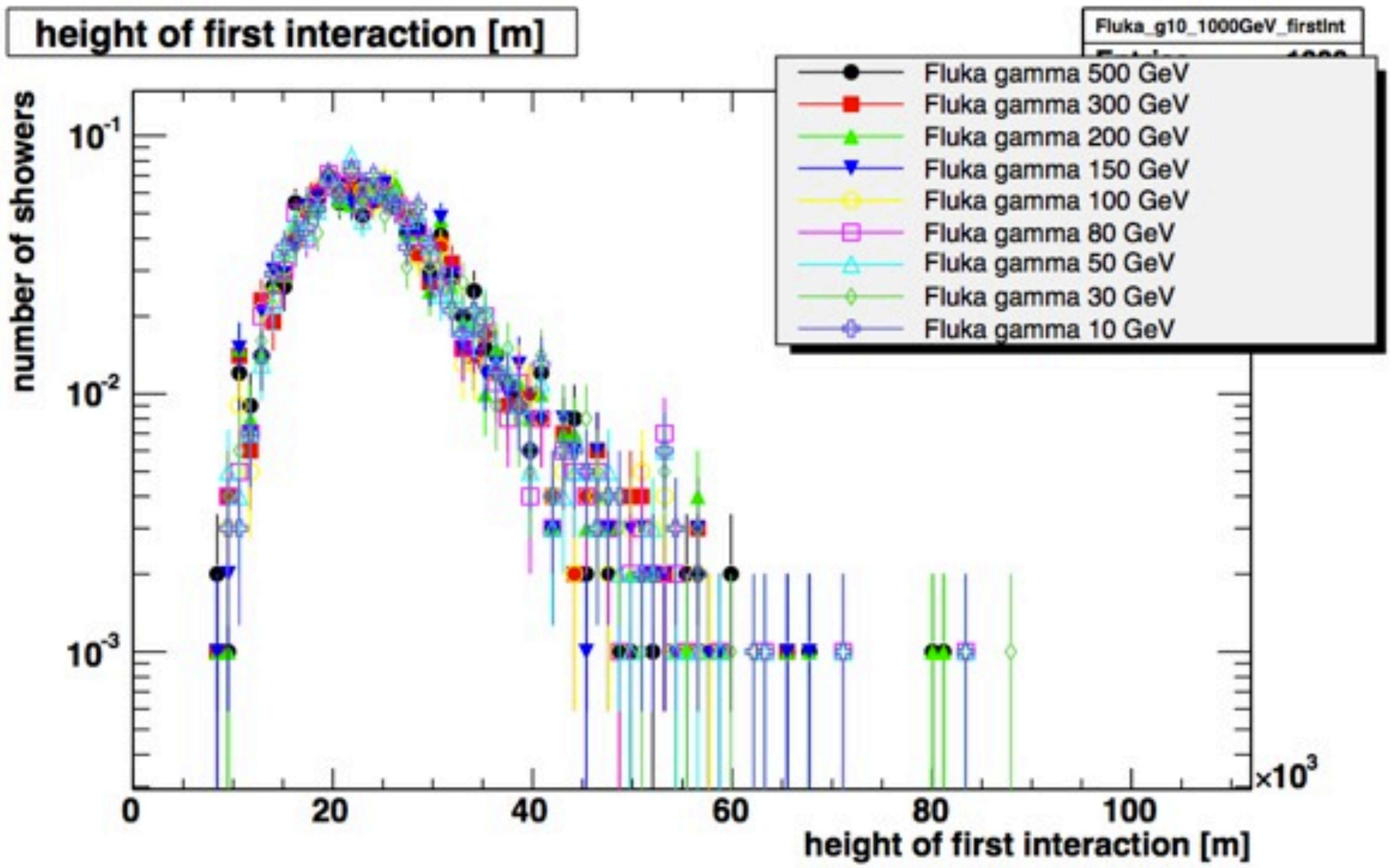

number of Cherenkov photons per shower fluctuates by a factor of 1.1-2

Shower fluctuations

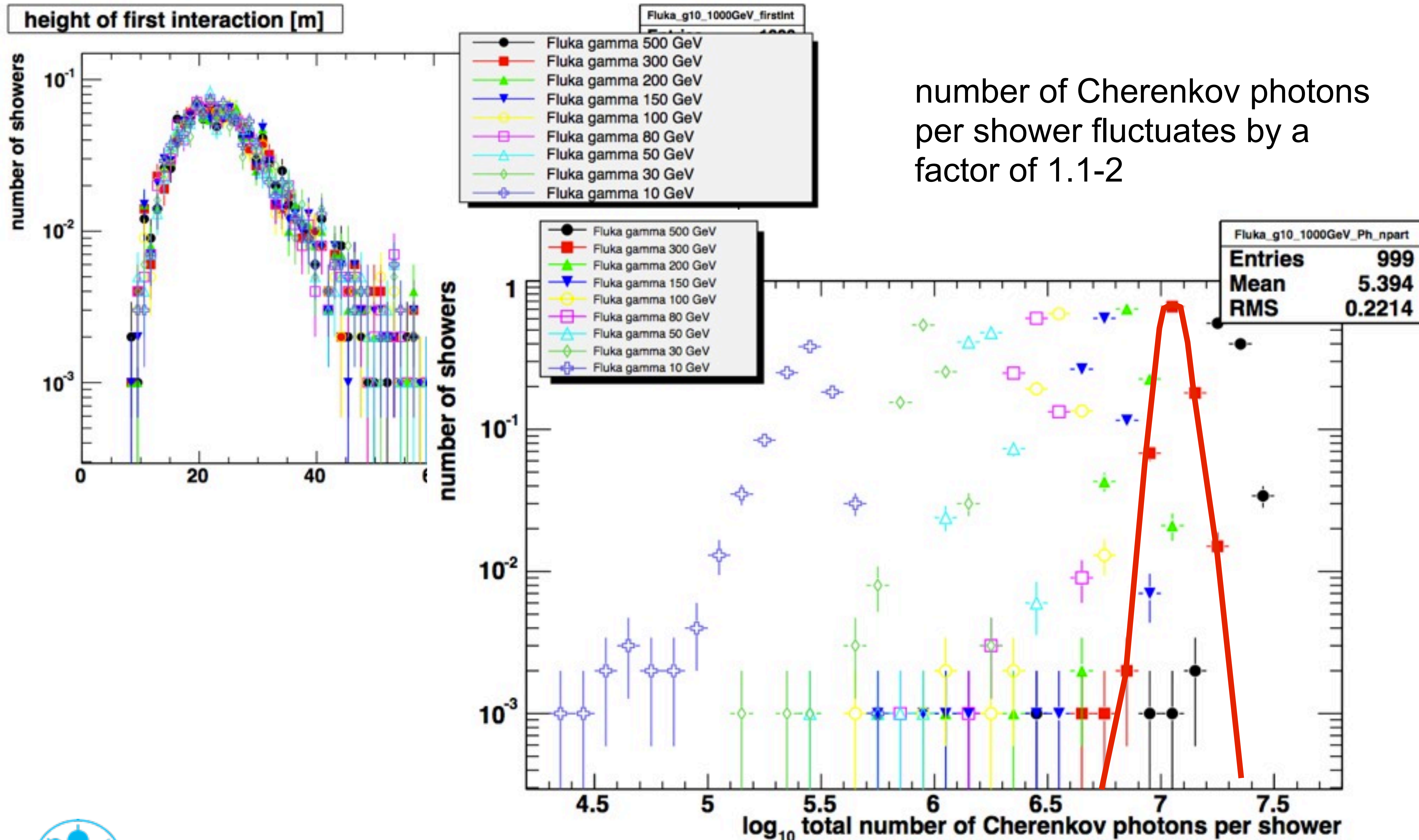

number of Cherenkov photons per shower fluctuates by a factor of 1.1-2

Geomagnetic Field

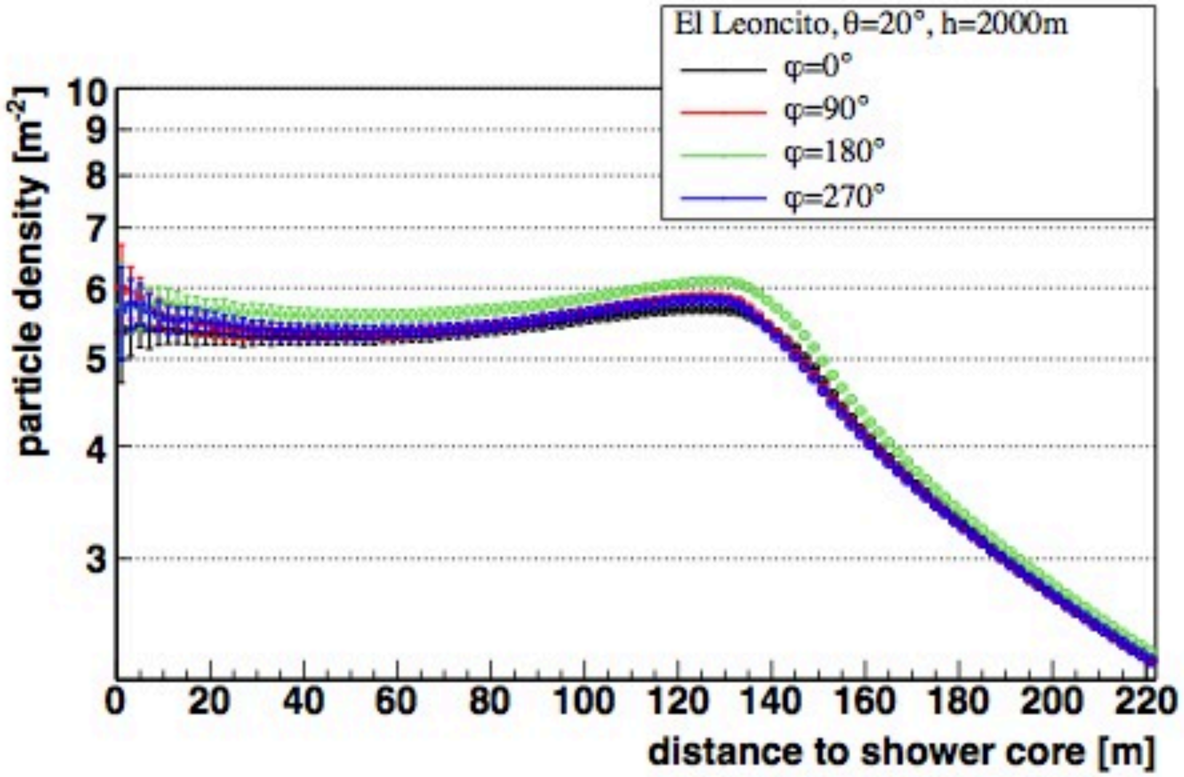

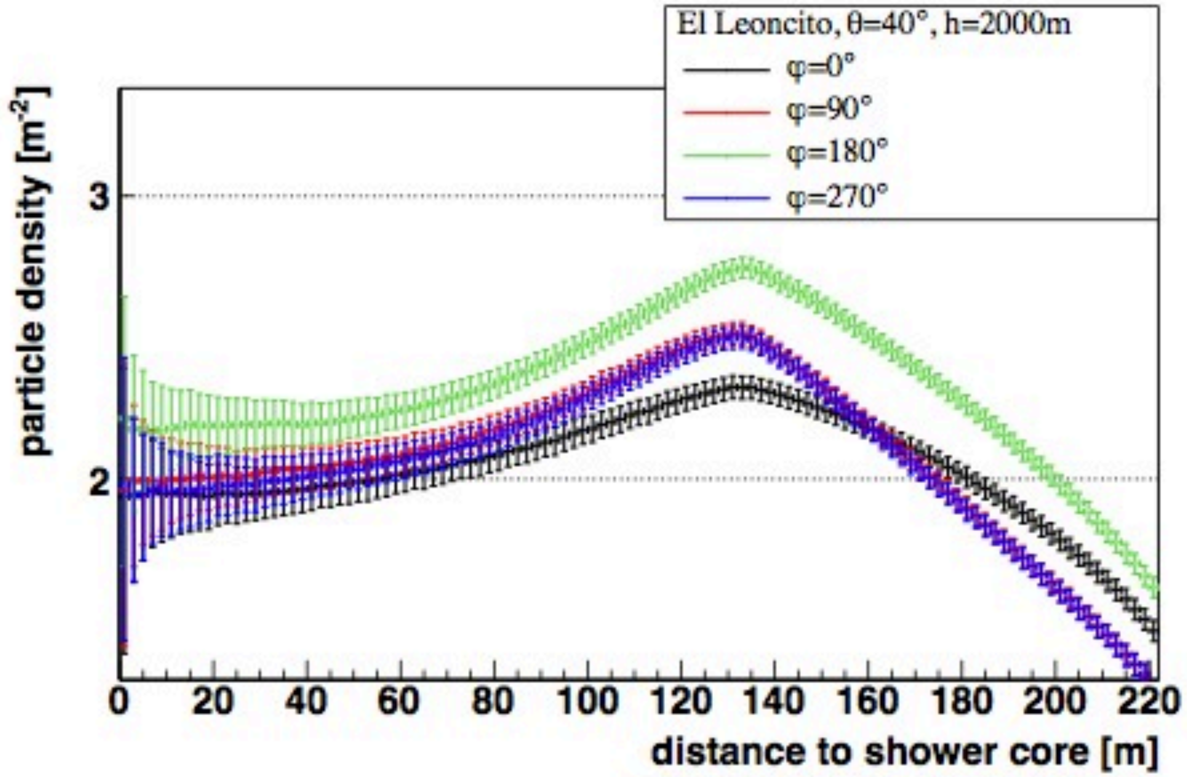

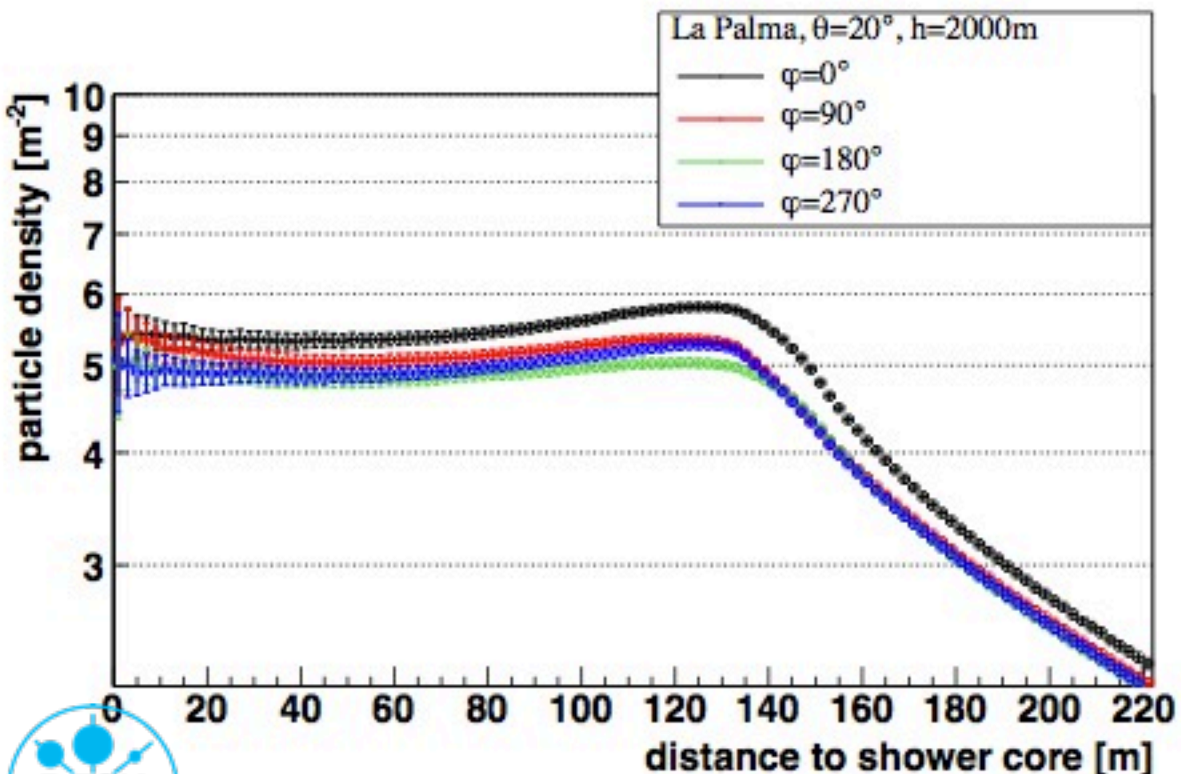

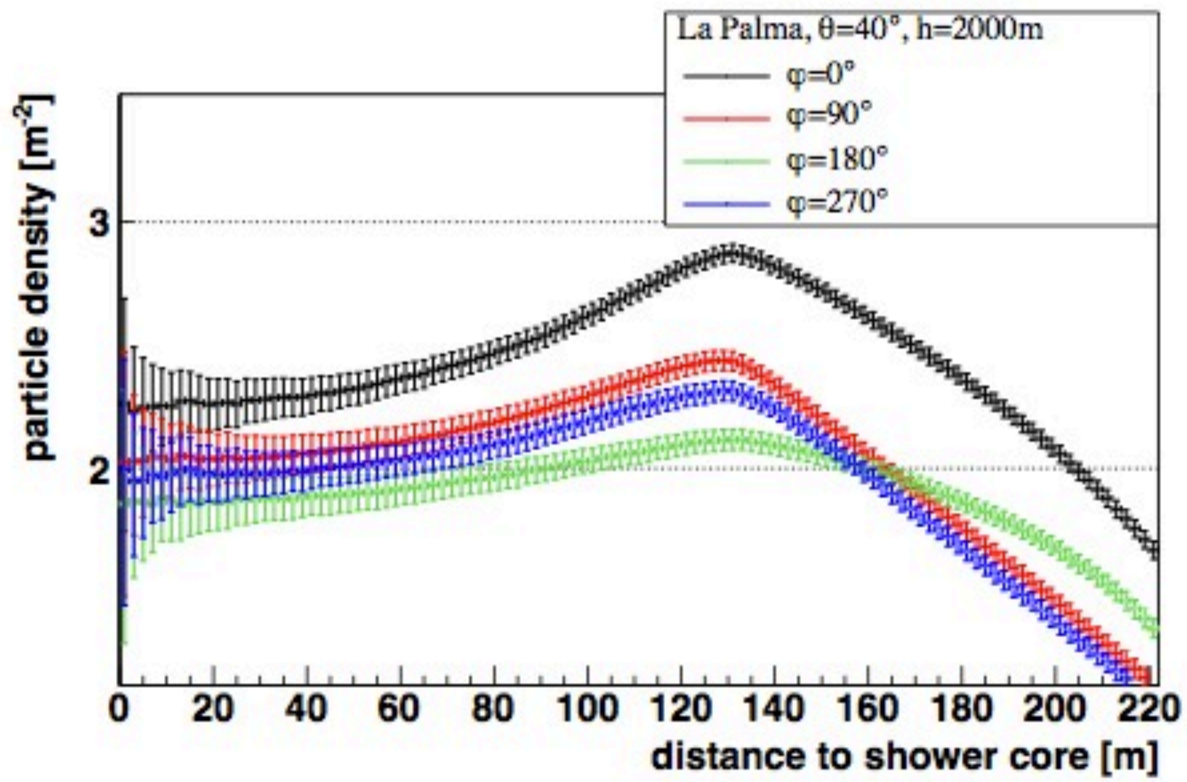

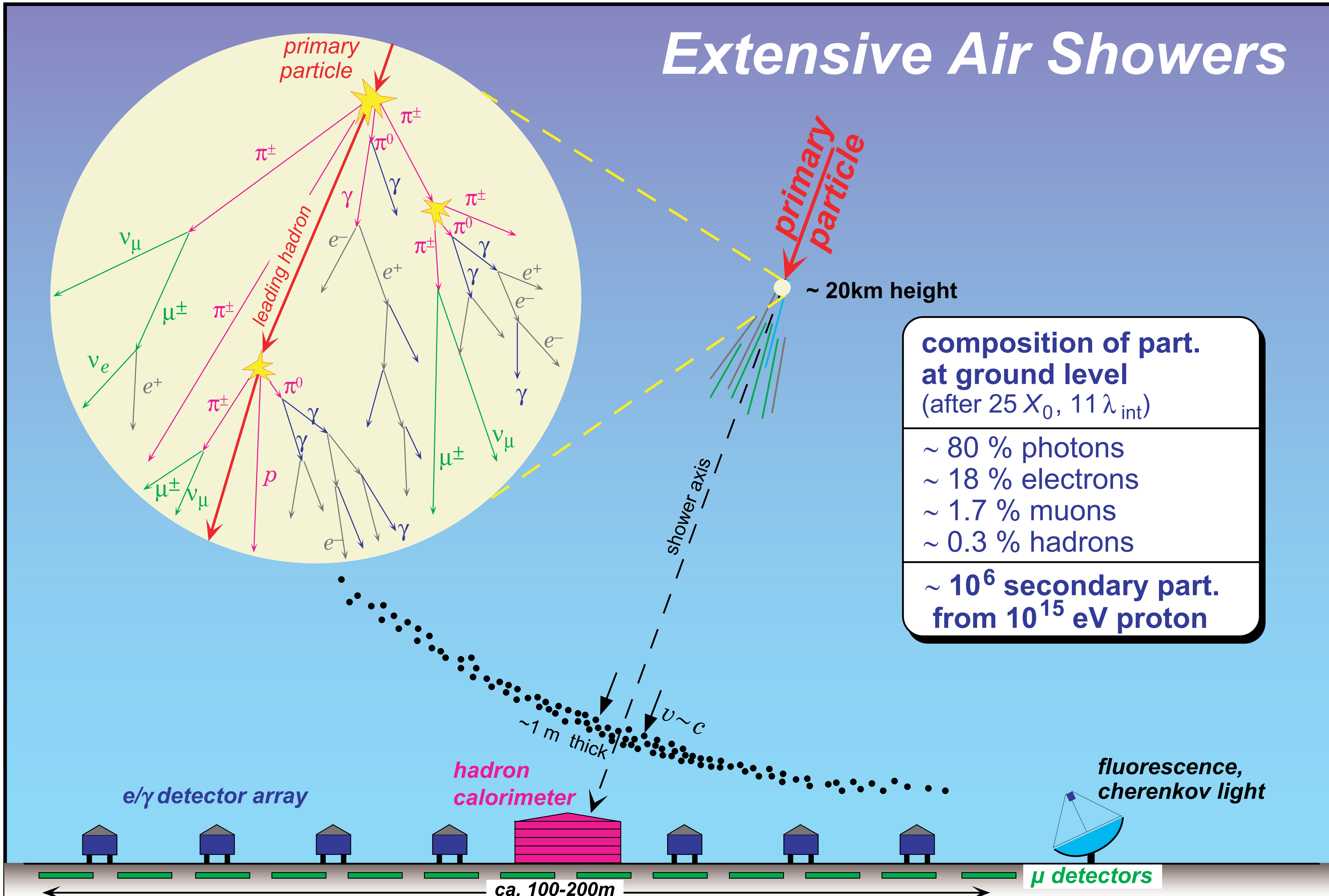

Extensive Air Showers
primary particle
π±
π0
γ
leading hadron
νμ
μ±
νe
e+
e−
p
primary particle
~ 20km height
shower axis
composition of part. at ground level
(after 25 X0, 11 λint)
~ 80 % photons
~ 18 % electrons
~ 1.7 % muons
~ 0.3 % hadrons
~ 10^6 secondary part. from 10^15 eV proton
~1 m thick
υ~c
hadron calorimeter
e/γ detector array
fluorescence, cherenkov light
μ detectors
ca. 100-200m

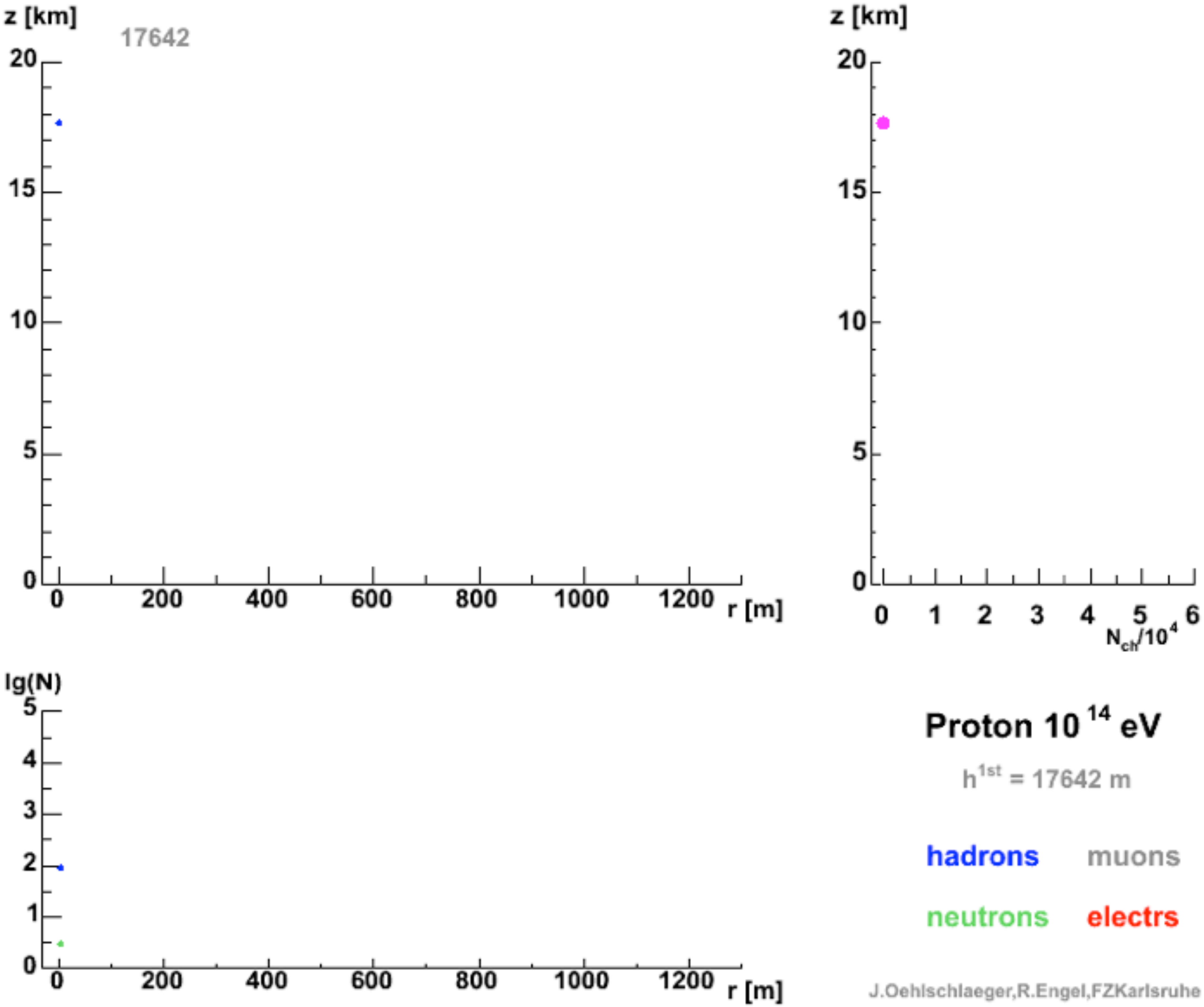

z [km]
17642
20
15
10
5
0
0
200
400
600
800
1000
1200
r [m]
z [km]
20
15
10
5
0
0
1
2
3
4
5
6
N_ch/10^4
lg(N)
5
4
3
2
1
0
0
200
400
600
800
1000
1200
r [m]
Proton 10 14 eV
h1st = 17642 m
hadrons
muons
neutrons
electrs
J.Oehlschlaeger,R.Engel,FZKarlsruhe

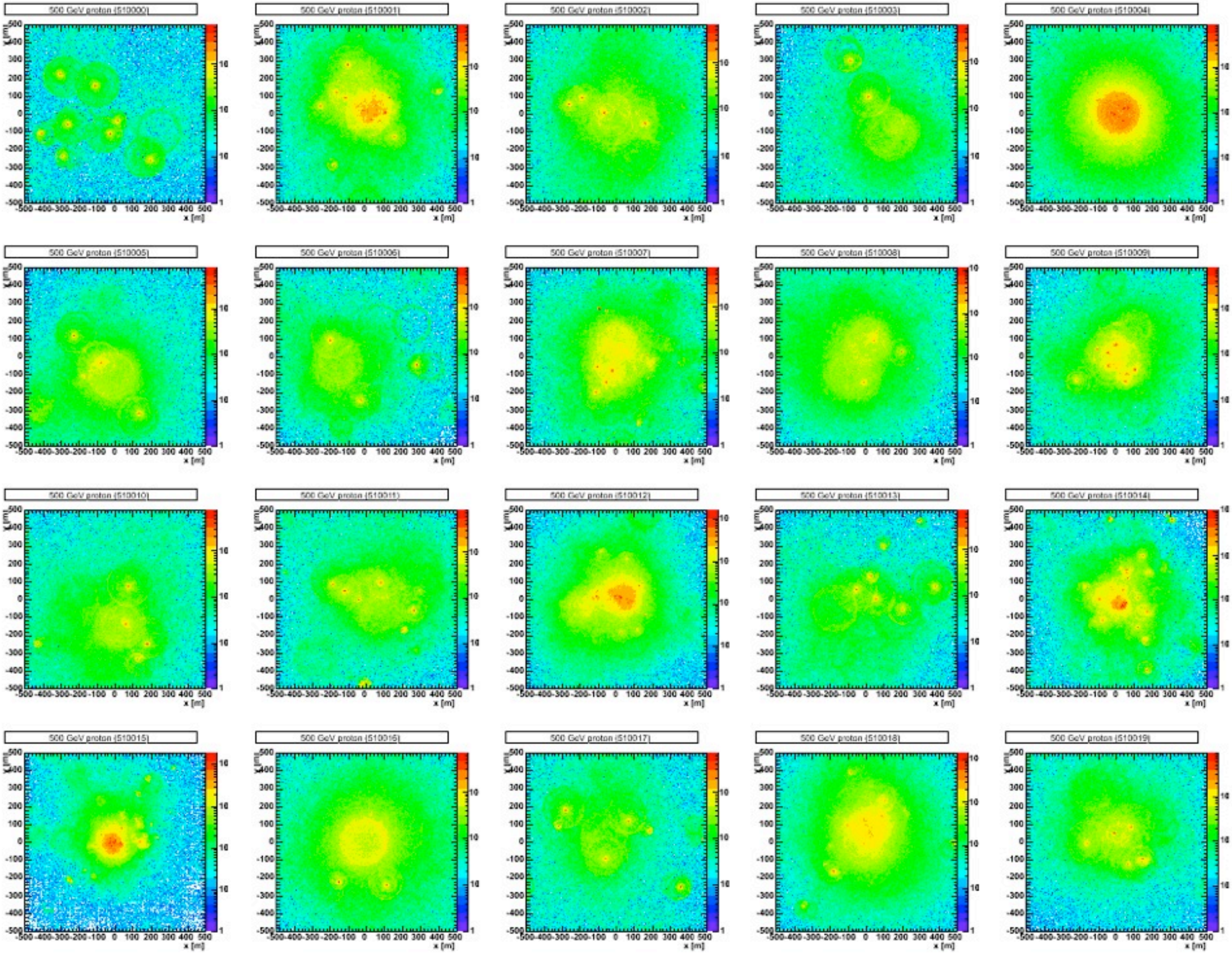
500 GeV proton (510000)
500 GeV proton (510001)
500 GeV proton (510002)
500 GeV proton (510003)
500 GeV proton (510004)
500 GeV proton (510005)
500 GeV proton (510006)
500 GeV proton (510007)
500 GeV proton (510008)
500 GeV proton (510009)
500 GeV proton (510010)
500 GeV proton (510011)
500 GeV proton (510012)
500 GeV proton (510013)
500 GeV proton (510014)
500 GeV proton (510015)
500 GeV proton (510016)
500 GeV proton (510017)
500 GeV proton (510018)
500 GeV proton (510019)
y [m]
x [m]

Proton vs Gamma-ray showers

γ-ray

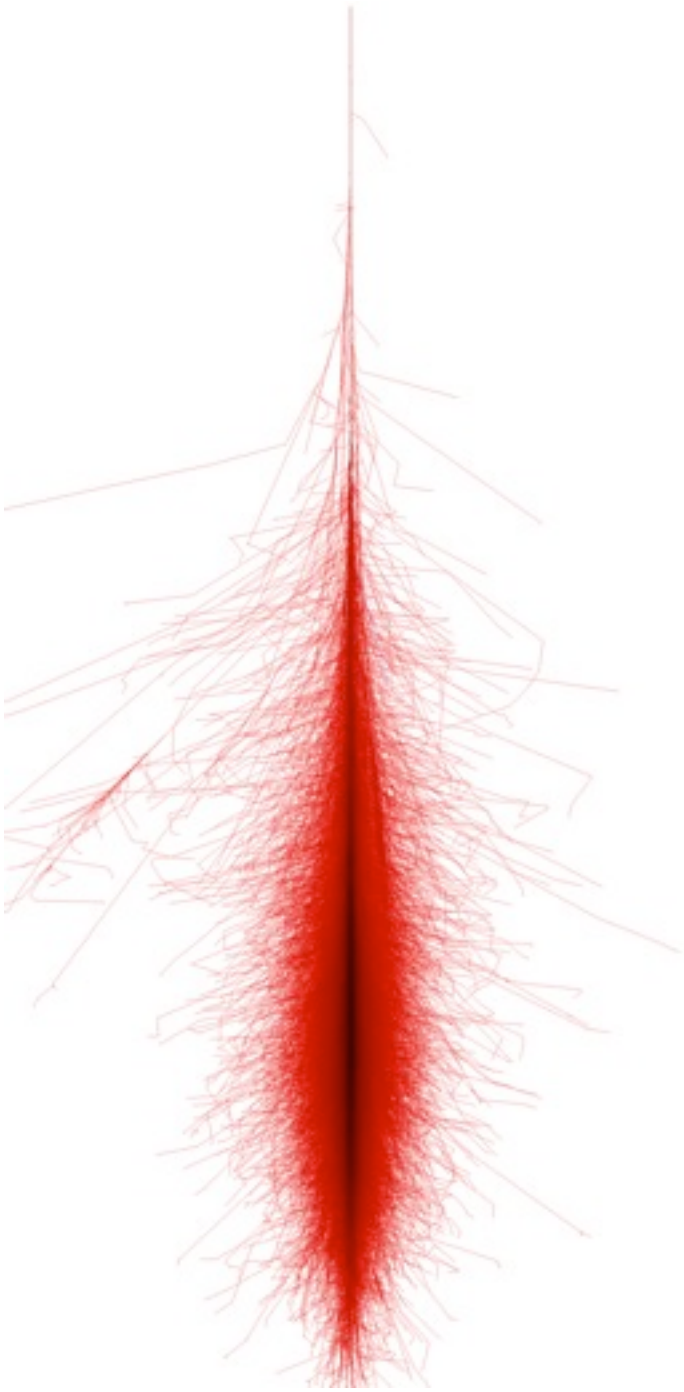

Cherenkov photons on ground

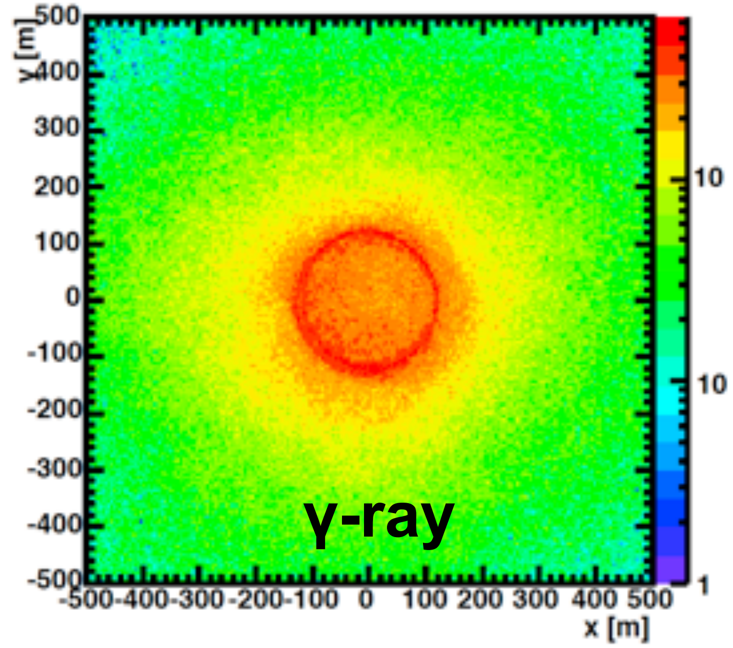

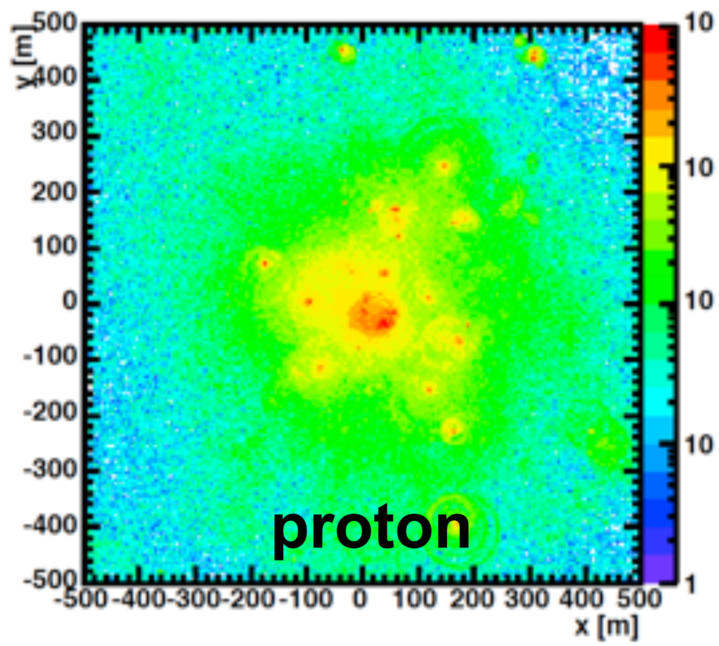

proton

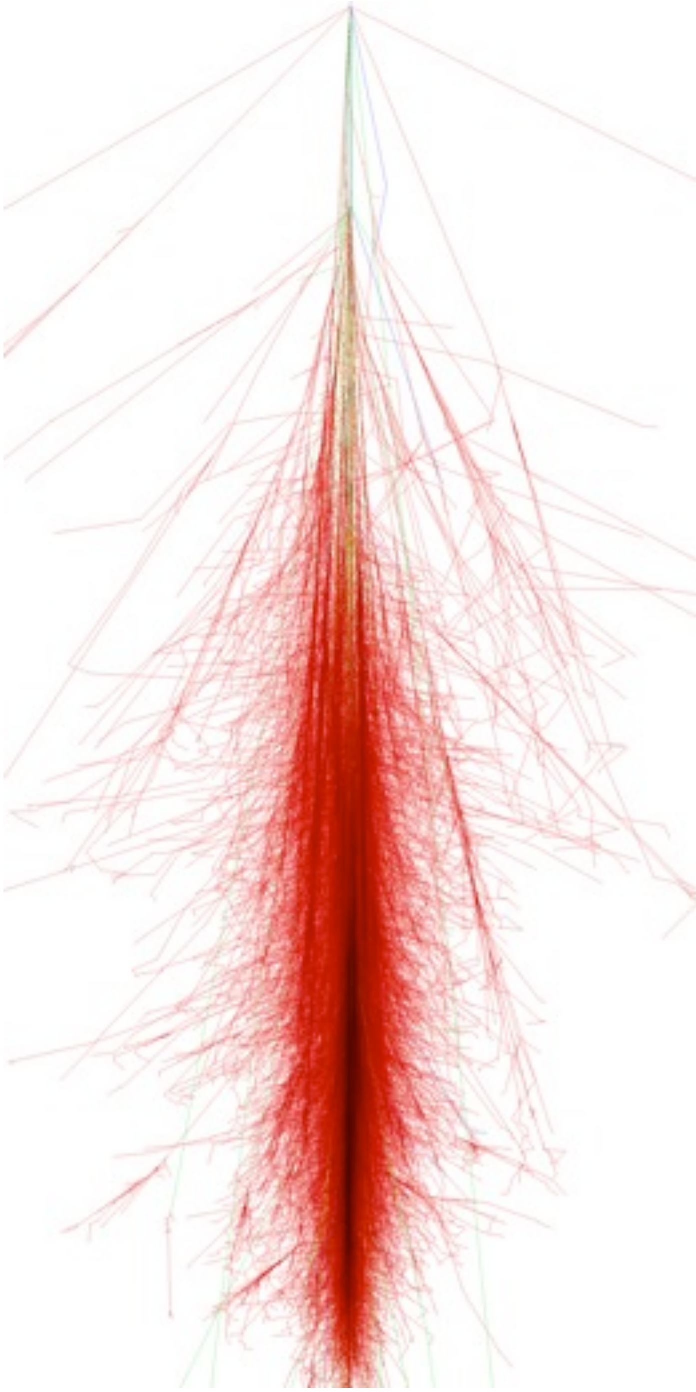

Atmosphere - Pressure profile variations

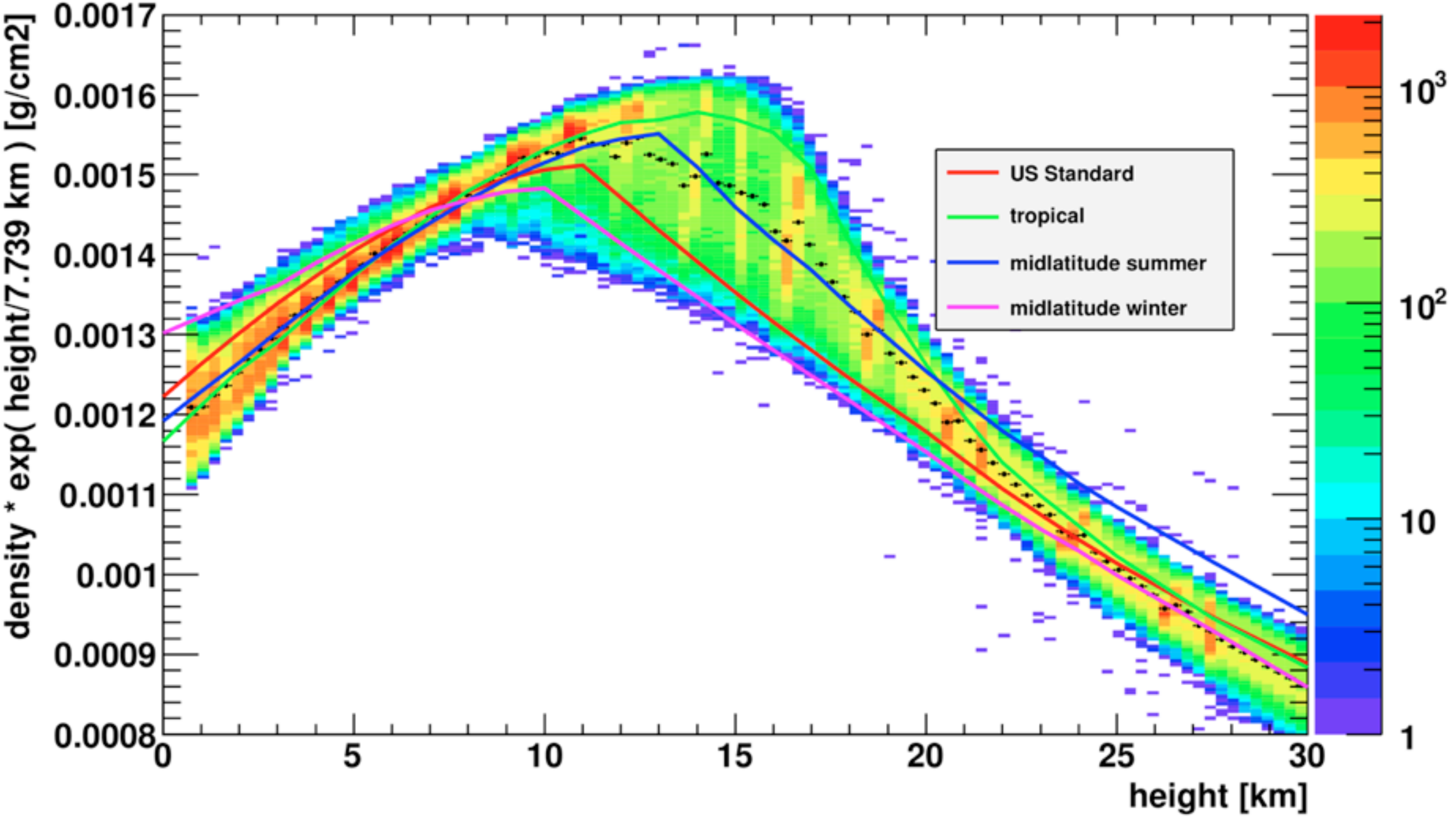

DESY

Atmosphere

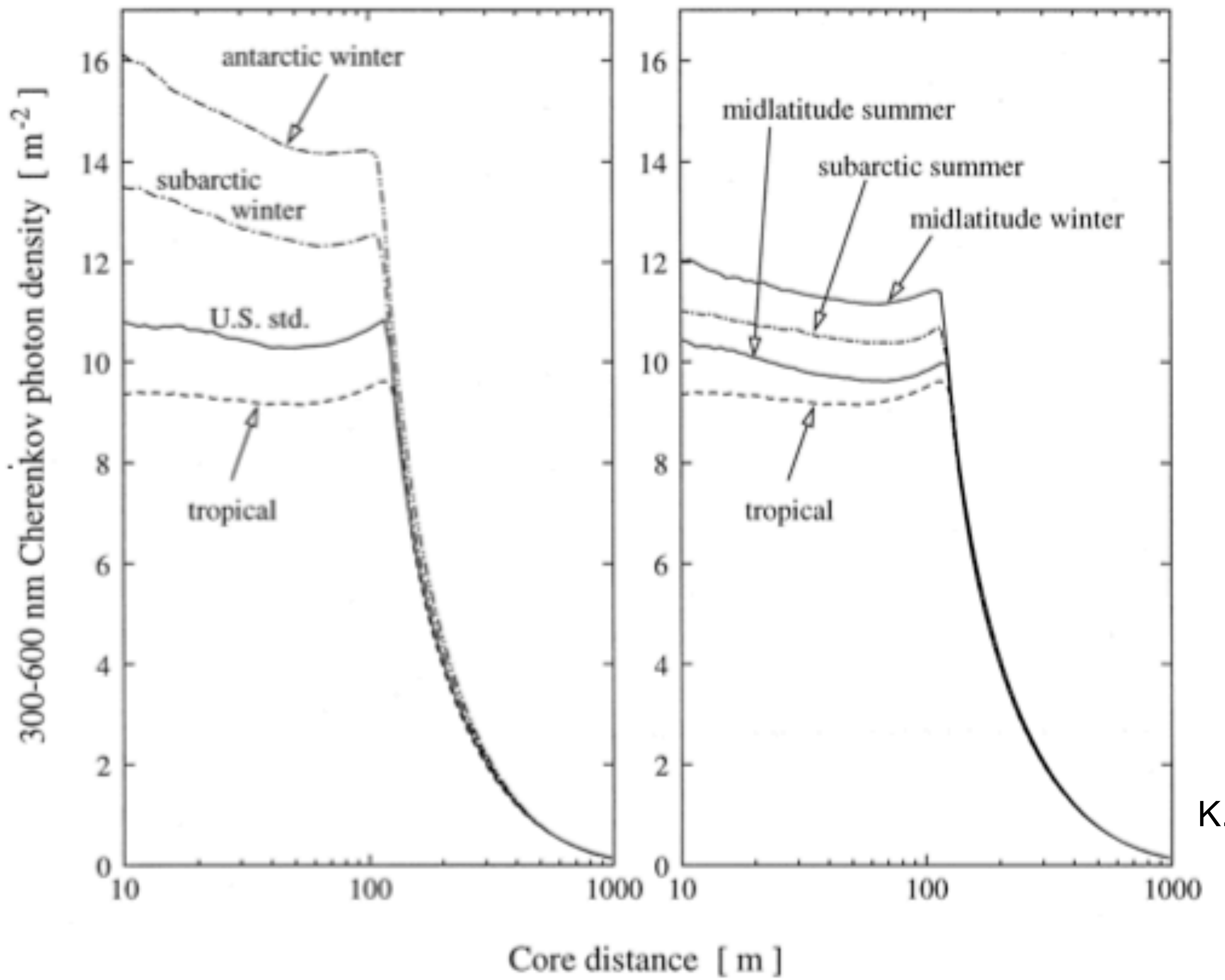

K. Bernlöhr (2000)

Fig. 1. Average lateral distributions of Cherenkov light photons in the wavelength range 300–600 nm for vertical 100 GeV gamma-ray showers in CORSIKA 5.71 simulations with different atmospheric profiles (2000 showers simulated for each profile). Absorption of Cherenkov light is taken into account (see Section 3). Observation altitude is 2200 m above sea level.

Atmospheric extinction

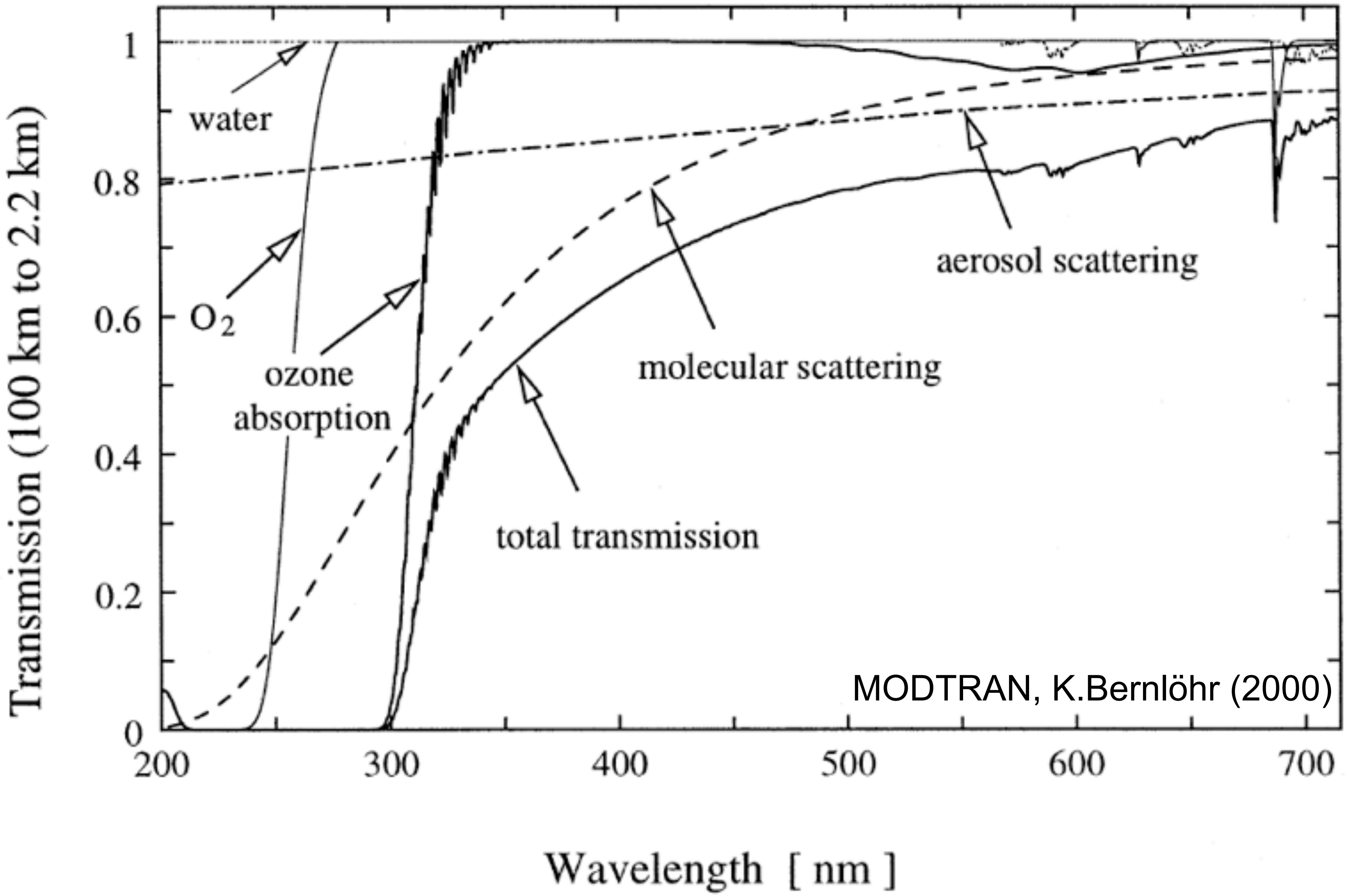

site dependent: use MODTRAN to calculate exact values

Atmospheric extinction

MODTRAN & K.Bernlöhr (2000)

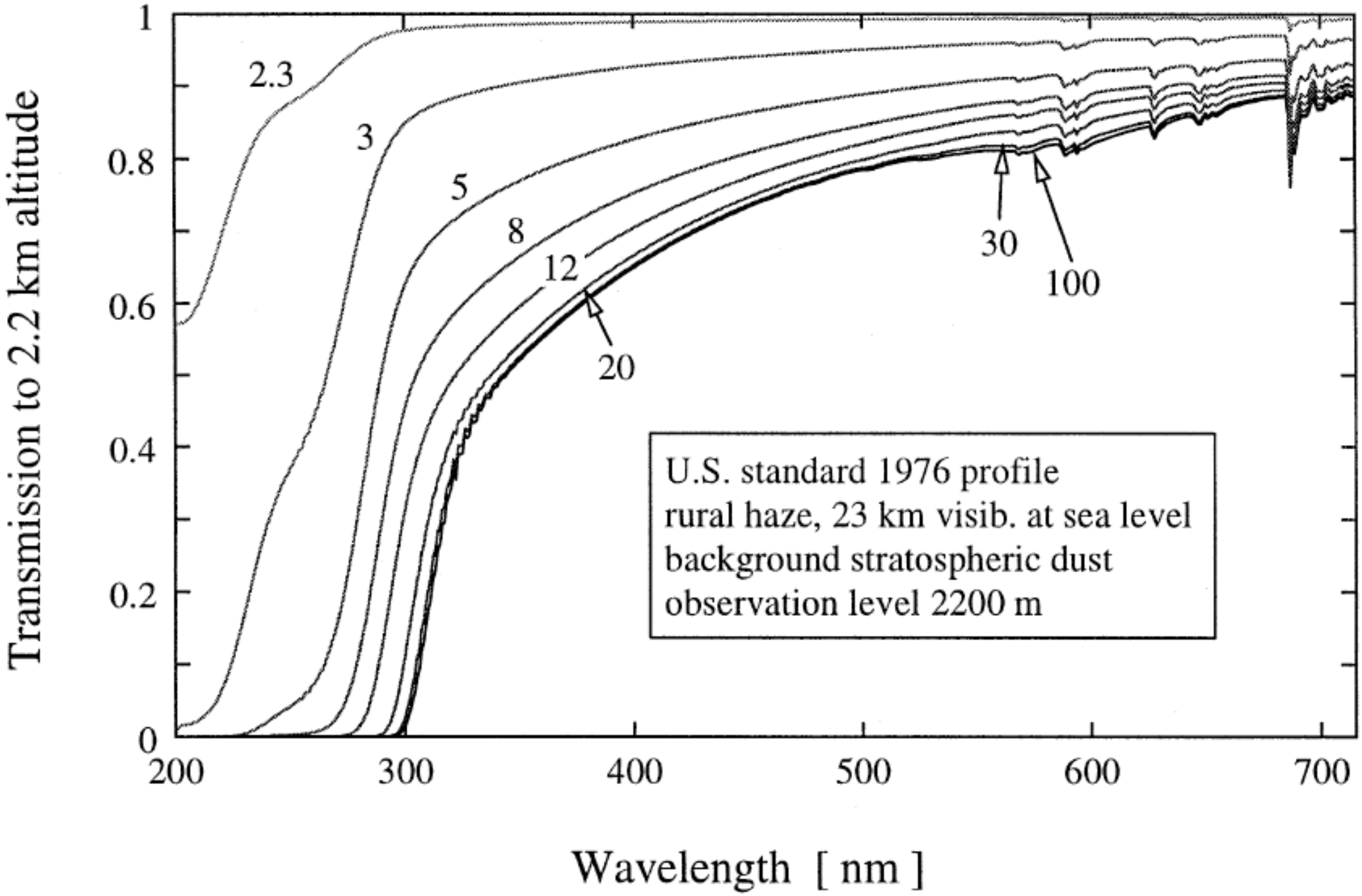

Cherenkov radiation: wavelength distribution

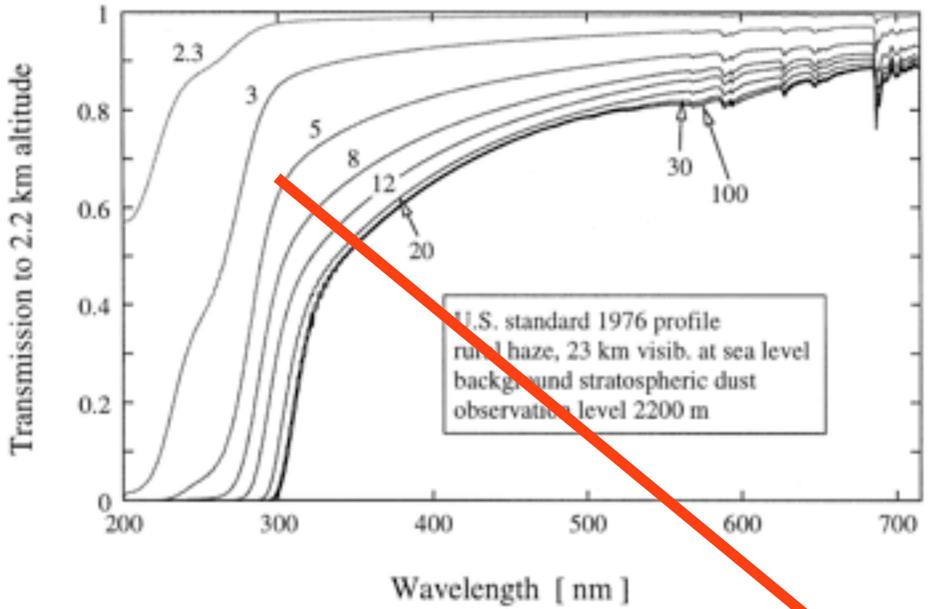

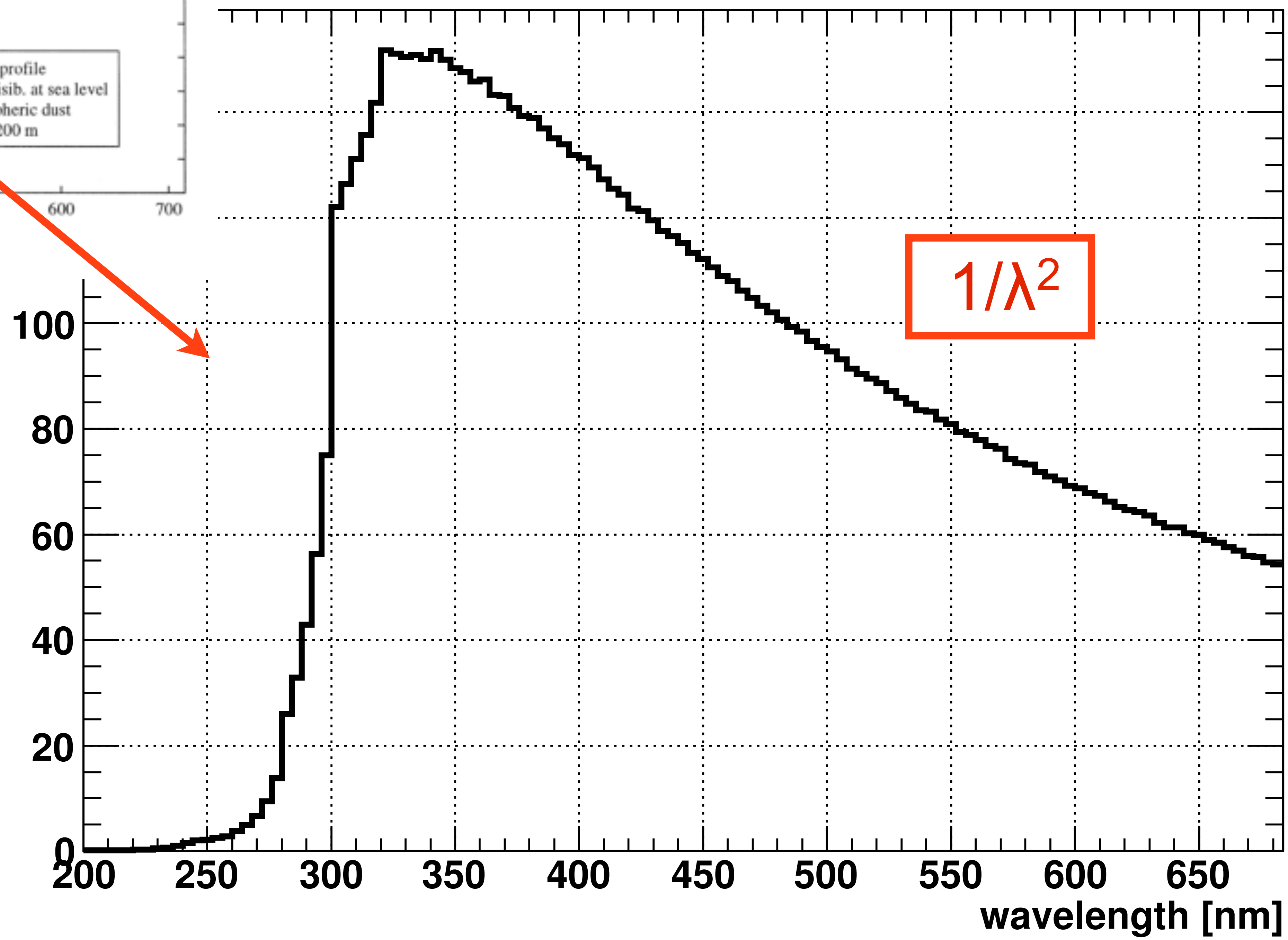

Telescopes

T.Weekes astro-ph/0811.1197

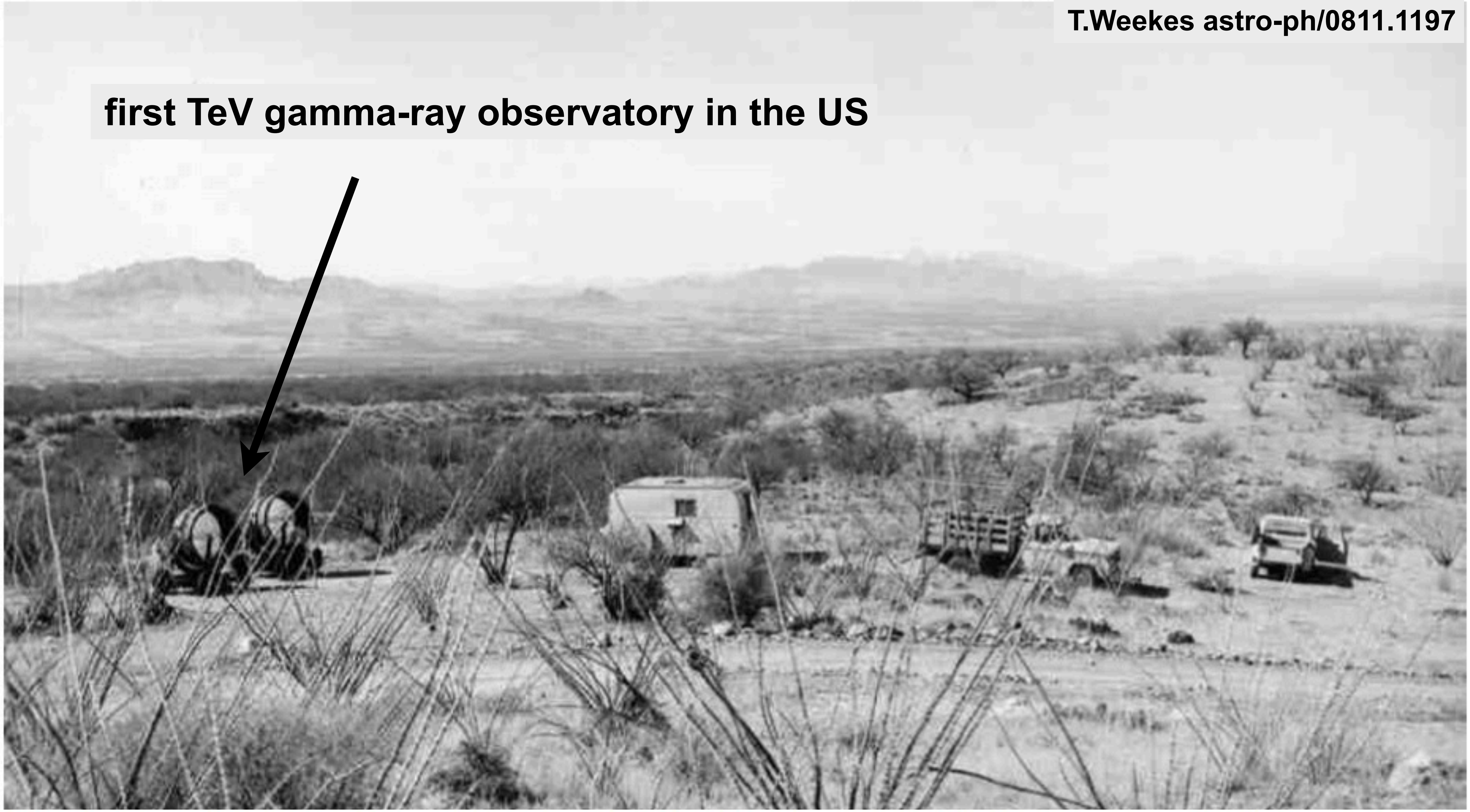

FIGURE 1. The first TeV gamma-ray observatory in the United States consisted of two 1.5m telescopes (made from World War II searchlight reflectors) above (left center); the telescopes were manually operated and were located at a dark site in southern Arizona during the winter of 1967-8 [10]. The telescopes were directed (by eye) at a point ahead of the position of the putative source so that the earth's rotation swept the source through the field of view. Power came from an electric generator on the back of the truck (center right) and the pulse counting electronics were housed in a small trailer (center). The system was mercifully free of computers and the analysis was done offline with a mechanical calculator. No sources were detected.

completed in 1968
upgrade with imaging camera proposed 1977
first detection (Crab Nebula) 1986

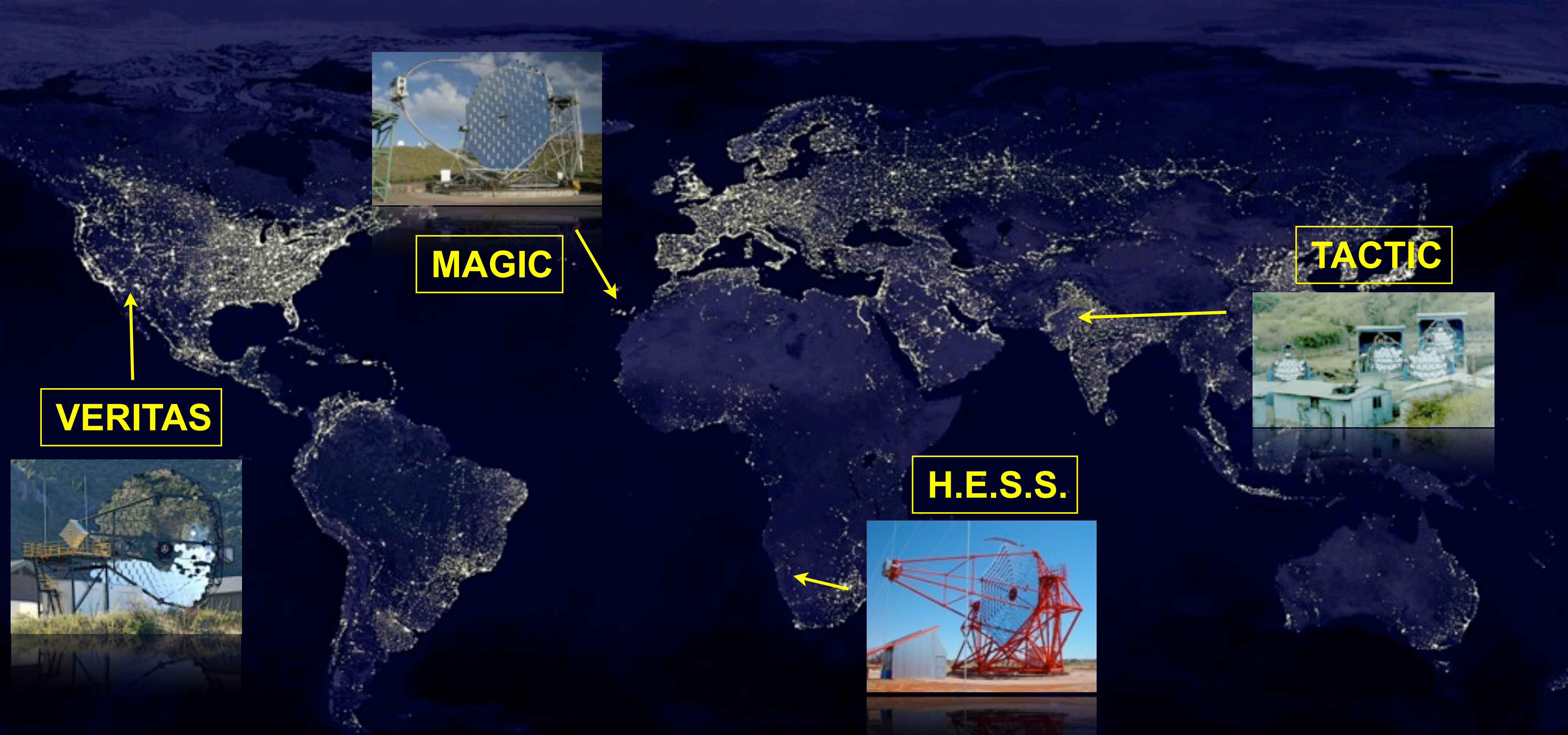

Observatory	Elevation (km)	Telescopes #	Mirror Area (m^2)	FoV (degrees)	First Light	Threshold (GeV)	Sensitivity (%Crab)
H.E.S.S.	1.8	4	428	5	2003	100	0.7
VERITAS	1.3	4	424	3.5	2007	100	1
MAGIC	2.2	1	236	3.5	2005	50	1.6
HAGAR	4.3	7	31	3	2008	60	9
Whipple	2.3	1	75	2.2	1985	400	10
CANGAROO III	0.1	3(4)	172 (230)	4	2006	400	10
PACT	1.1	24	107	3	2001	750	11
TACTIC	1.3	1	10	2.8	2001	1500	70
SHALON	3.3	1	11.2	8	1996	1000?	?

Davies-Cotton f/1.0-1.4 optics

12 m diameter reflector (110 m^2 mirror area)

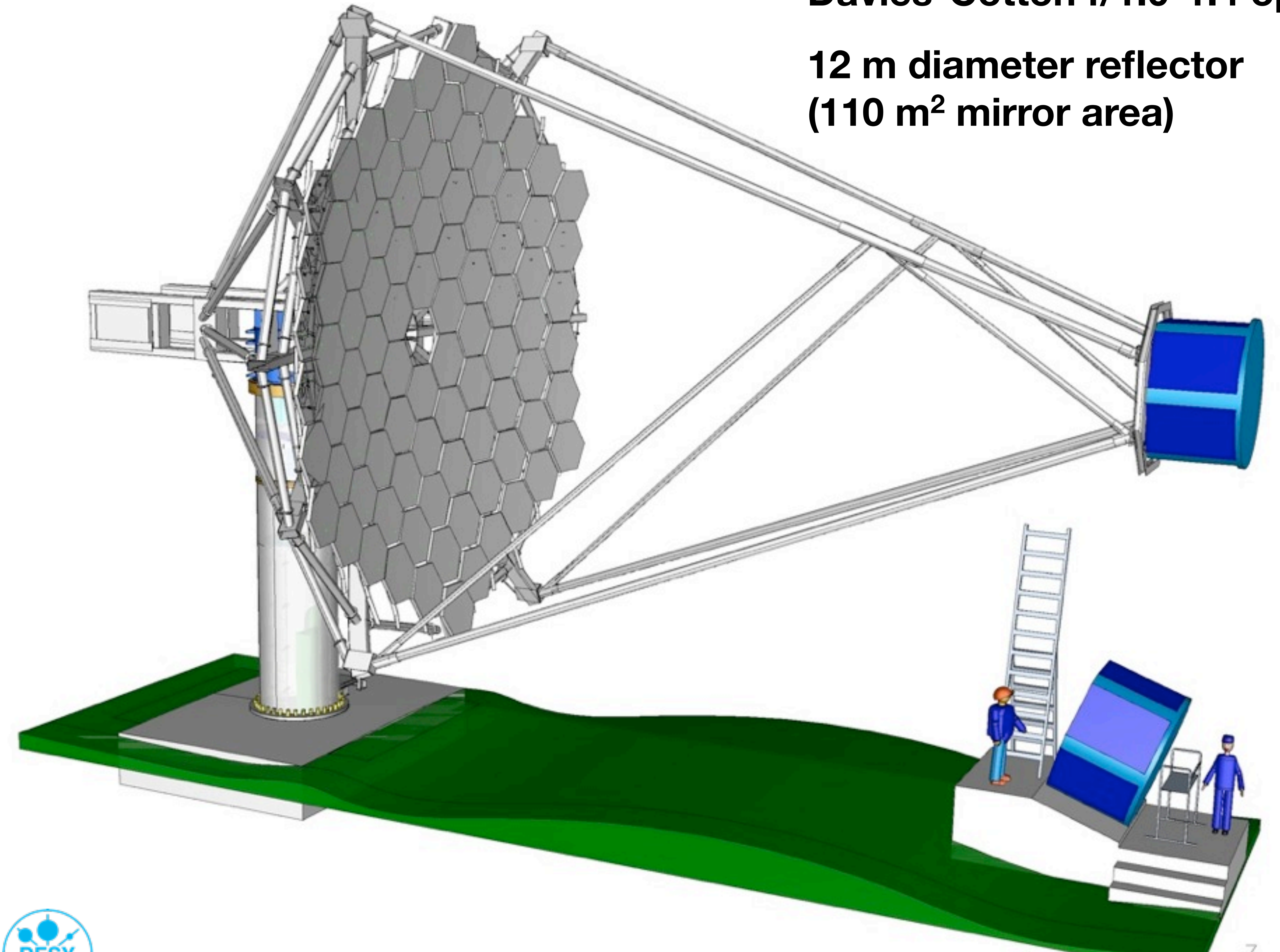

Imaging Atmospheric Cherenkov Telescopes

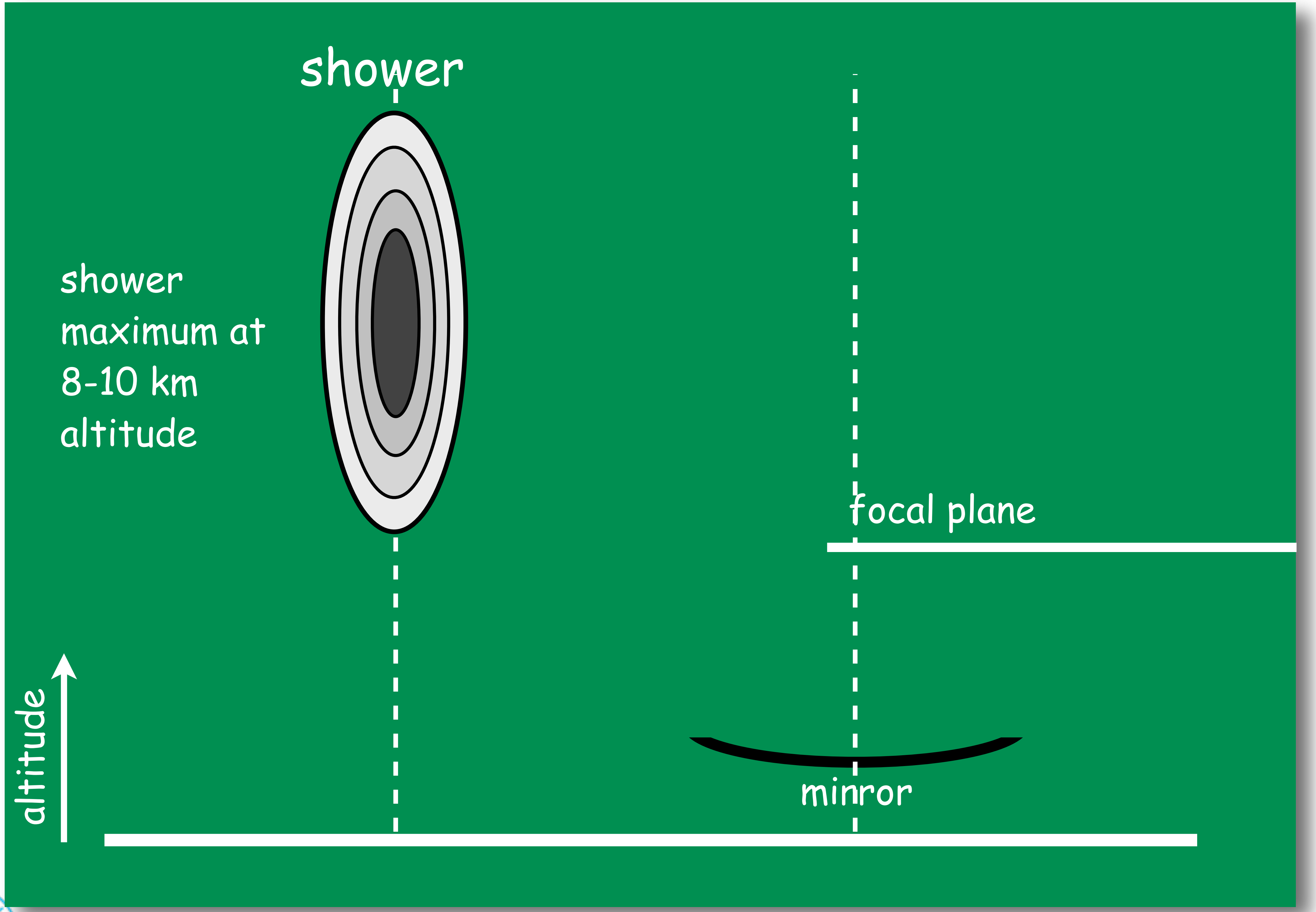

Imaging Atmospheric Cherenkov Telescopes

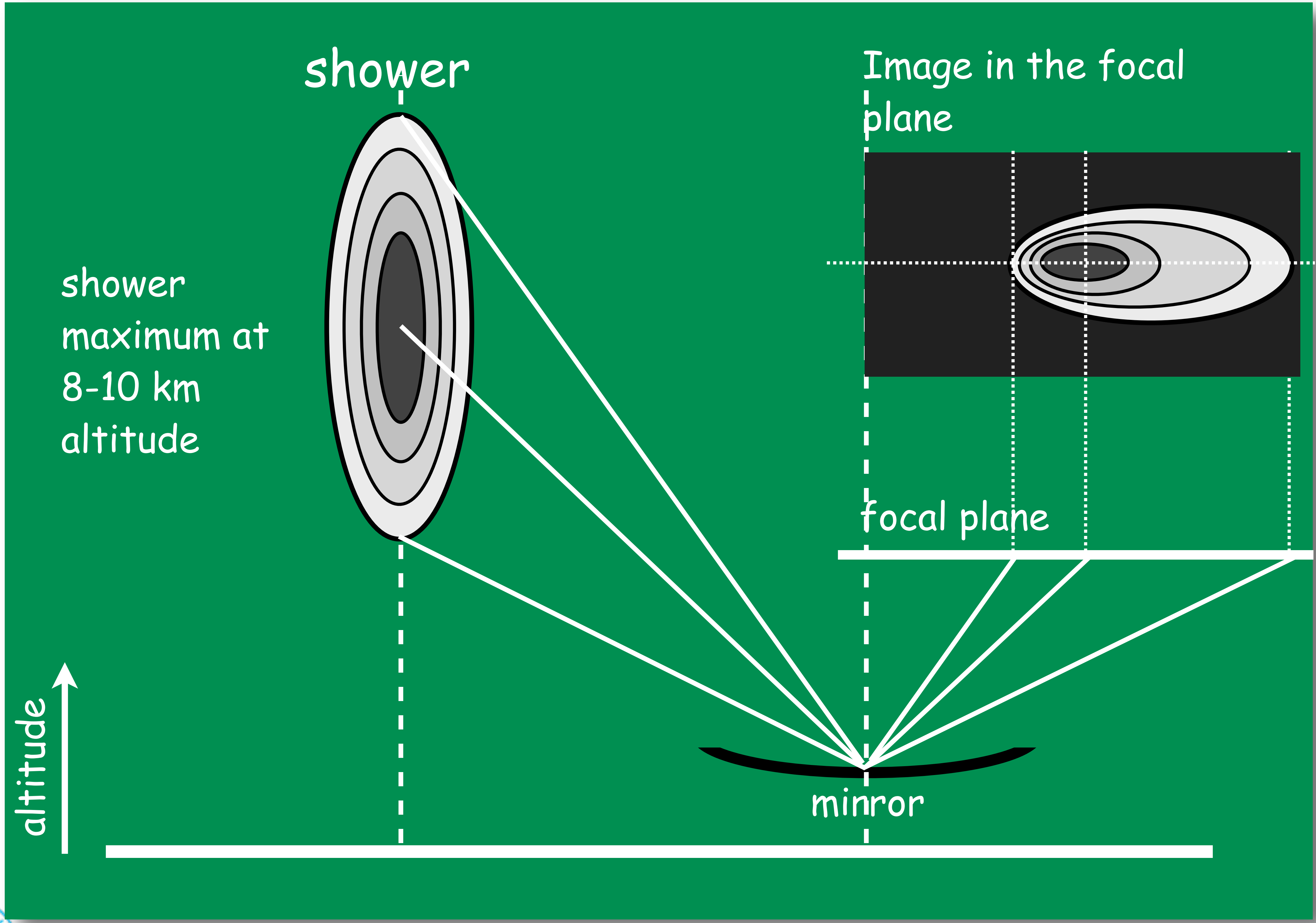

Camera, electronics and data acquisition

- 499 PMTs (Photonis XP 2970/02)
- 0.15° pixel separation, 3.5° field of view
- light concentrator
- 500 MSample/s flash ADC (2 ns)
- 8 bit dynamic range (dual range)
- typical data rate 6 Mbyte/s per telescope
- dead time for typical array rate of 300 Hz is 8-10%

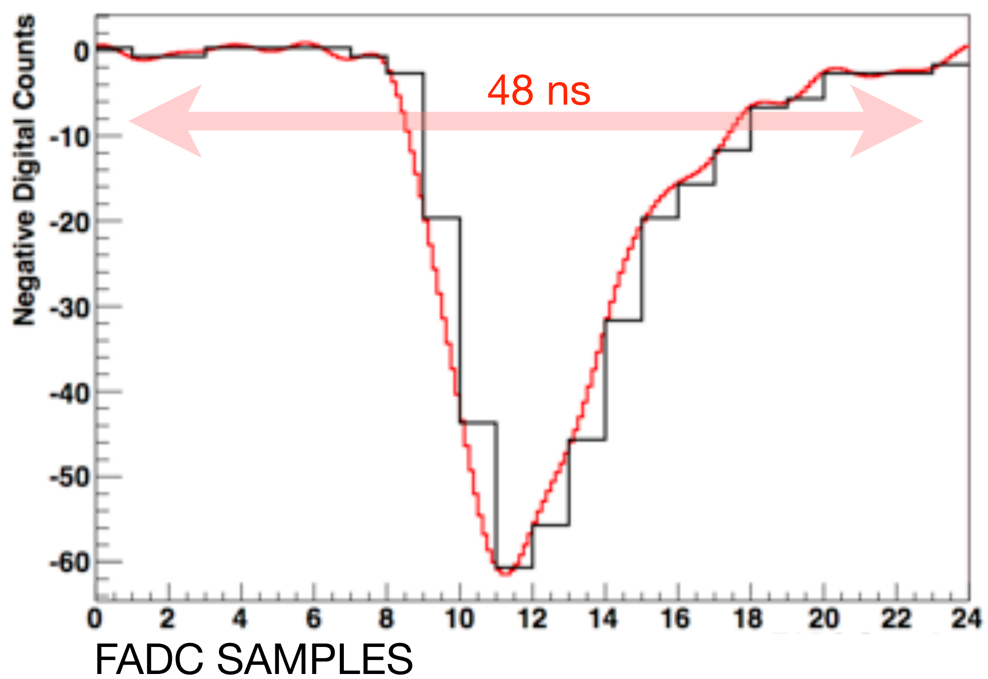

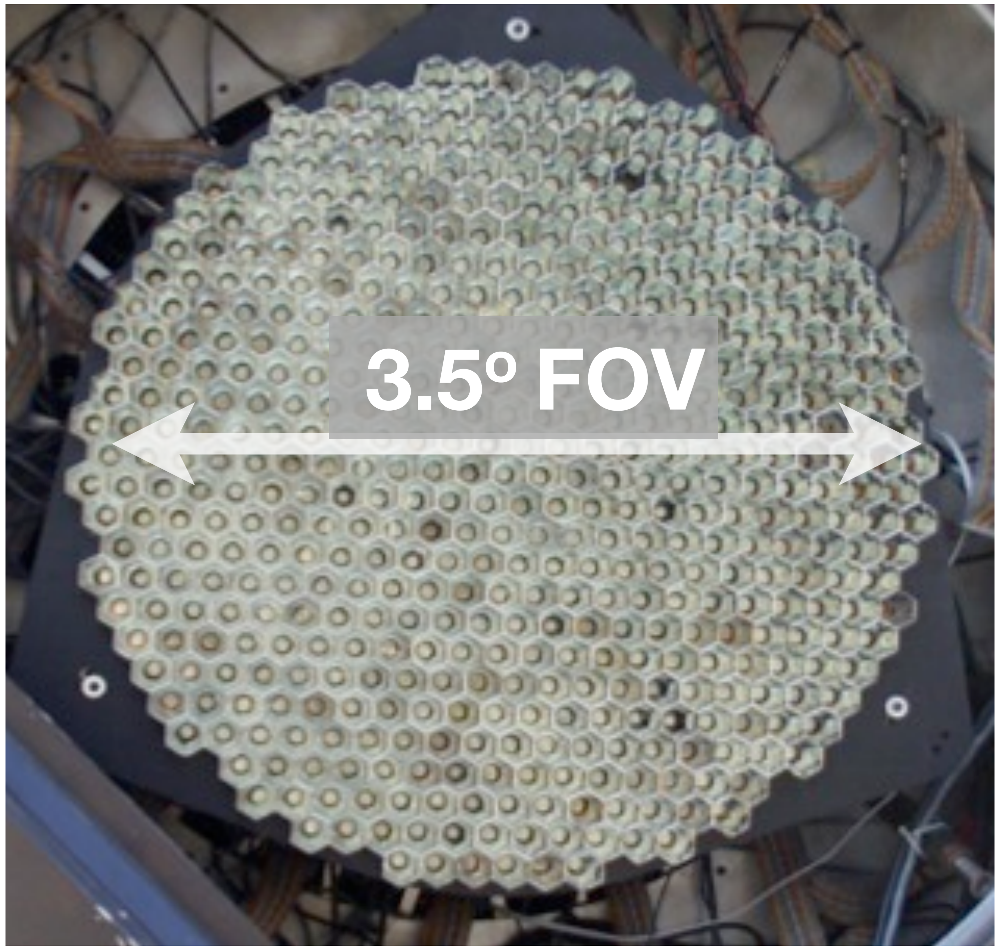

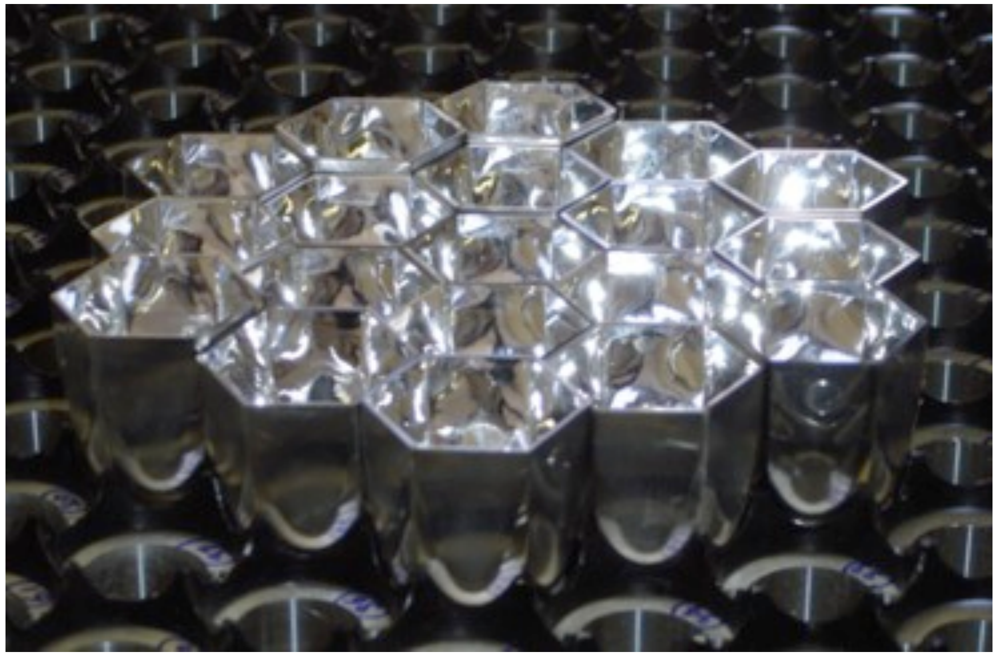

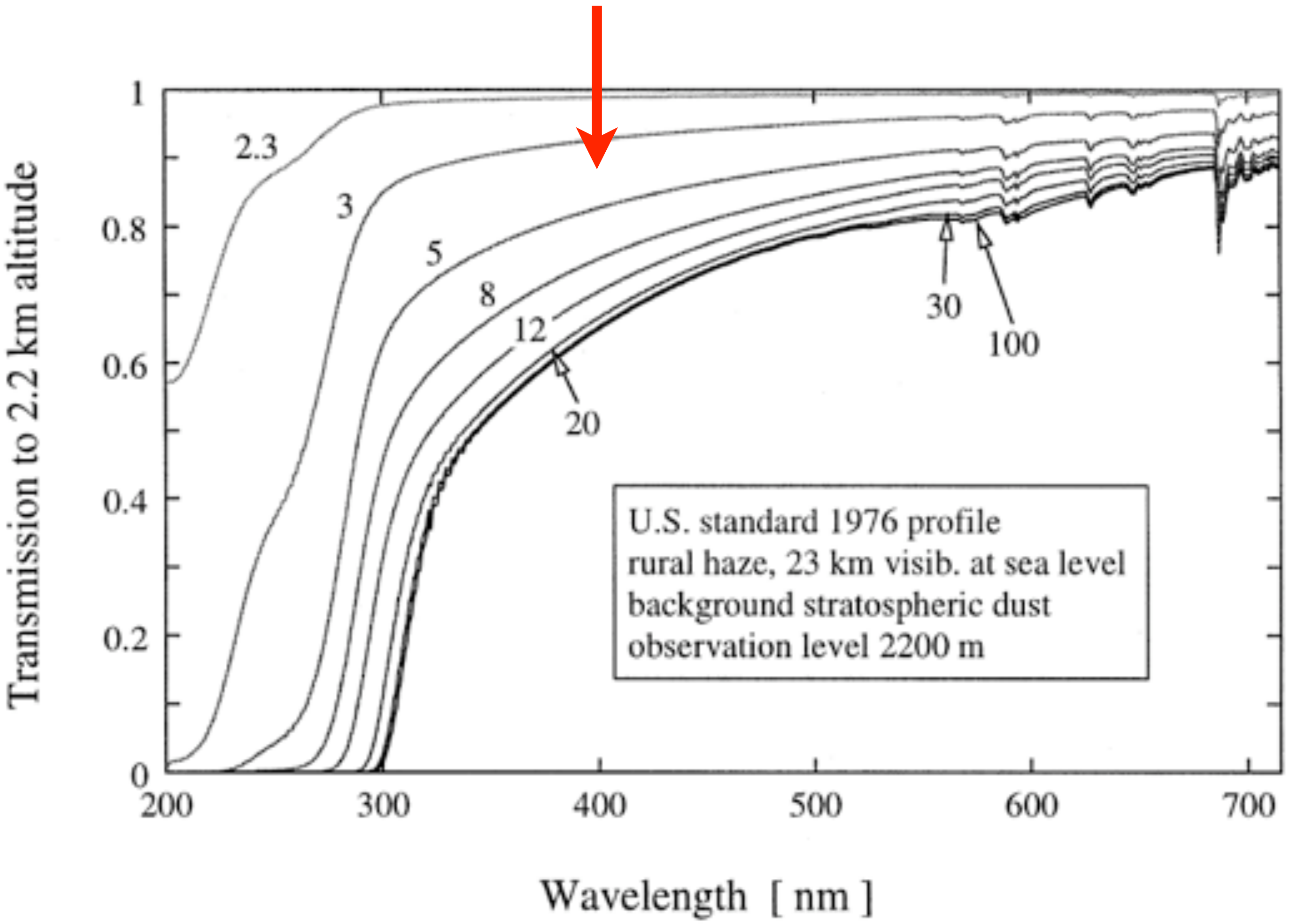

atmospheric extinction

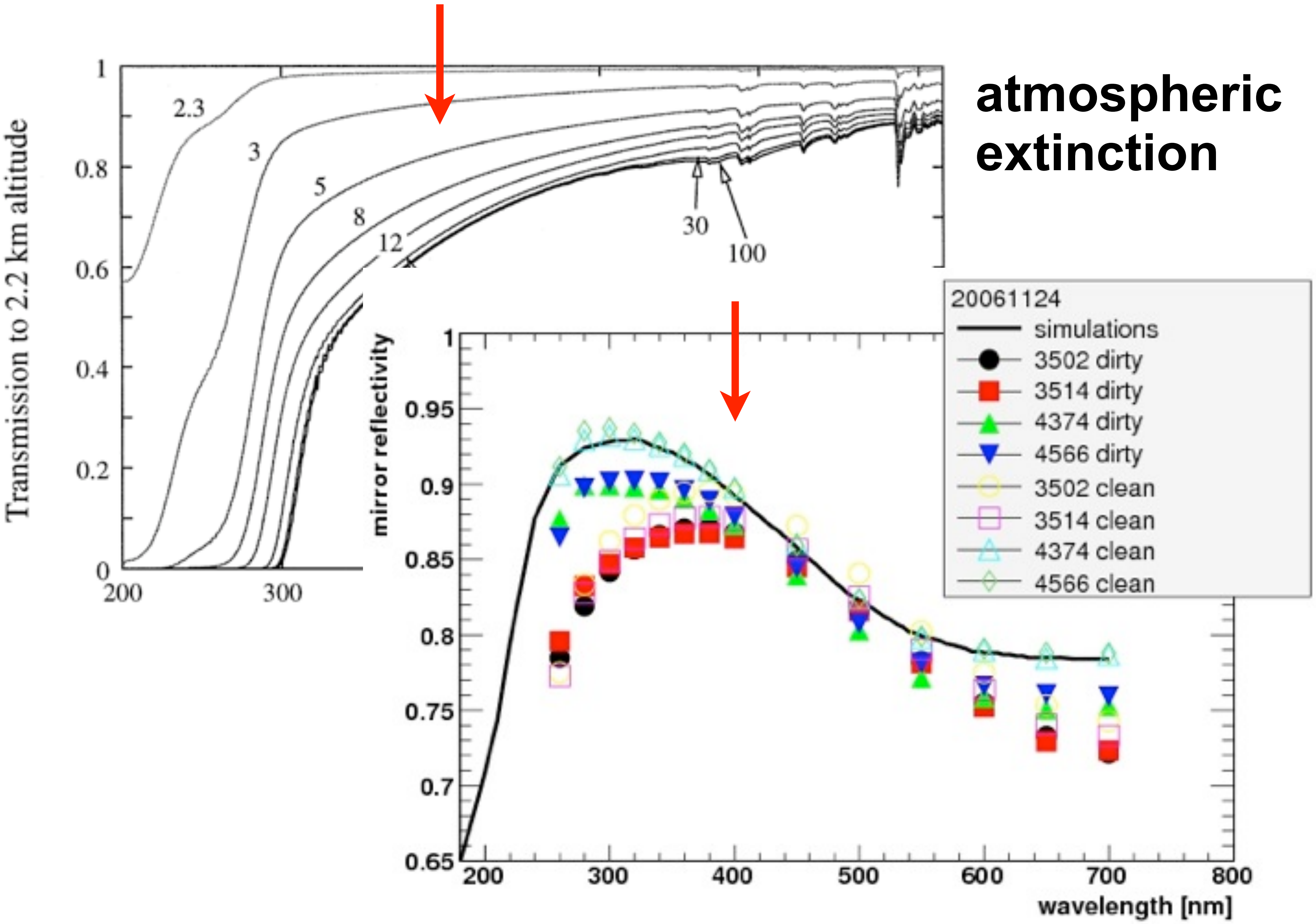

atmospheric extinction

mirror reflectivity

atmospheric extinction

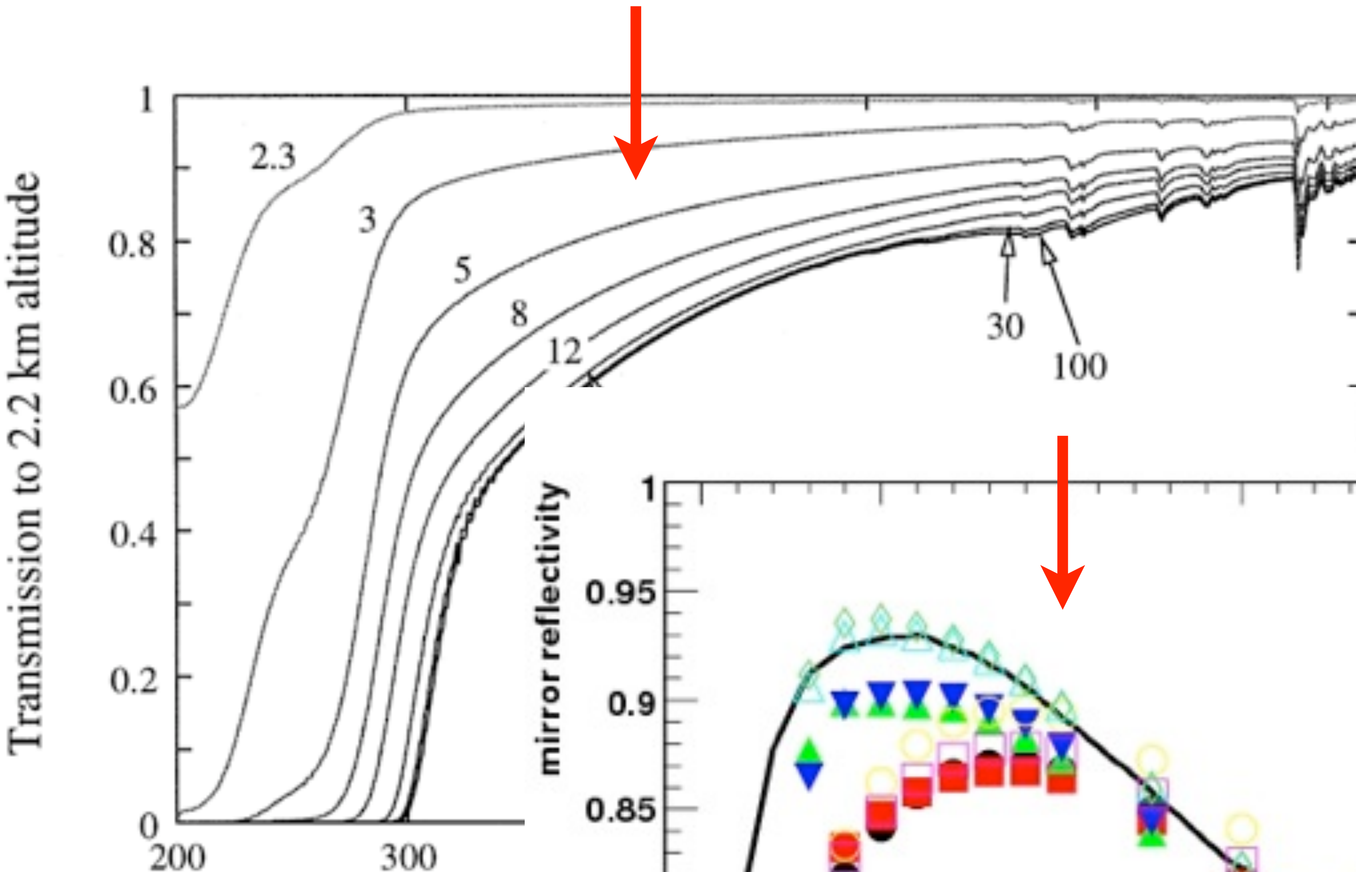

mirror reflectivity

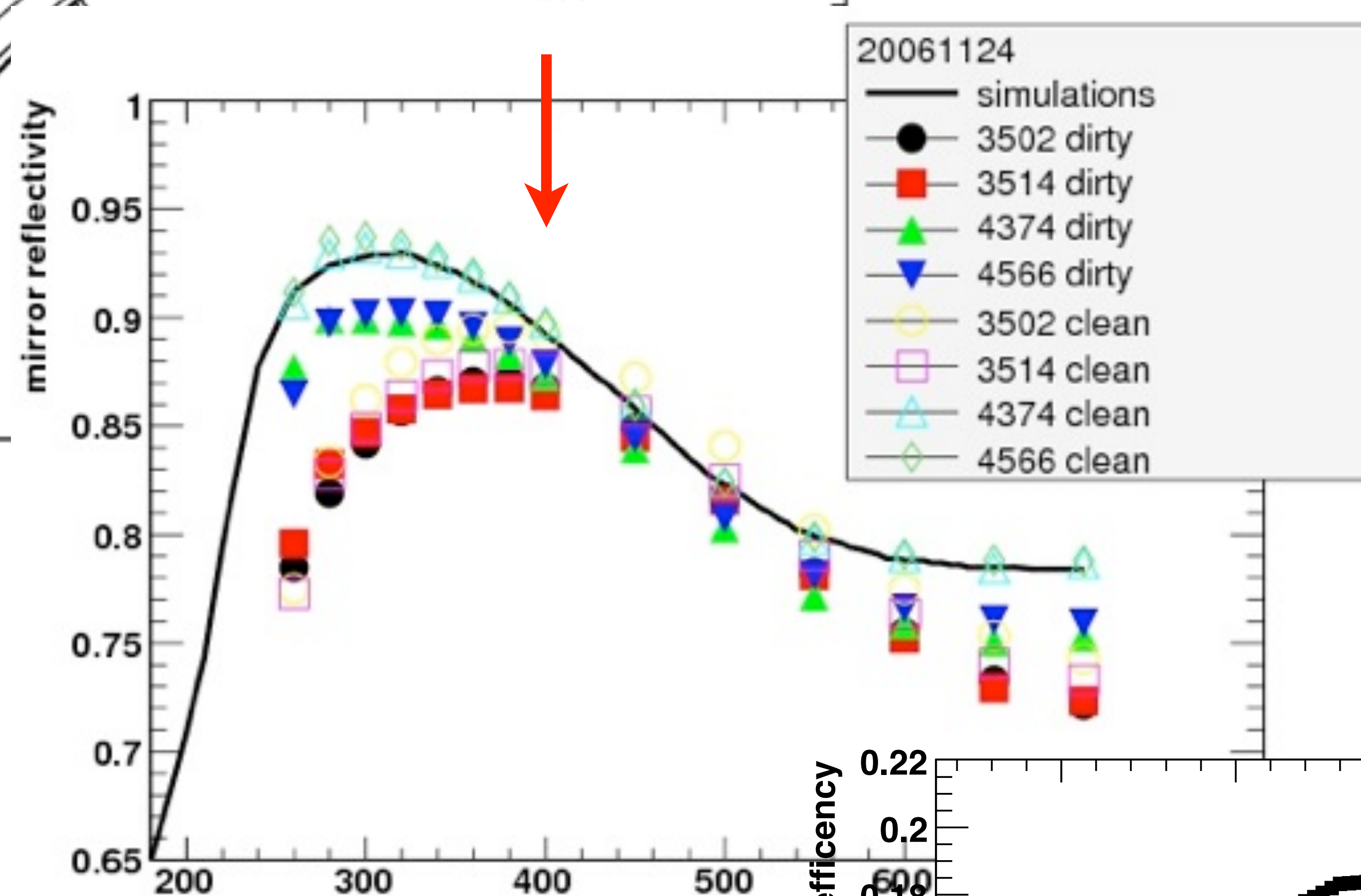

quantum efficiency

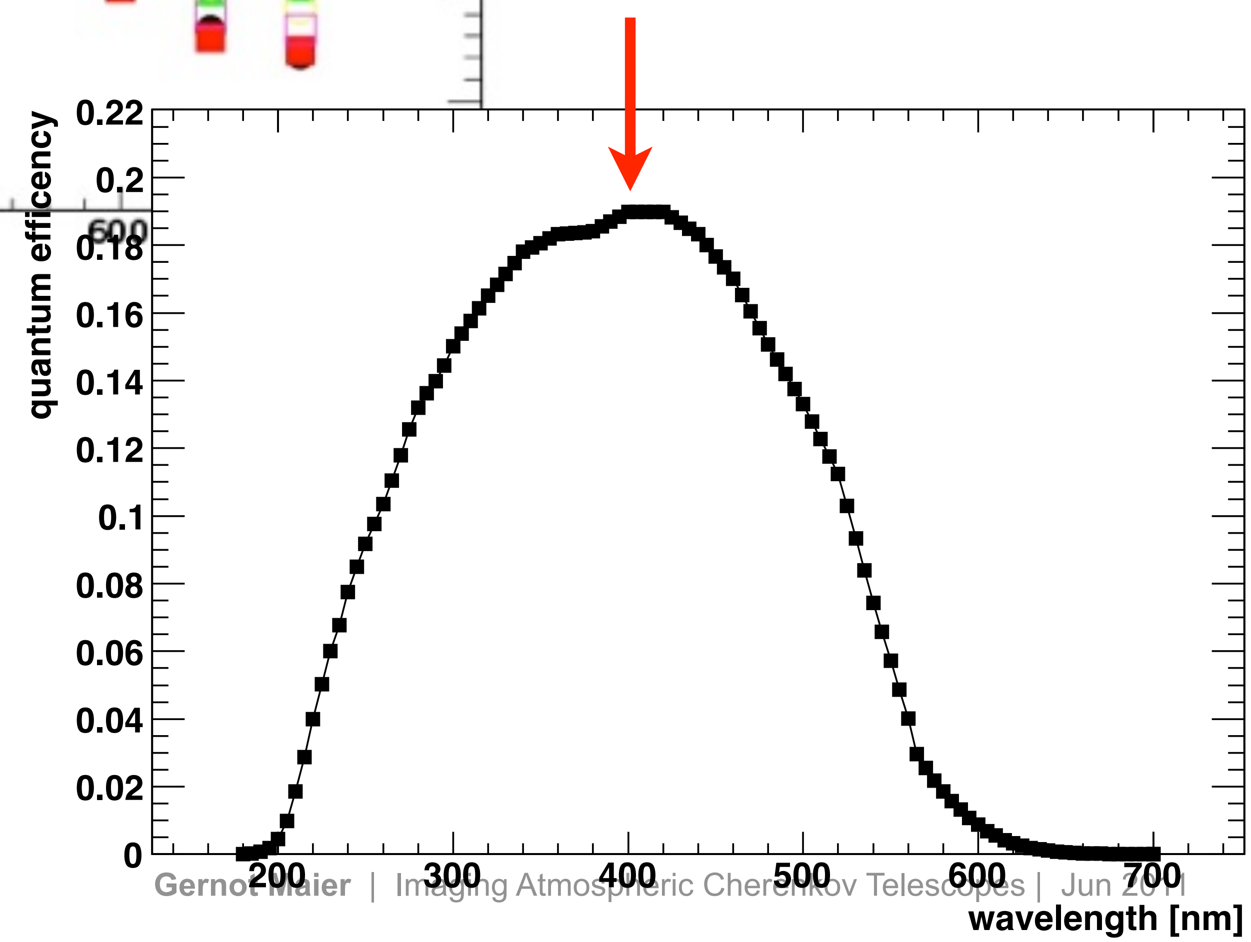

Background....

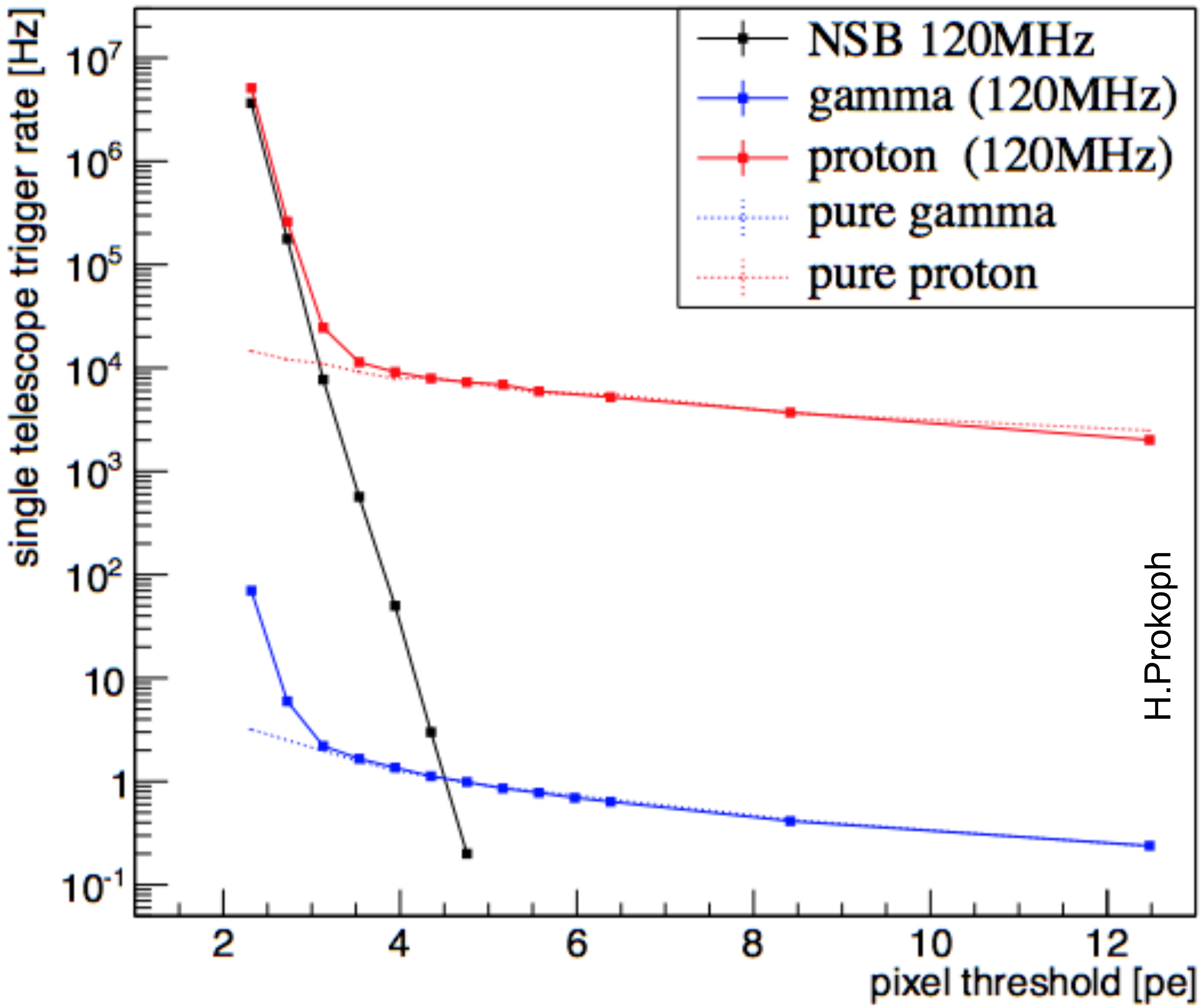

(for a mid-size CTA telescope)

Level 1 (Pixel) Trigger:

Constant fraction discriminators with rate feedback
(typical threshold at 50 mV or ~4-5 photoelectrons)

Level 2 (Pattern) Trigger:

Recognize patterns of trigger pixel in the camera
(default is three adjacent pixels in a time window of 6 ns)

Level 3 (Array) Trigger:

Telescope coincidence trigger
(i.e. in a time window of ~100 ns)

Tracking

slew speed in the order of 1 (VERITAS) - 5 (MAGIC) deg/s

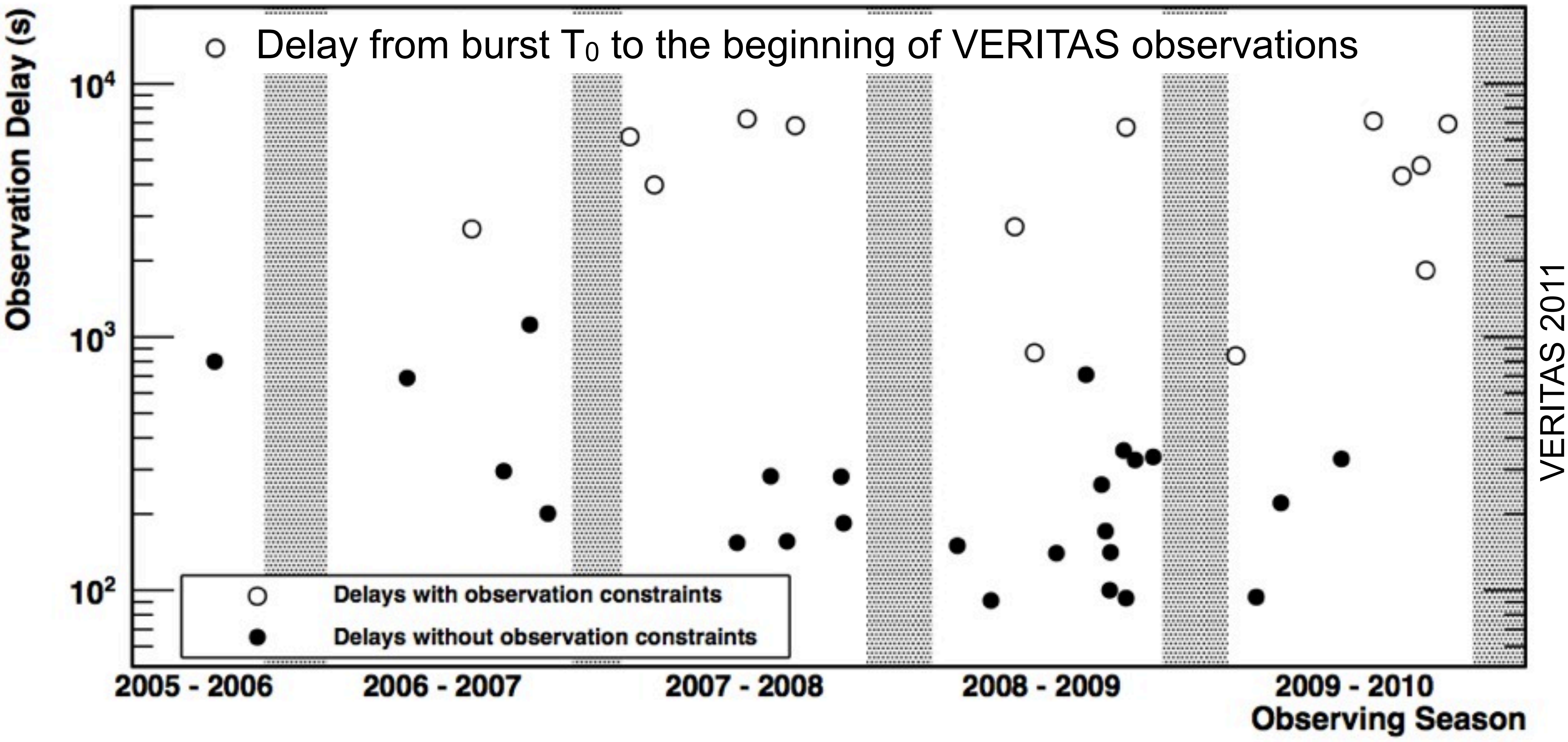

Field of View

Vela Supernova Remnant

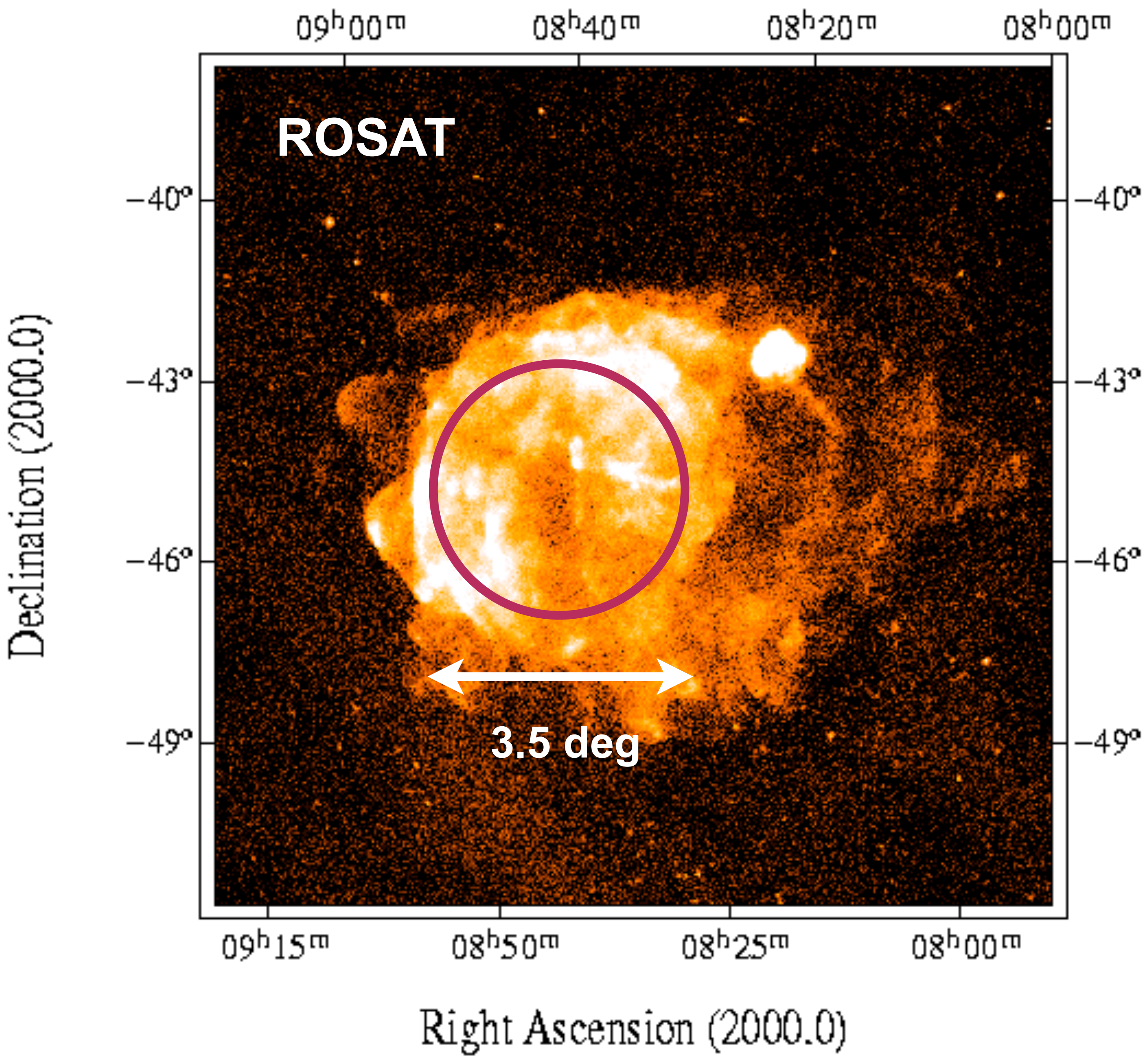

GRB 091123

```
//////////////////////////////////////////////////////
TITLE:           GCN/FERMI NOTICE
NOTICE_DATE:     Mon 23 Nov 09 01:56:15 UT
NOTICE_TYPE:     Fermi-GBM Flight Position
RECORD_NUM:      47
TRIGGER_NUM:     280634161
GRB_RA:          338.883d {+22h 35m 32s} (J20
                 339.007d {+22h 36m 02s} (cur
                 338.257d {+22h 33m 02s} (195
GRB_DEC:          +7.850d {+07d 50' 60"} (J20
                  +7.901d {+07d 54' 05"} (cur
                  +7.591d {+07d 35' 27"} (195
GRB_ERROR:       13.70 [deg radius, statistic
GRB_INTEN:       137 [cnts/sec]
DATA_SIGNIF:     [illegible] [sigma]
INTEG_TIME:      2.048 [sec]
GRB_DATE:        15158 TJD;    327 DOY;    09/1
```

Visibility

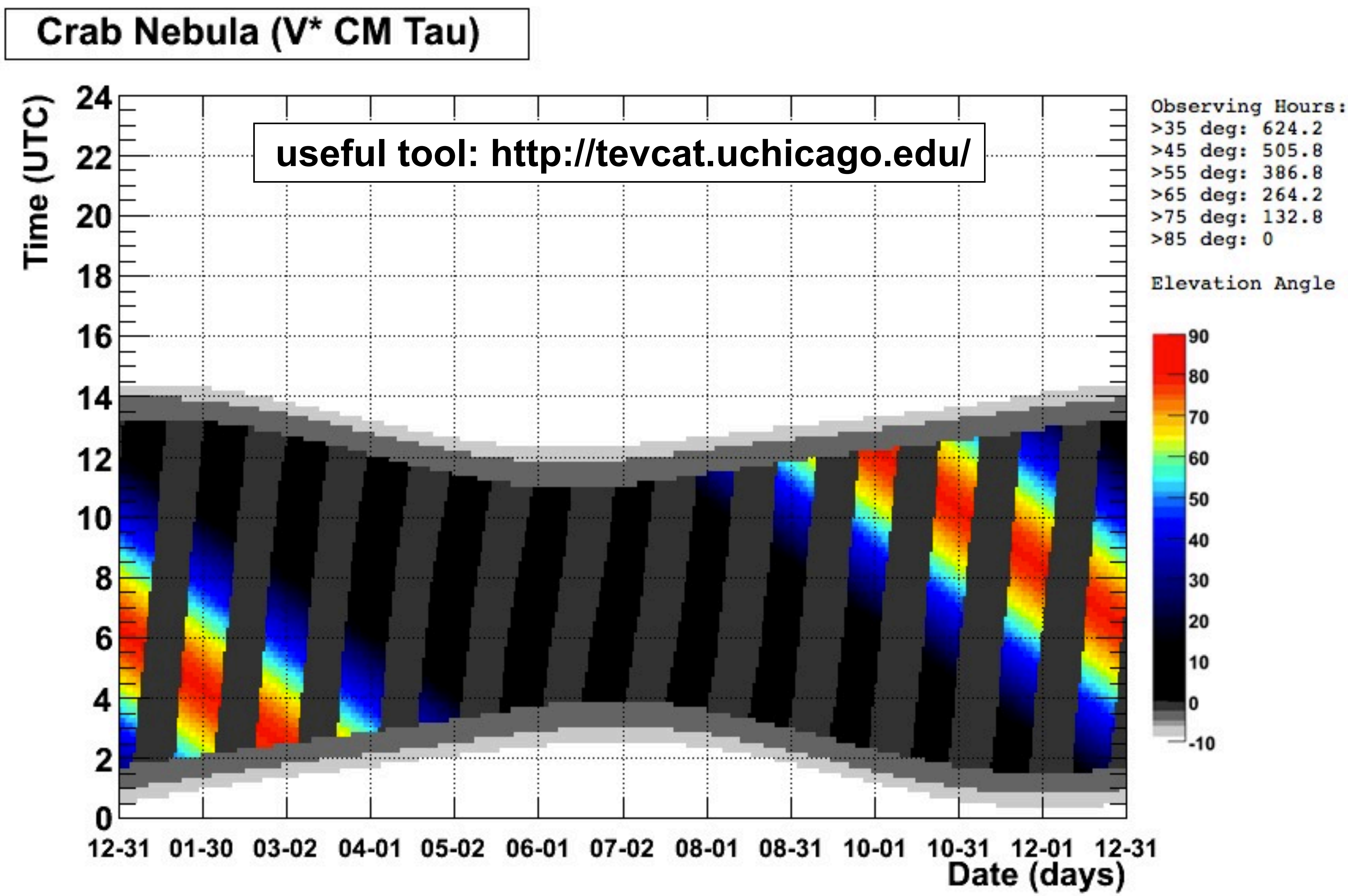

Plotted Crab Nebula (V* CM Tau) RA,Dec = (83.6331,22.0145) for year 2011 at lat,lon = 31.68,-110.86

Observational Constrains

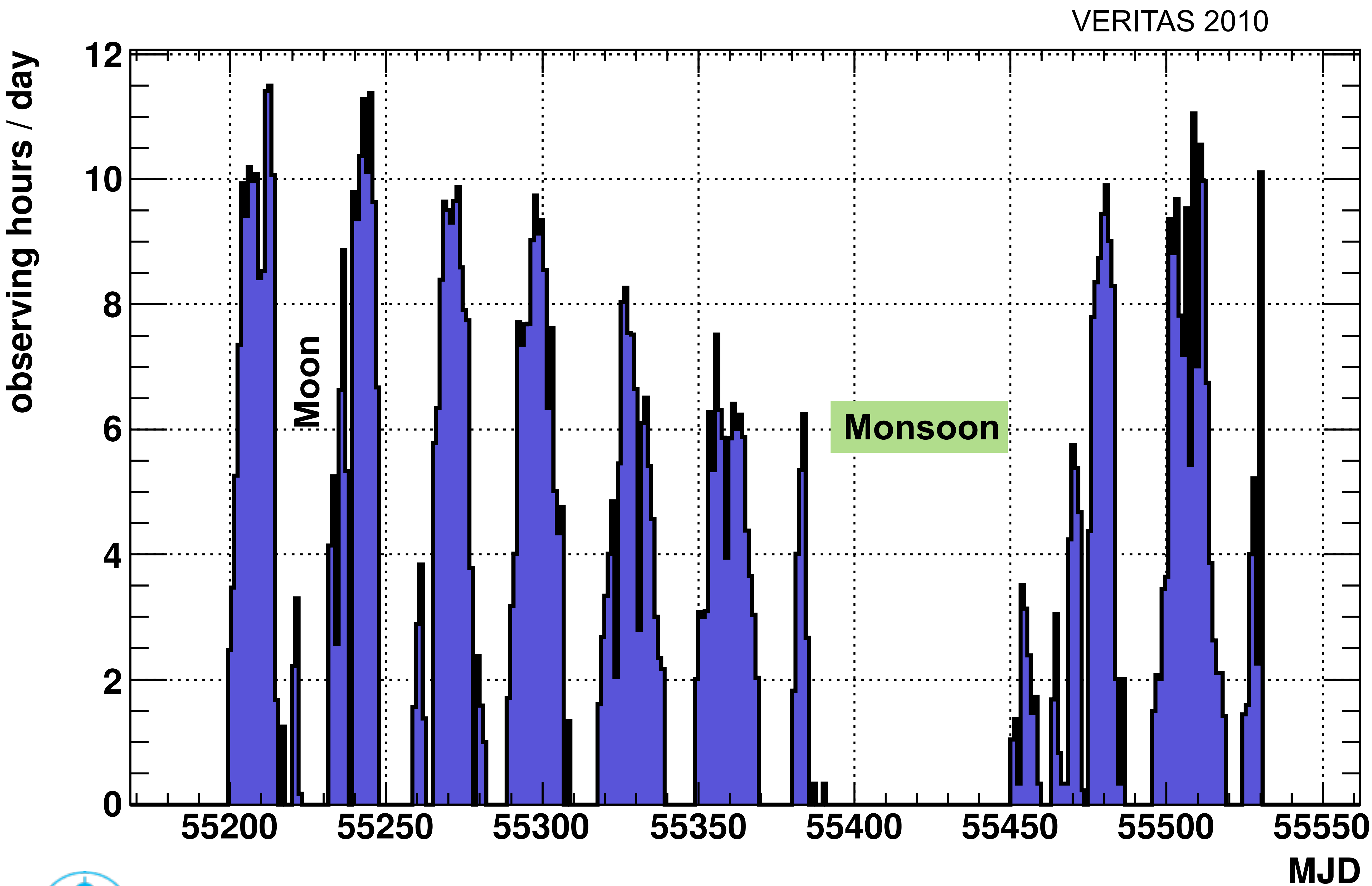

Sky Coverage - 1 day

typical field of view: 3.5 - 5 deg

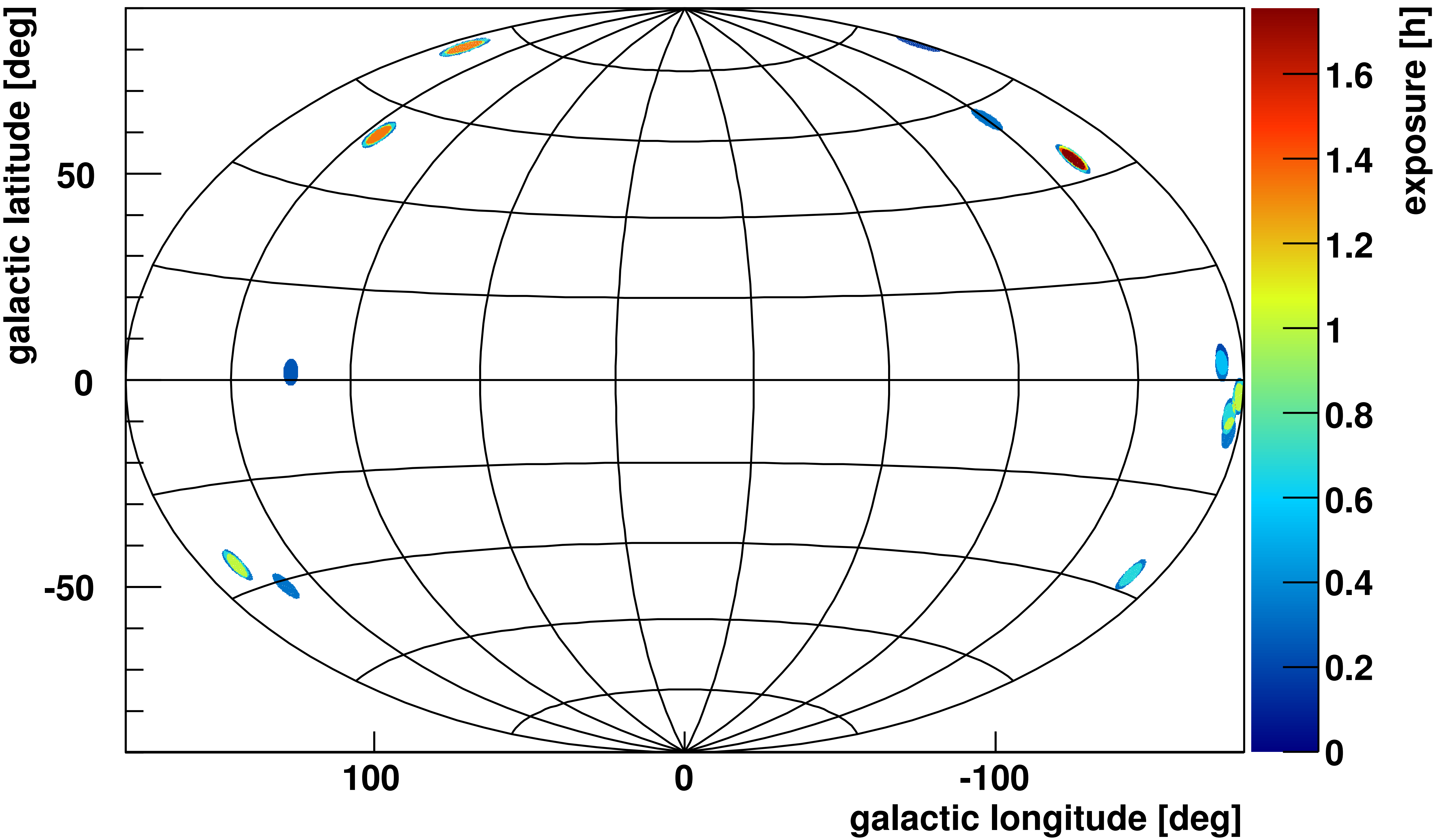

Sky Coverage - 1 day

typical field of view: 3.5 - 5 deg

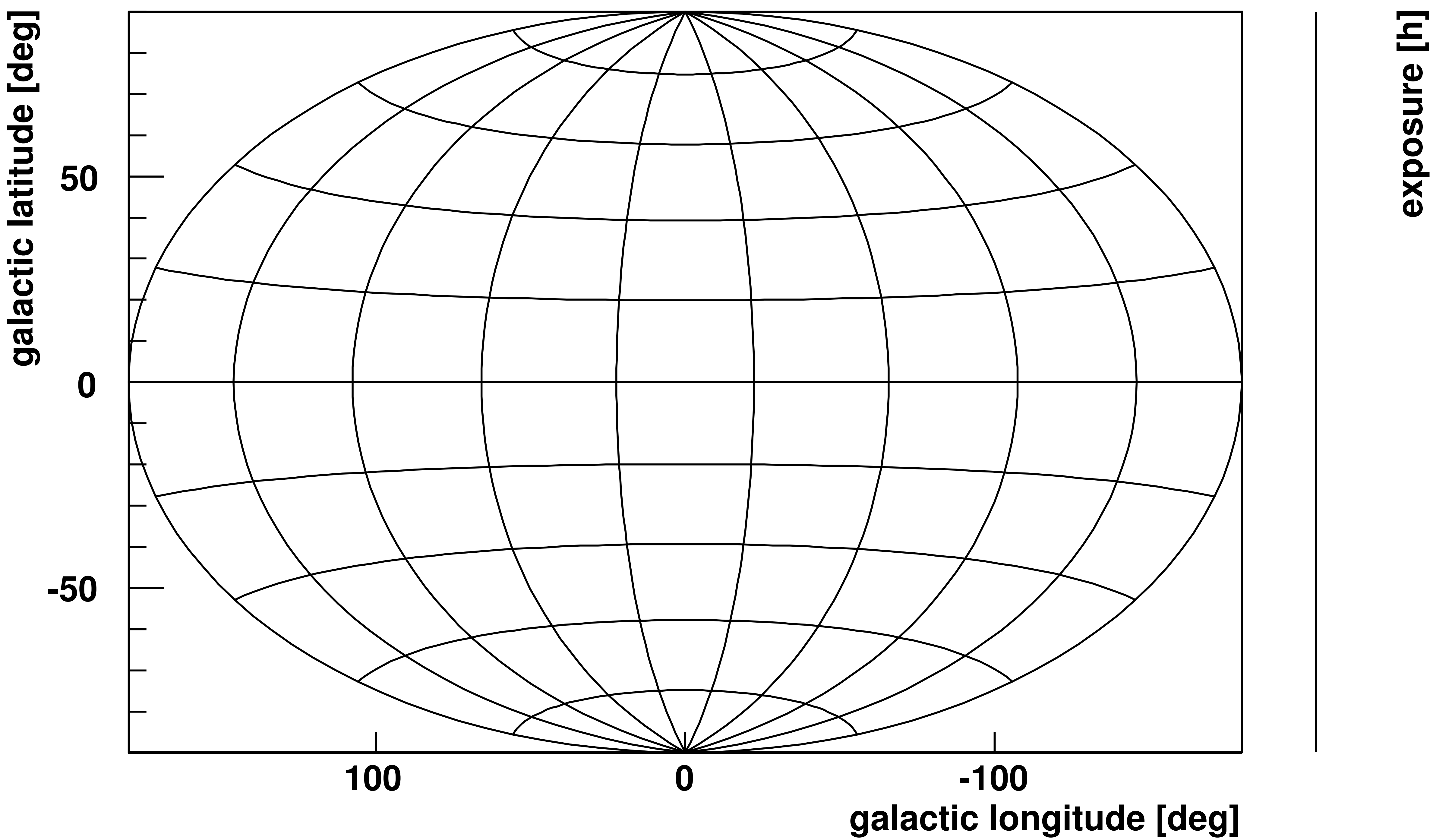

Sky Coverage - 1 week

typical field of view: 3.5 - 5 deg

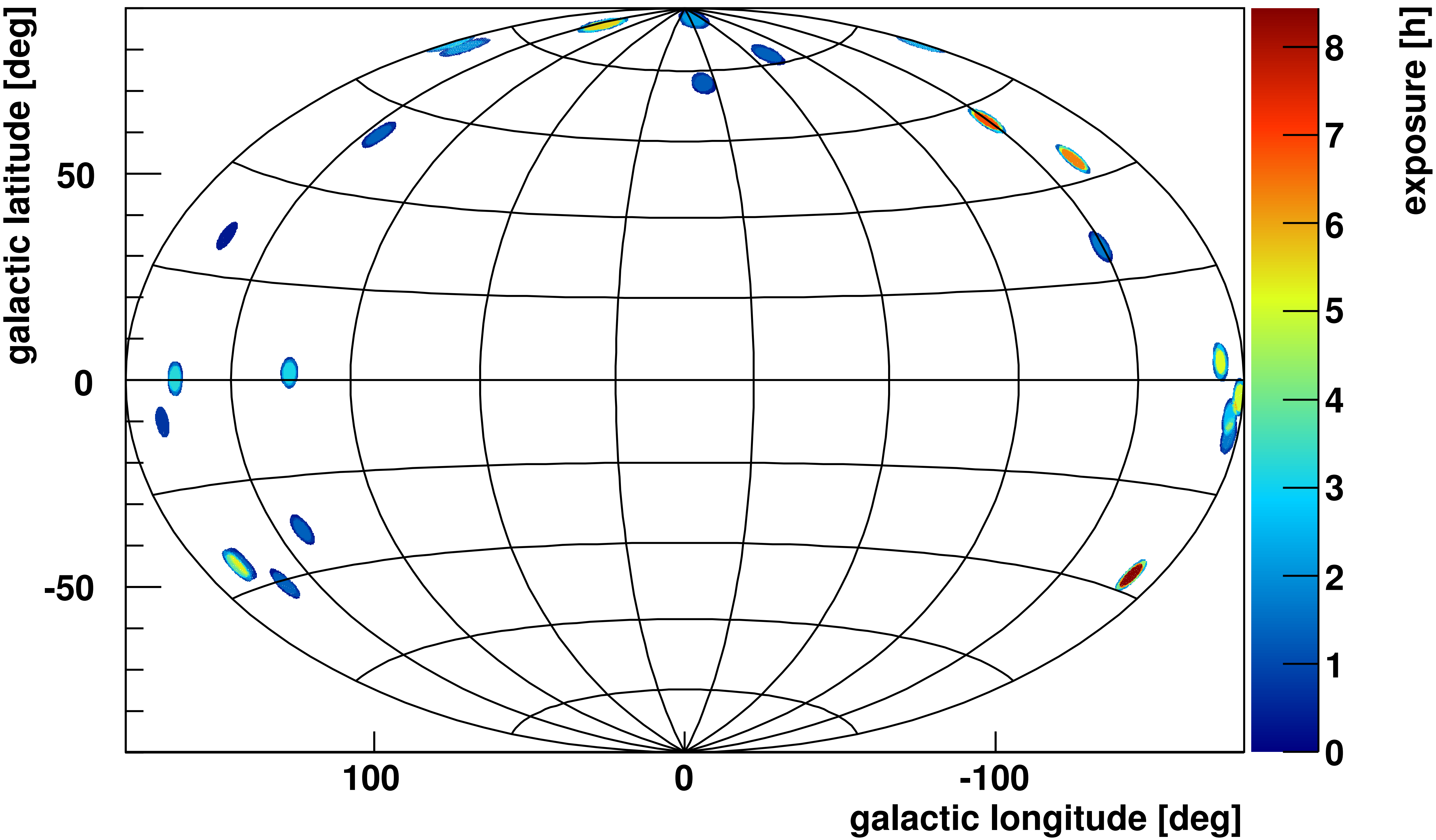

DESY

Sky Coverage - 1 month

typical field of view: 3.5 - 5 deg

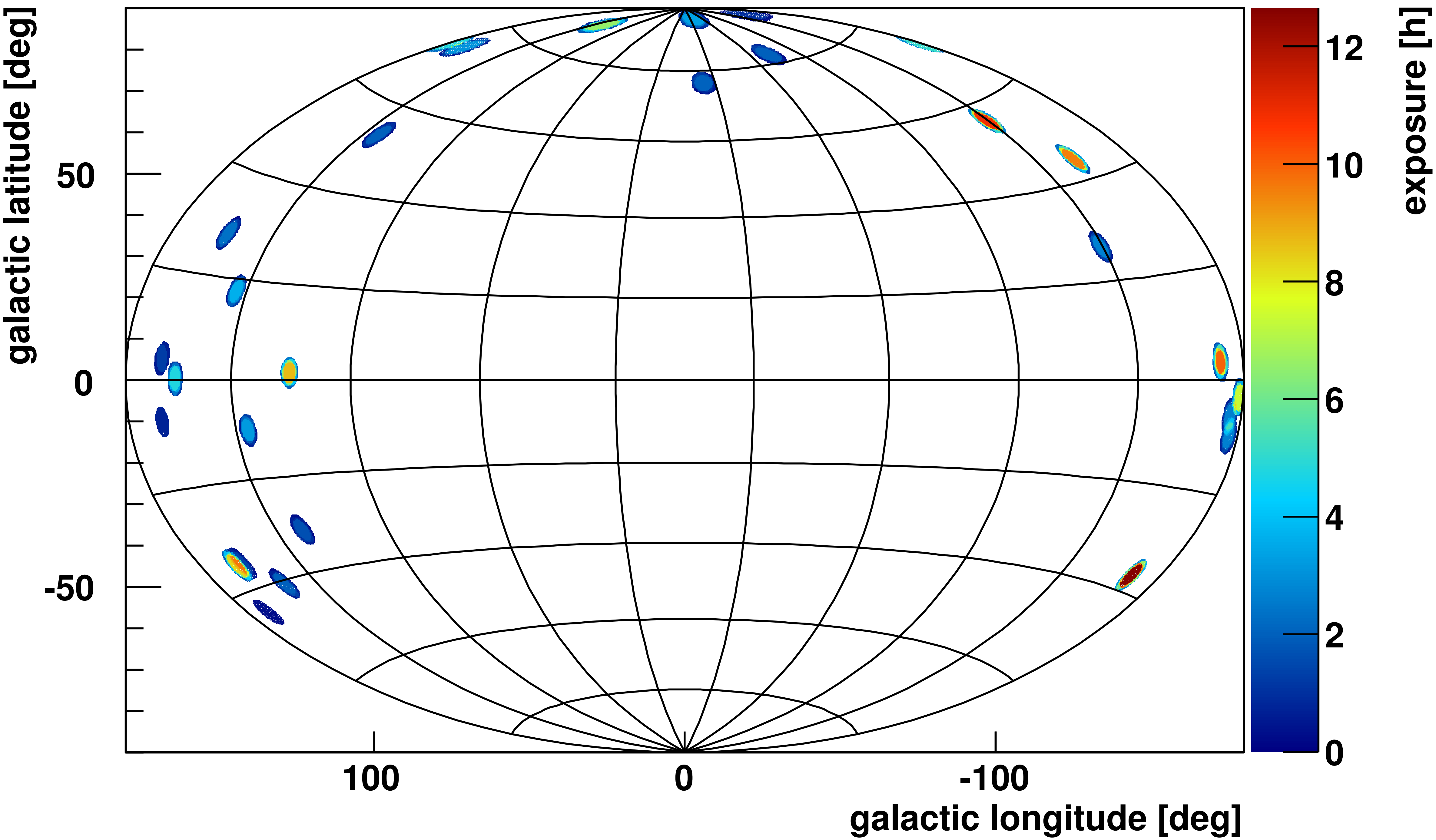

Sky Coverage - 1 year

typical field of view: 3.5 - 5 deg

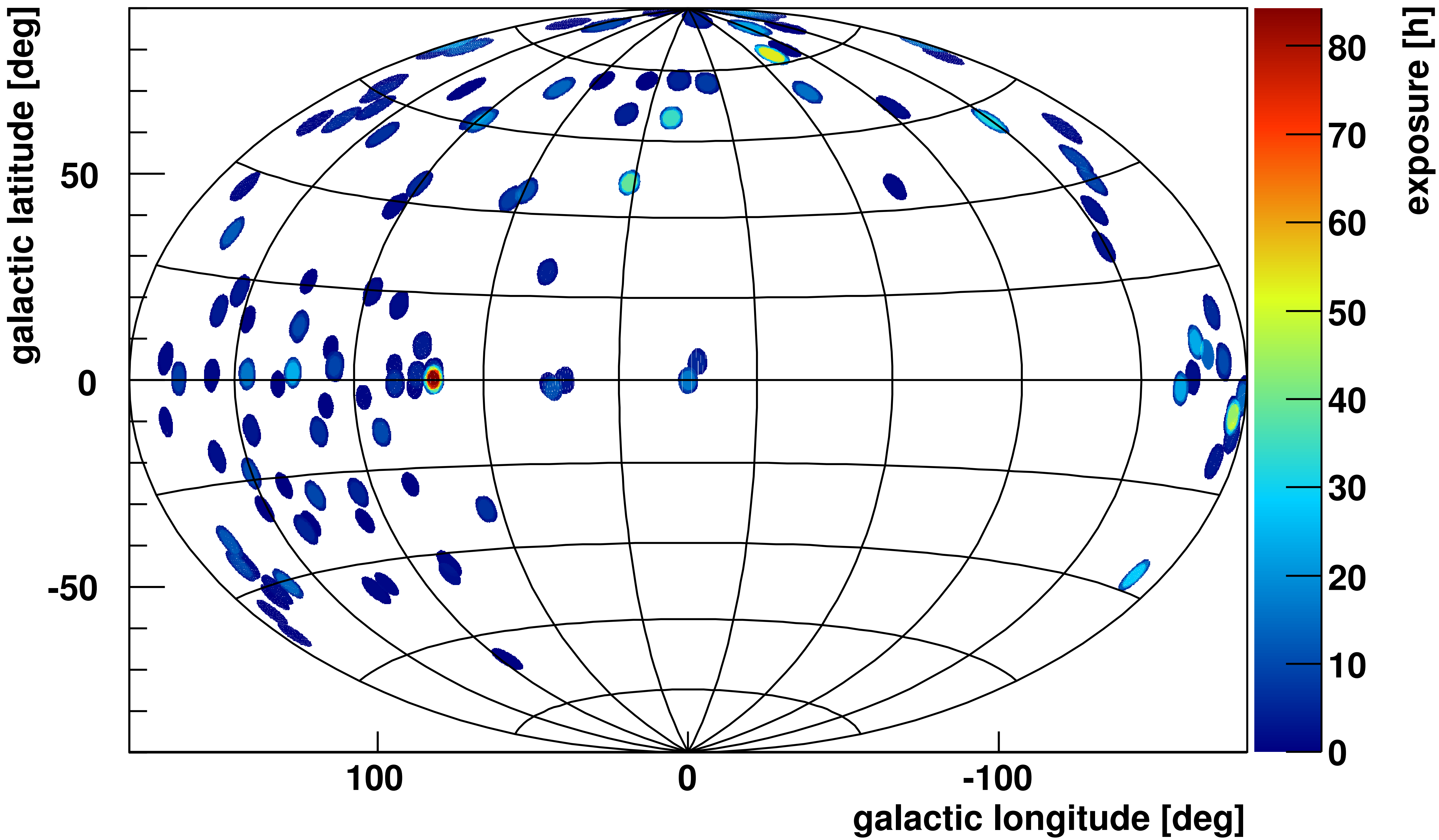

Sky Coverage - 1 year

typical field of view: 3.5 - 5 deg

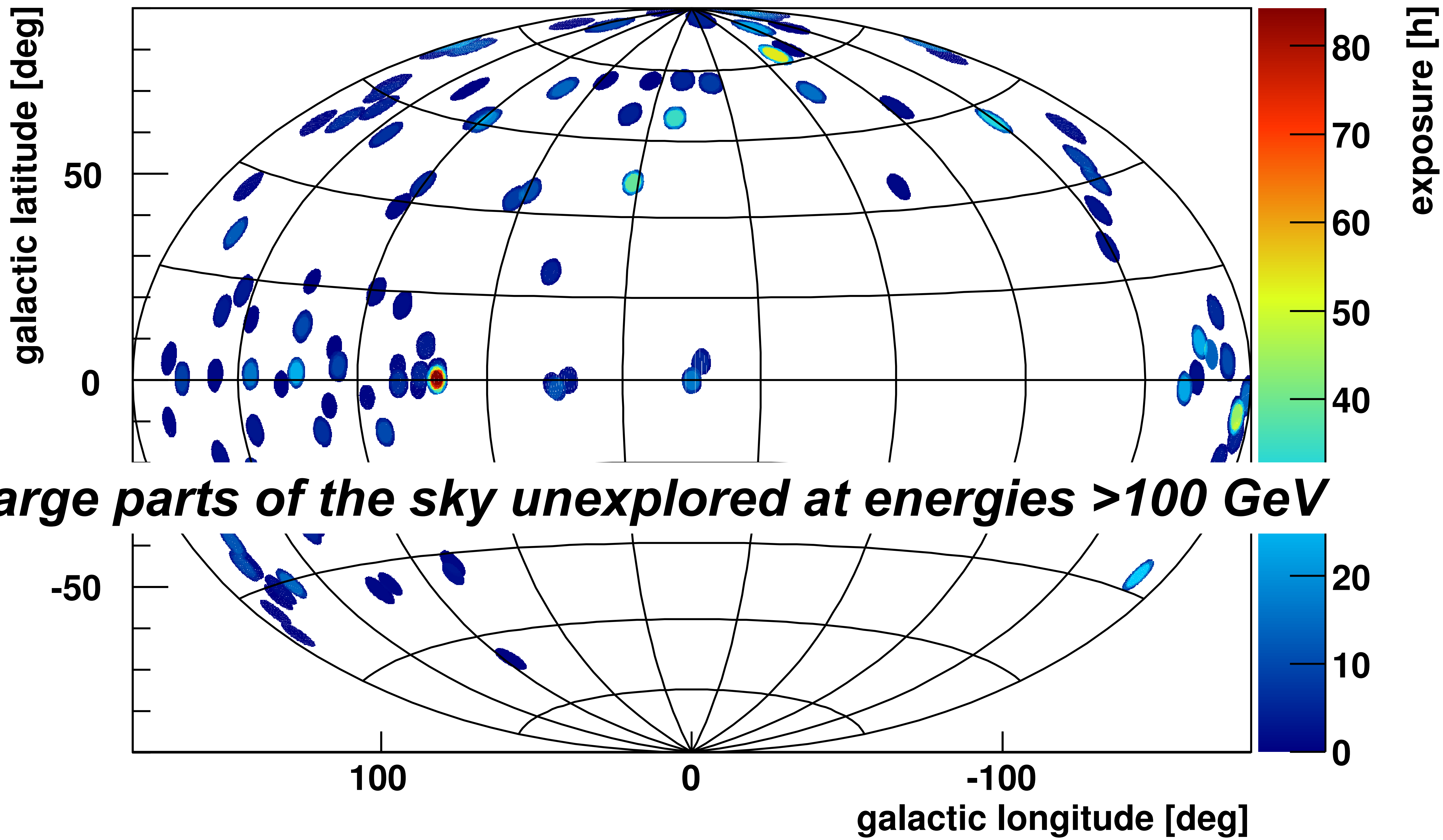

large parts of the sky unexplored at energies >100 GeV

IACT Analysis

IACT Analysis

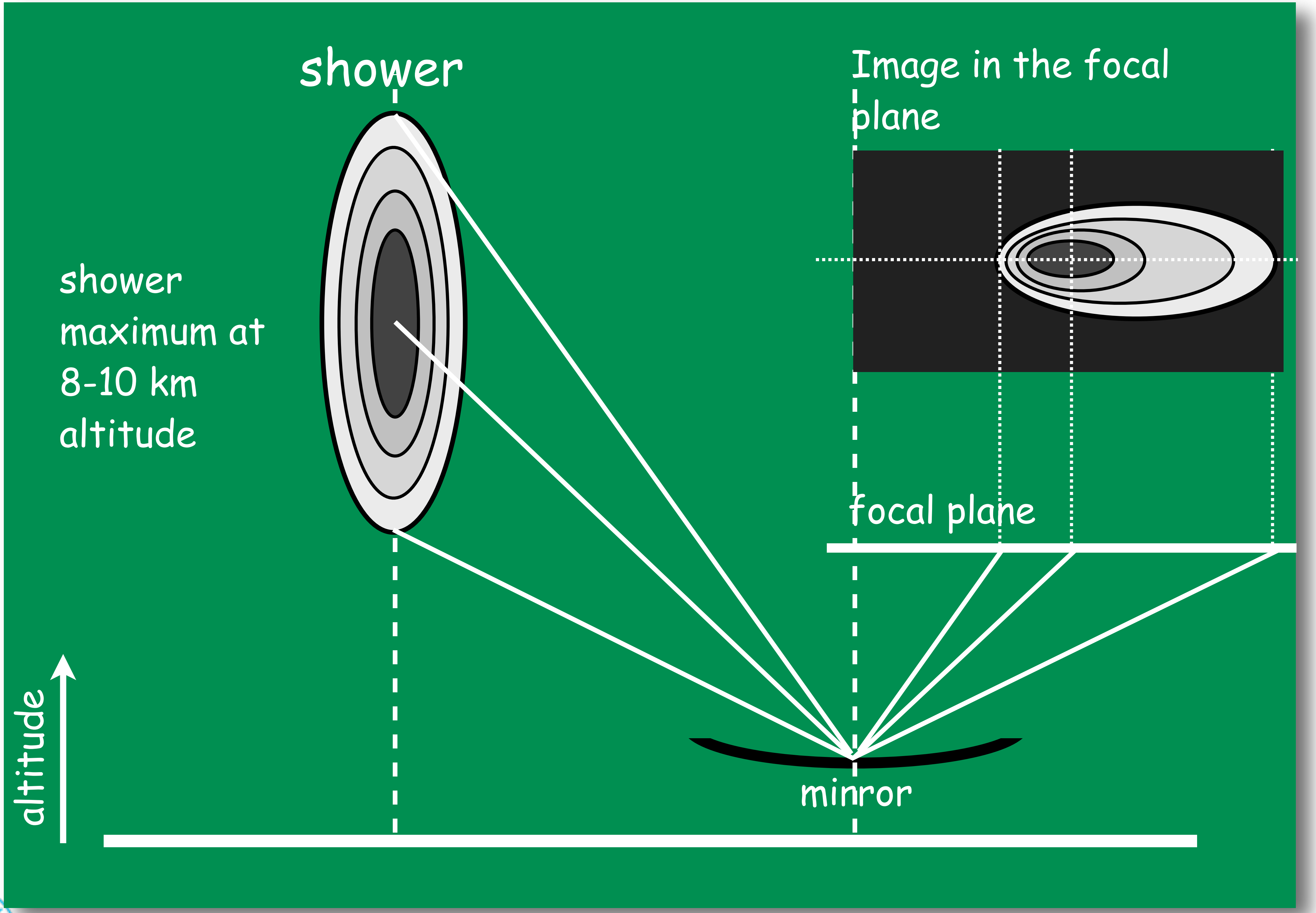

Gamma-ray Events - Monte Carlo Simulations

event display VERITAS

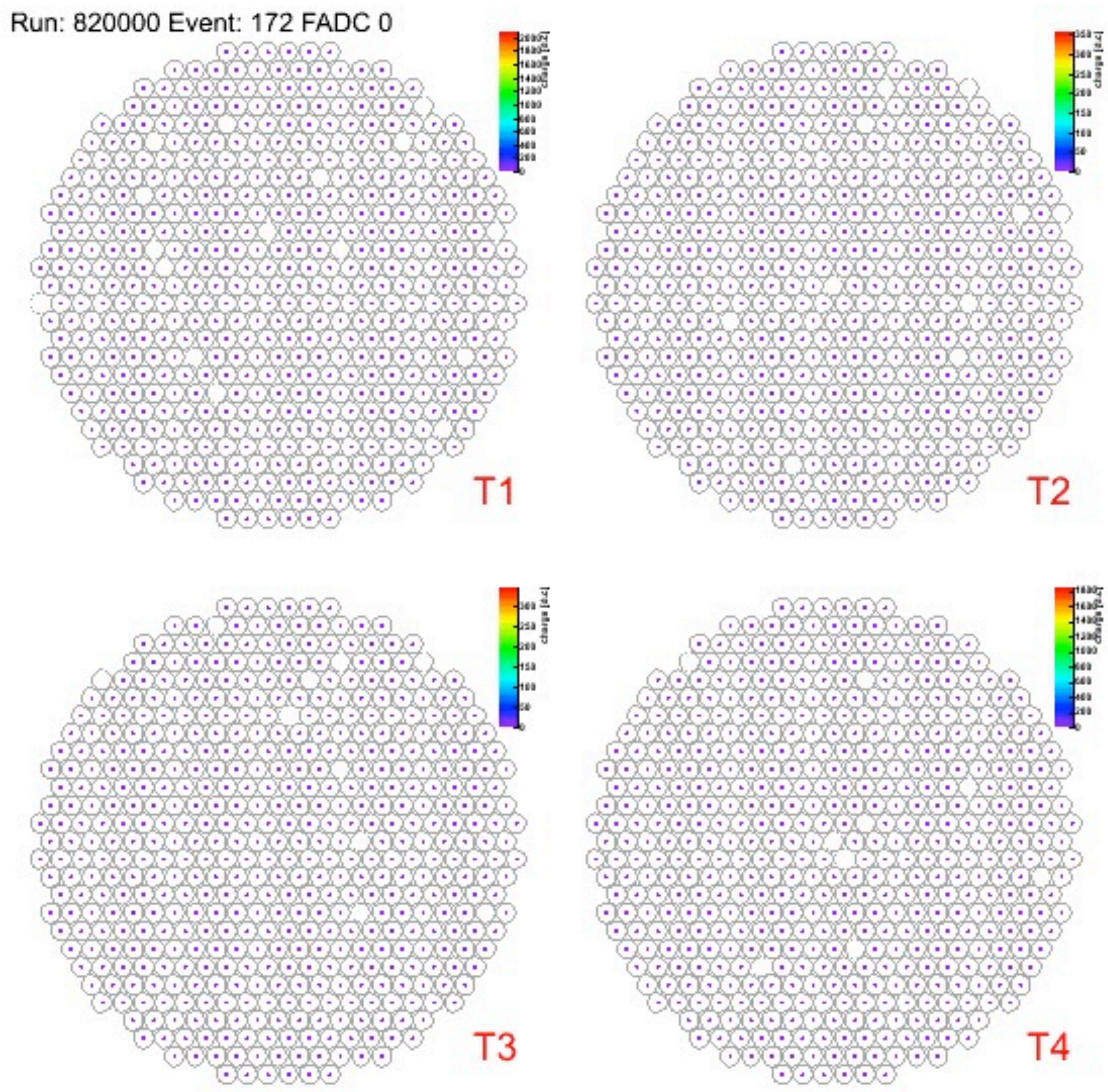

(each frame 2 ns long)

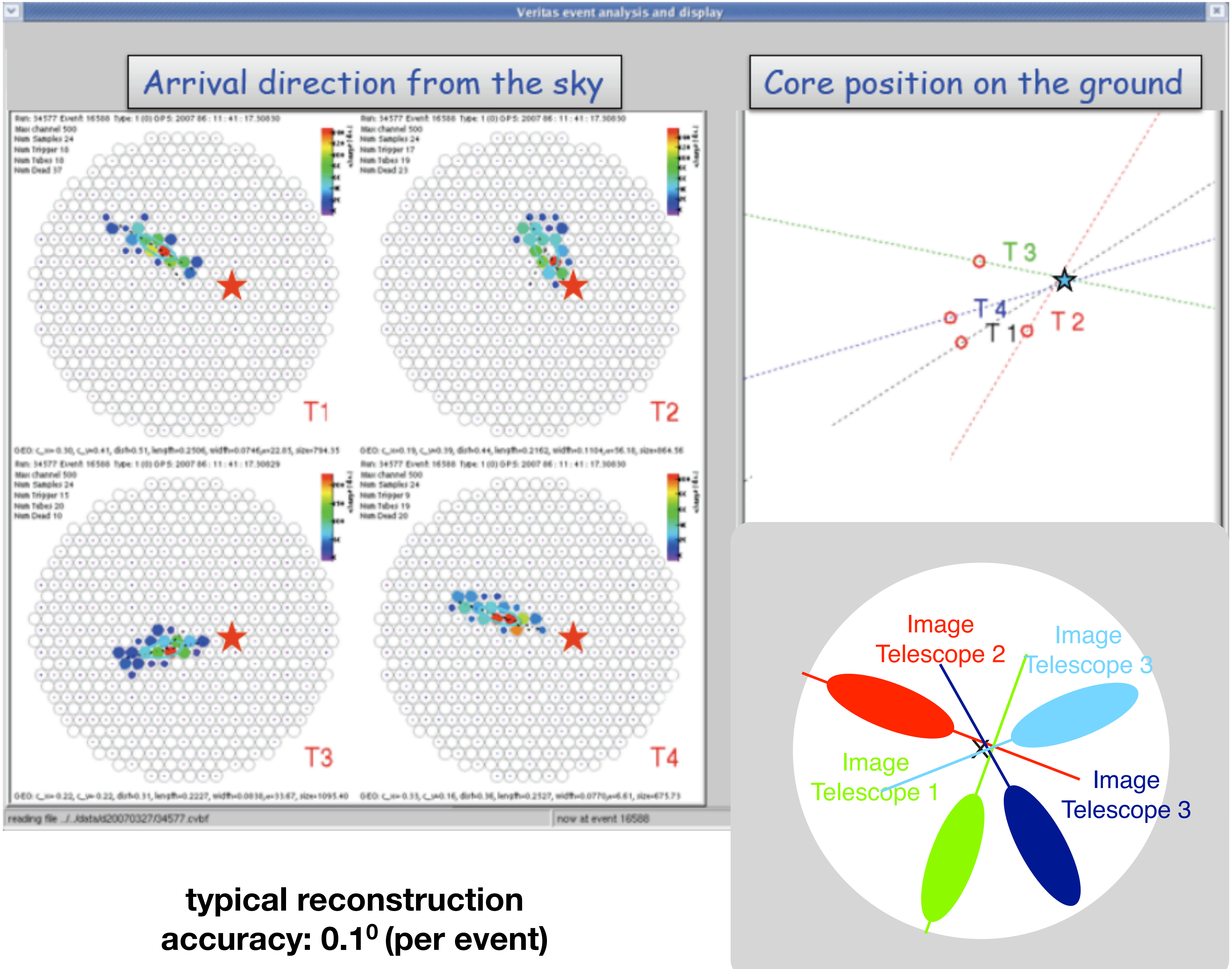

typical reconstruction accuracy: 0.1^0 (per event)

Observations

event display VERITAS

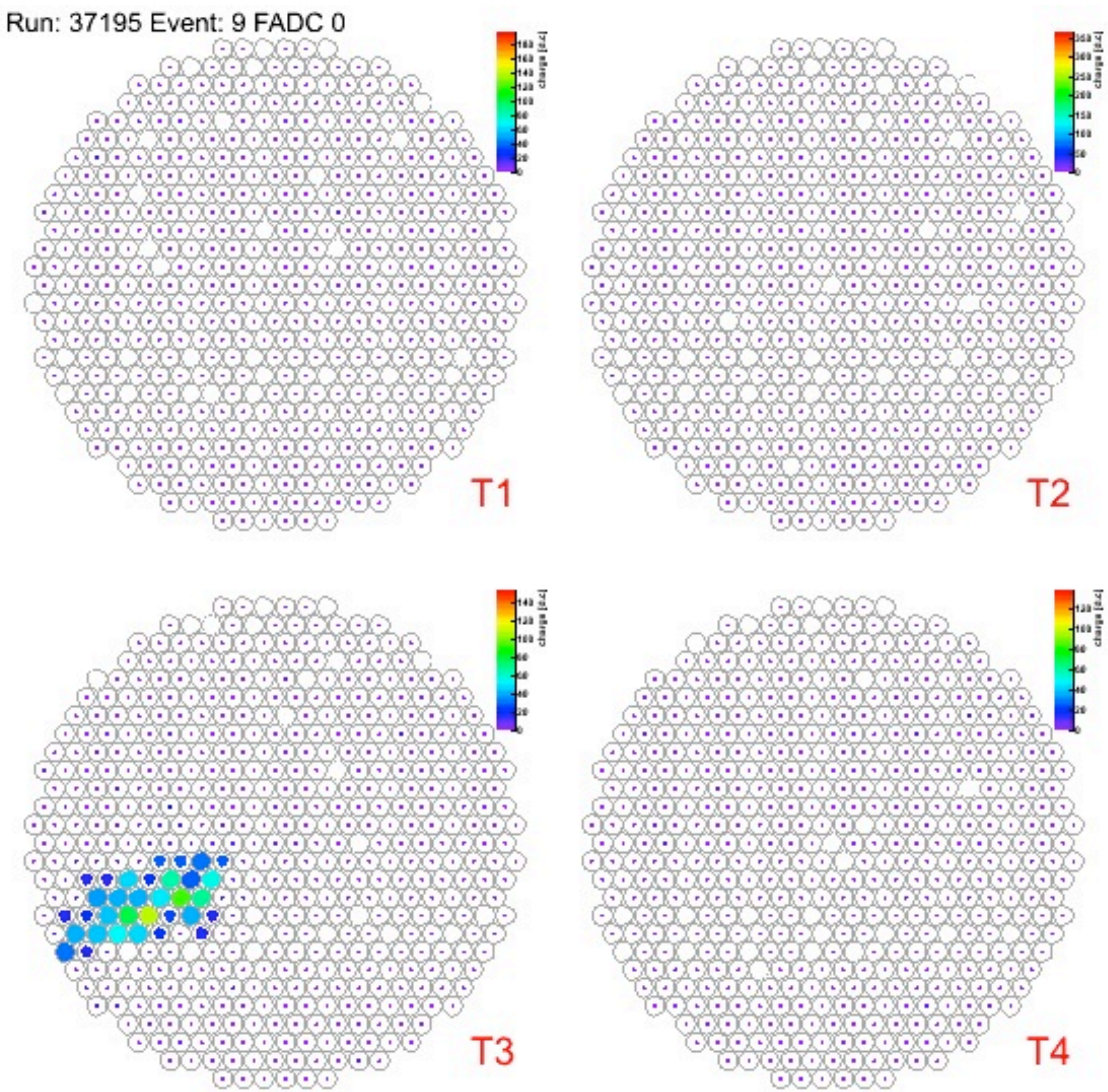

about every 1000th event is a γ-ray

(each frame 2 ns long)

gamma/hadron separation

(based on Image/Hillas parameters)

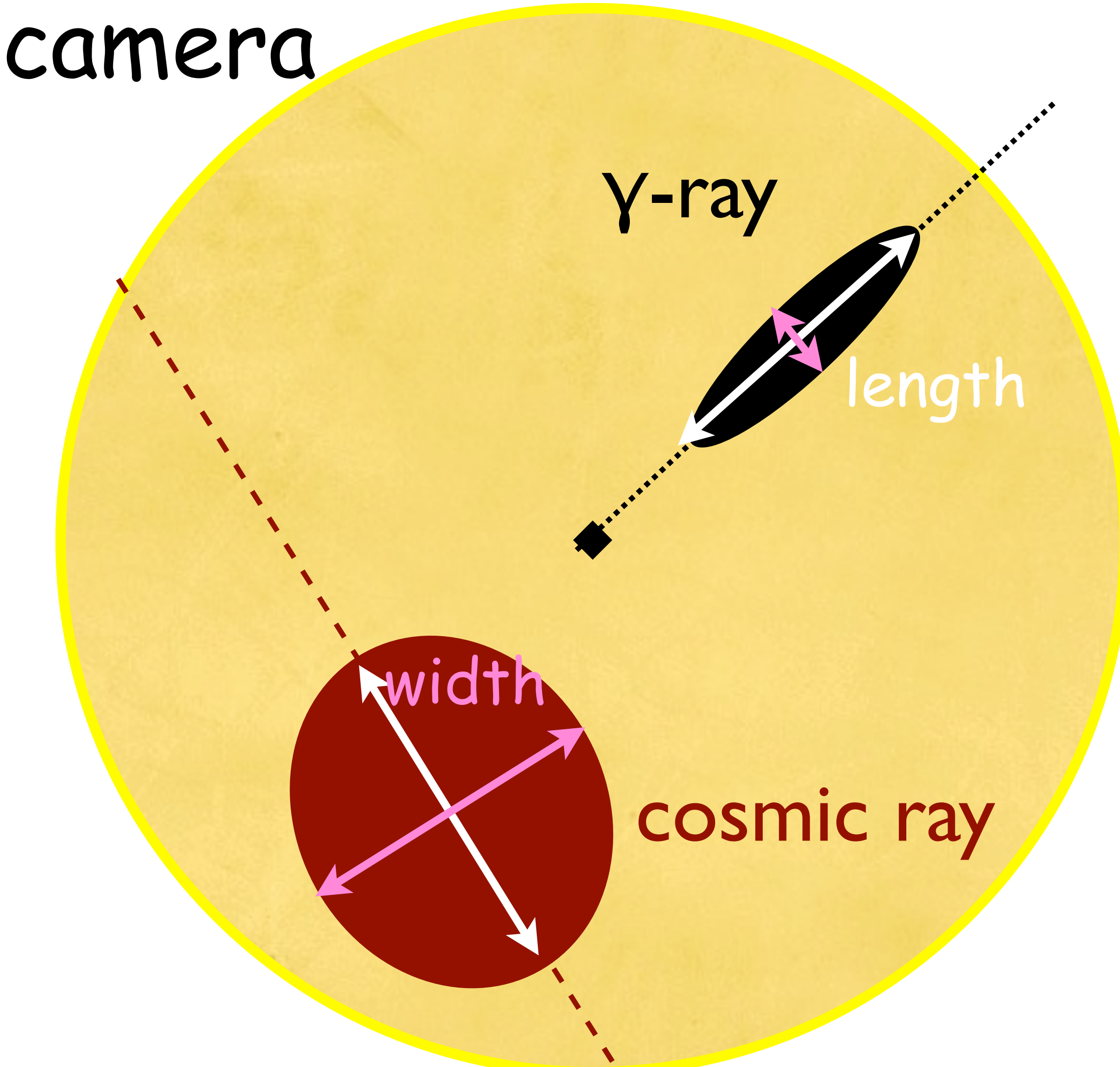

mean scaled width

$$mscw = \frac{1}{N_{\text{images}}} \left[\sum_{i}^{N_{\text{images}}} \frac{\text{width}_i - w_{\text{MC}}(R,s,\Theta)}{\sigma_{\text{width, MC}}(R,s,\Theta)} \right]$$

(same for length)

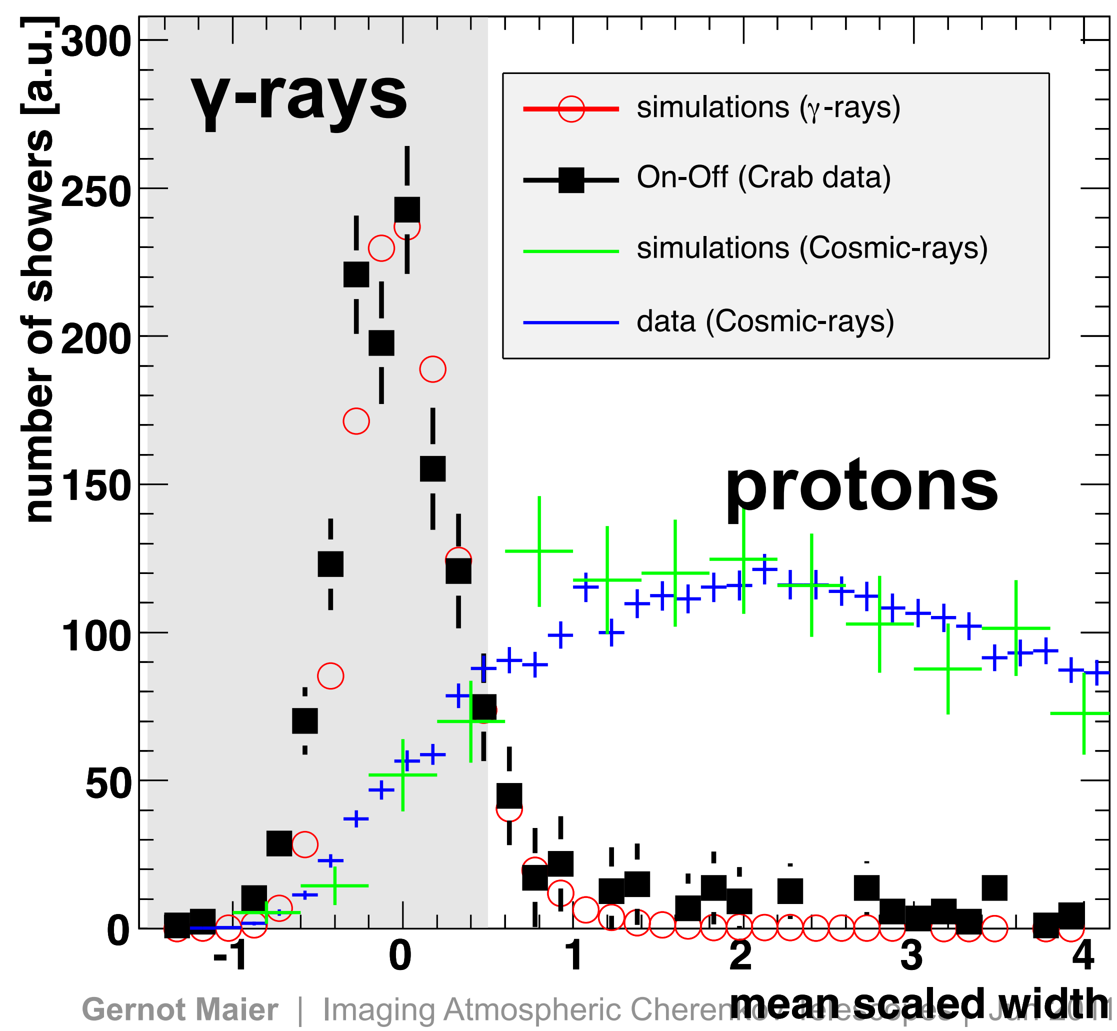

background suppression

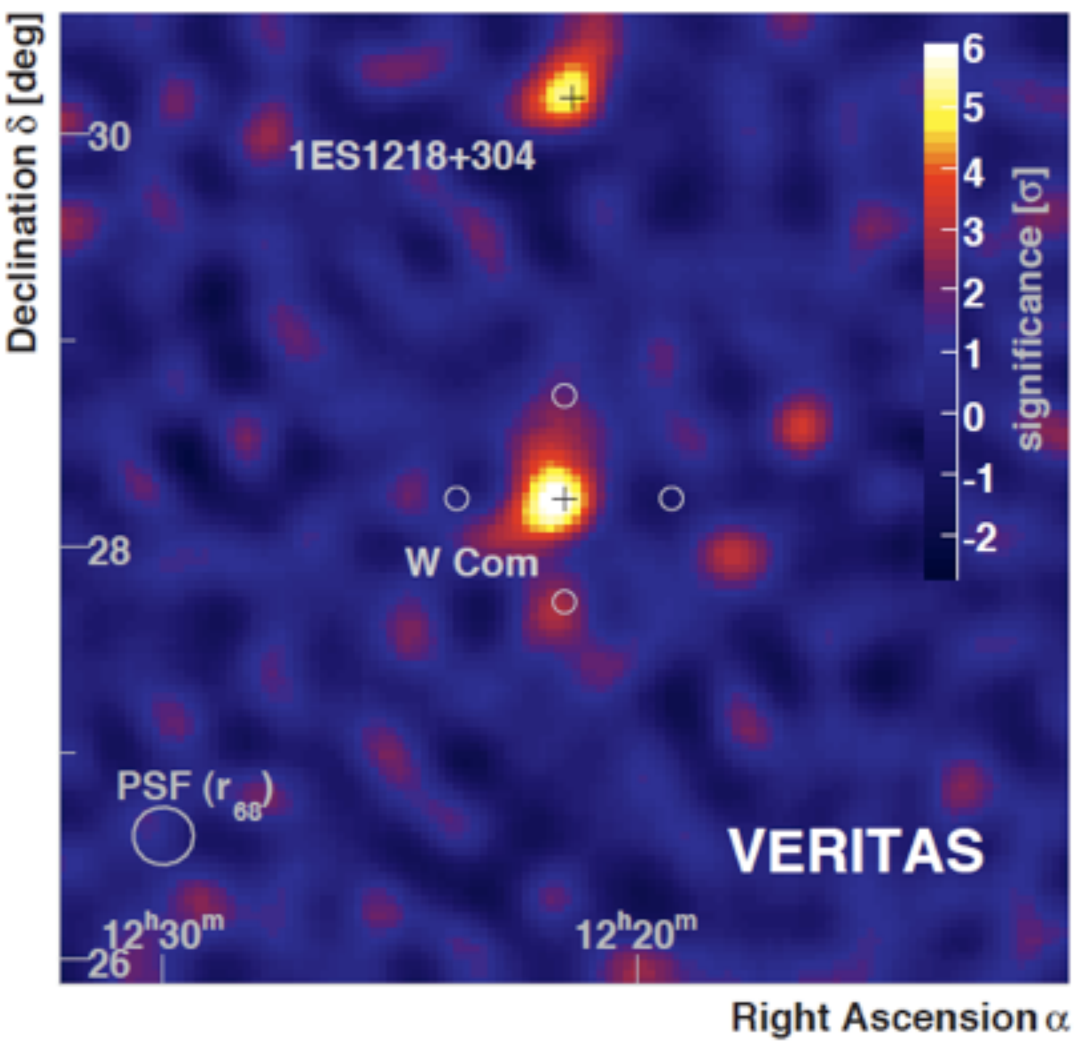

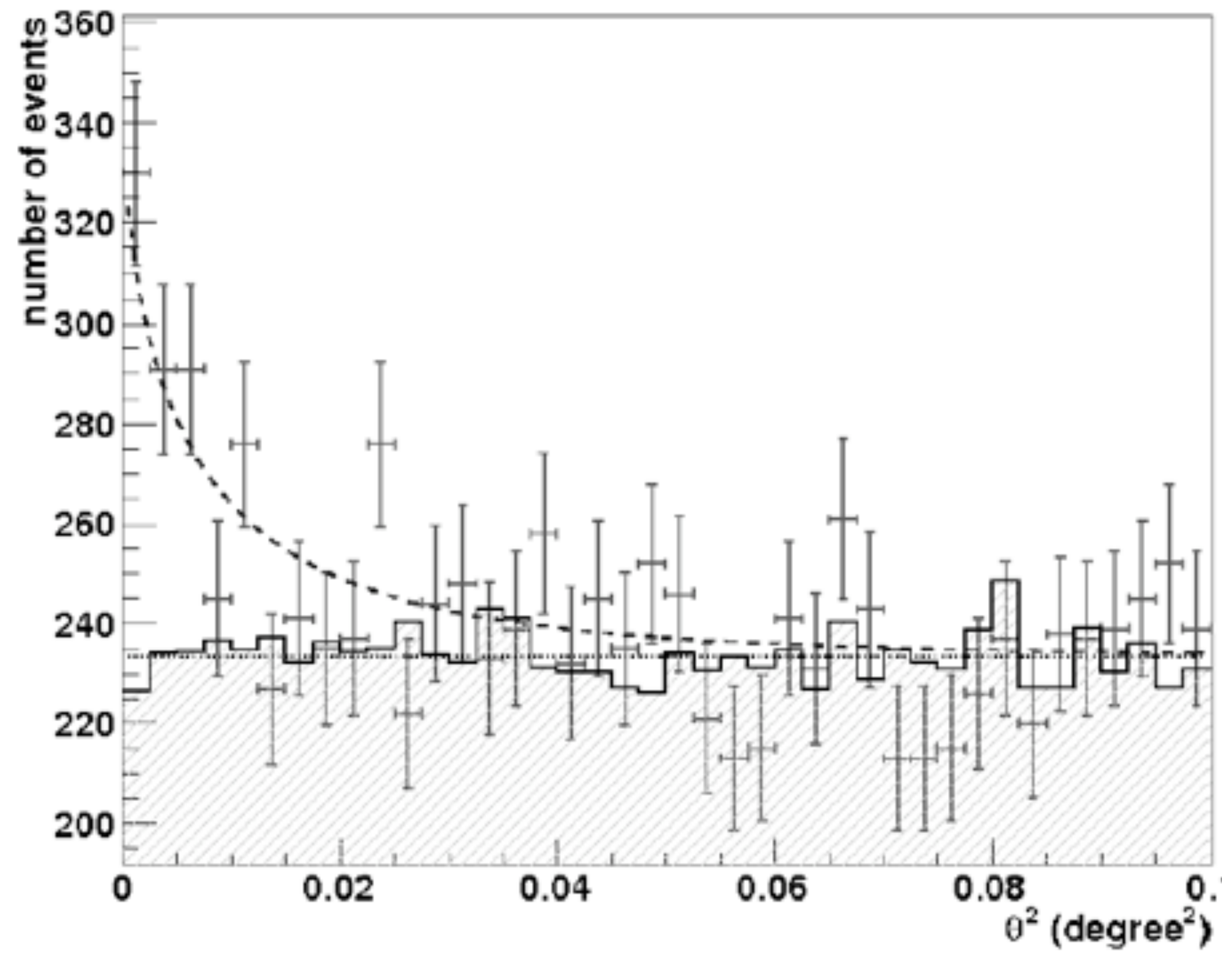

angular resolution single most important factor for background suppression (for point sources only)

Background Models

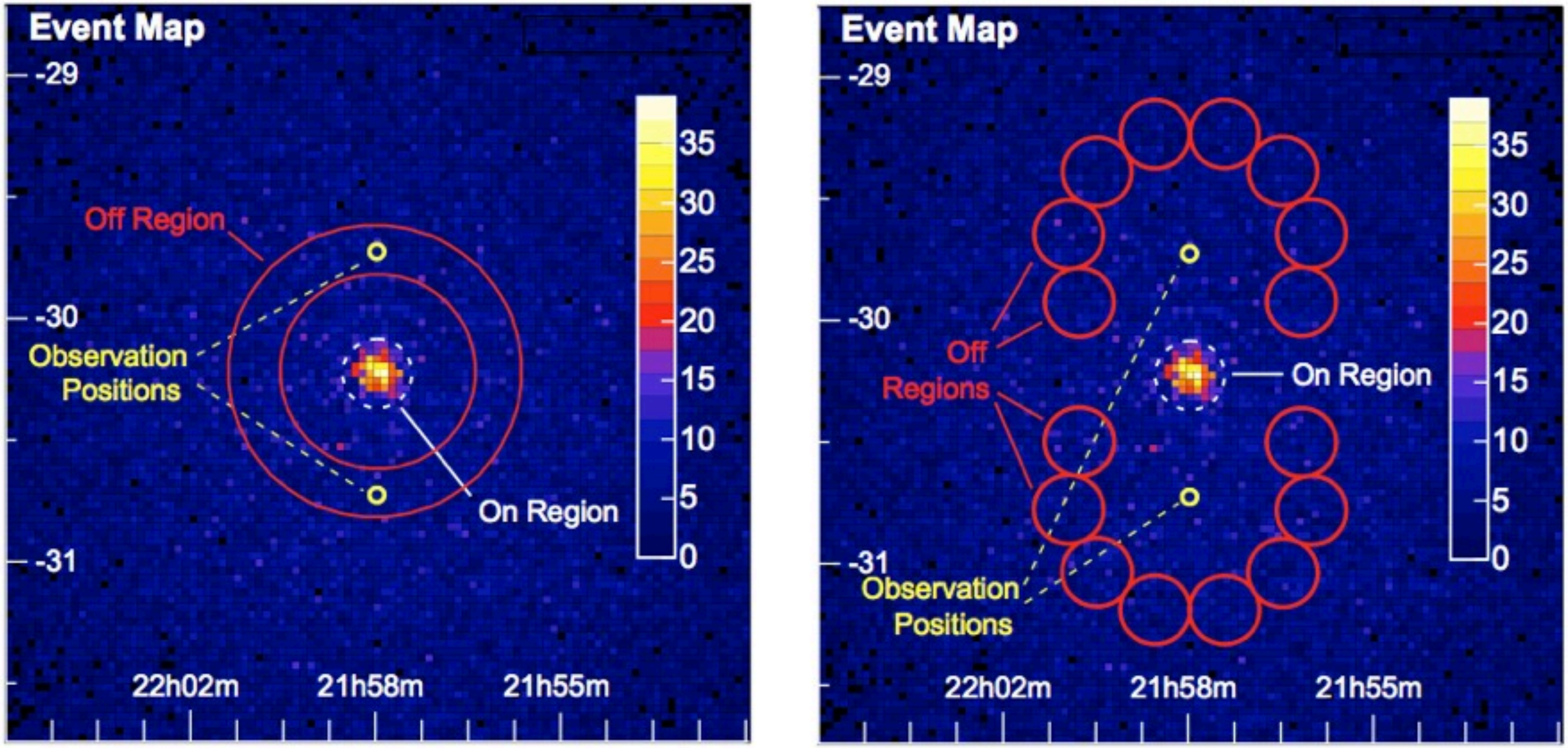

Fig. 4. Count map of γ-ray-like events from 5 h of HESS observations of the active galaxy PKS 2155–304 (Aharonian et al. 2005d). Note that the data were taken in wobble mode around the target position with alternating offsets of $\pm 0.5°$ in declination. The *ring-* (*left*) and *reflected-region-* (*right*) background models are illustrated schematically.

Angular Resolution

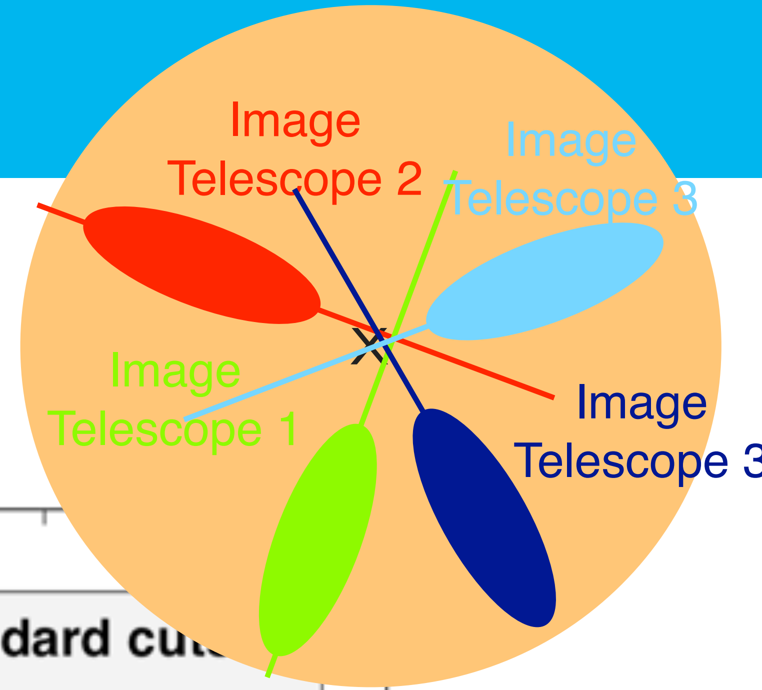

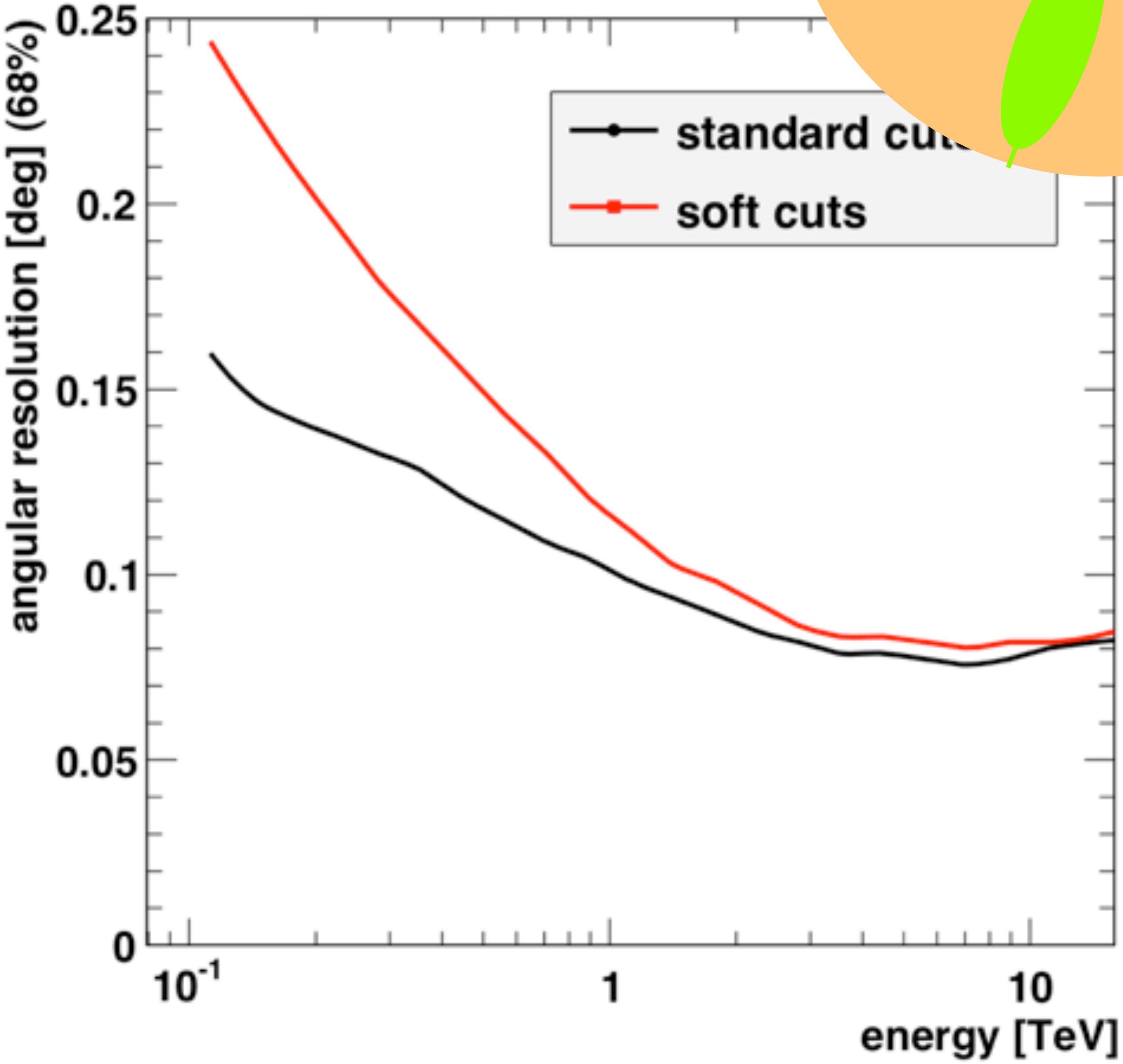

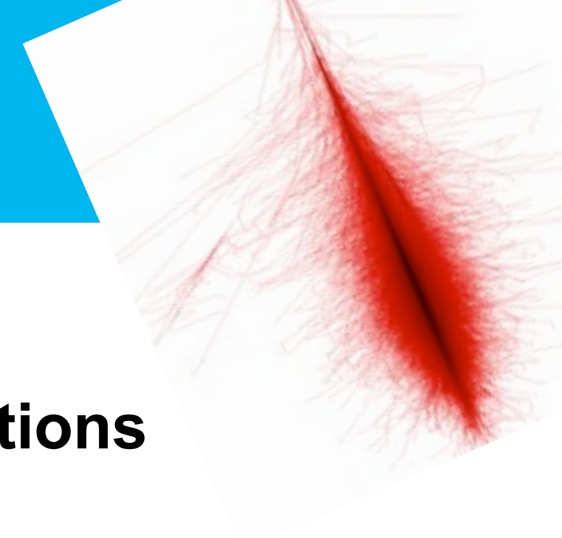

Limitations

lateral spread of shower (multiple scattering)

gamma-ray collection efficiency

geomagnetic field

number of telescopes

array geometry

optical point spread function

pixel size

Angular Resolution and Geomagnetic Field

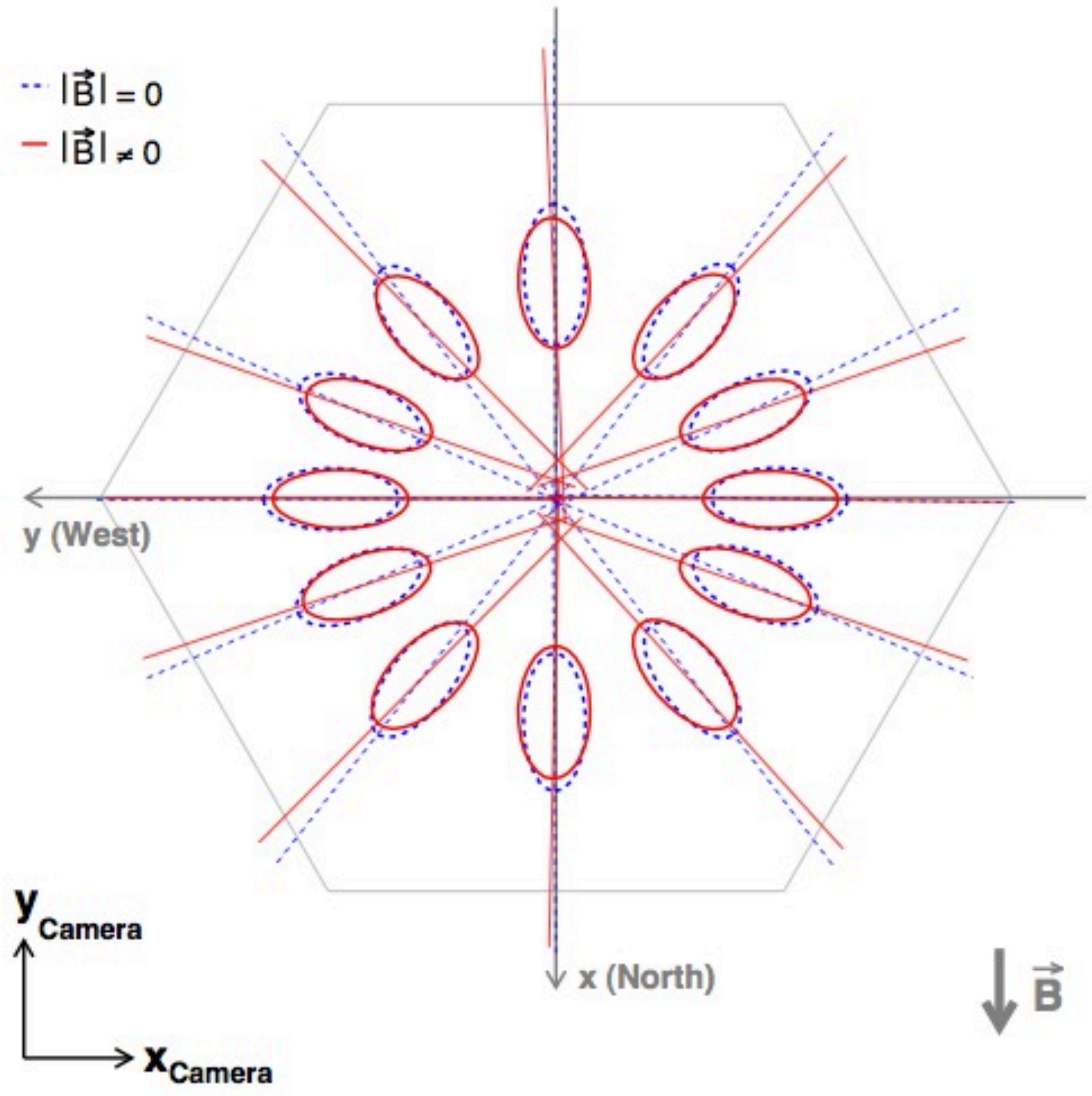

(b) $Az = 180°, \theta = 87°.$

Commichau 2008

Energy Resolution

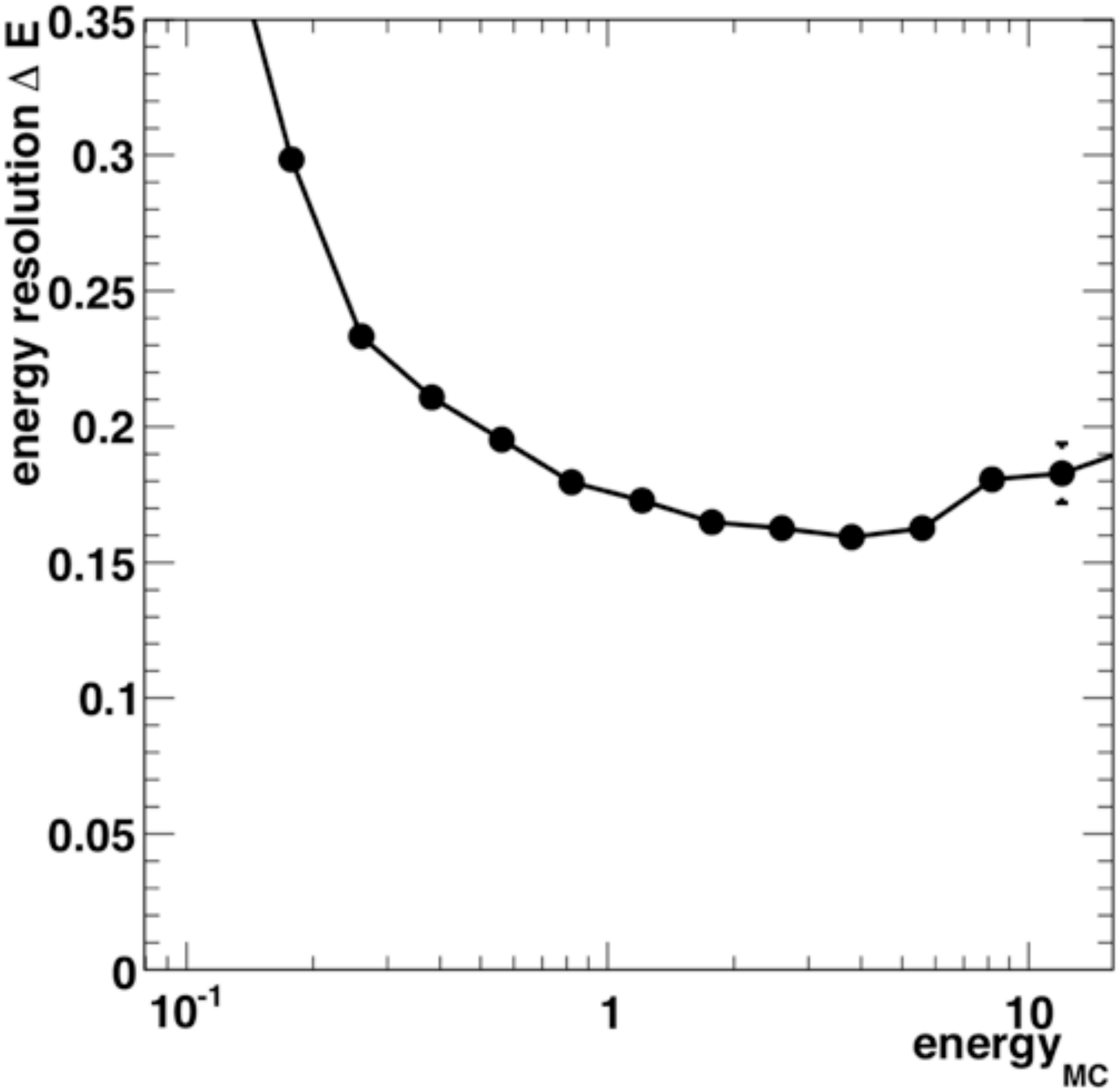

Limitations

shower-to-shower fluctuations (height of emission maximum)

Poisson statistics

background noise (NSB)

shower core reconstruction

Systematic Error in Energy Reconstruction

TABLE 4
CONTRIBUTION TO THE SYSTEMATIC UNCERTAINTIES

Albert et al (MAGIC) 2008

Source of Uncertainty	Class	Uncertainty (%)	Comments
Parametrization of atmosphere in MC simulation	A	3	Deviations due to yearly and daily pressure changes, deviations of real density distribution and standard atmosphere model
Atmospheric transmission losses due to Mie scattering	A, (C)	5	Lack of good measurements; short-term unpredictable changes possible
Incorrect NSB simulation	A	3	MC assumes uniform NSB; variations due to source location, air glow, variations due to man-made light; stars in the FOV
Reflectivity of main mirror	A	7	From measurements of reflected star images
Variation of the useful mirror area	A	3	Malfunctions of active mirror control resulting in focusing losses
Day-to-day reflectivity changes	A	2	Due to dust deposit variations and occasional dew deposit
Photon detection efficiency of the PMT/light catcher system	A, C	10–12	See text
Unusable camera channels	B	3	Dead PMTs (5–10 channels), problems in calibration (5–10 channels)
Trigger inefficiencies	B, C	4	Due to discriminator dead time, baseline shifts/drifts, level differences trigger branch and FADC branch, etc.
Signal drift in camera due to temperature drifts	A, C	2	Combination of PMT QE change (small), amplifier and optical transmitter drifts
Camera flat-fielding	A, B	2	Calibration problem
Signal extractor	B	5	Complex effect due to trigger jitter (early pulses from PEs generated on first dynode), etc.; baseline jitter, shifts in FADCs
Cuts and methods used in the analysis	B, C	5–30	Energy dependent; see discussion of differential energy spectrum
Losses of events during reconstruction	B(A)	8	Simplifications in MC simulation
Estimate of BG under source	B(A)	4	Camera nonuniformity not included in MC; hadronic events not perfectly simulated in MC
Small tracking instabilities	B	2	Source jitters around nominal camera position due to small tracking errors, small camera oscillations due to gusts, etc., resulting in a wider signal spread than predicted by MC
Nonlinearities in the analog signal chain (PMT-FADC)	C(A)	3–10	Saturation and nonlinearities of electronic and optoelectronic components

lass A: contributions to the uncertainty on the energy scale. Class B: contributions to the uncertainty in the event rate. Class B(A): error contributes more to the leading term. Some of the uncertainties are energy
d are averaged. Class C: contribution affecting the spectral slope.

typical systematic uncertainty on flux: 15-20%

DESY

Effective Areas

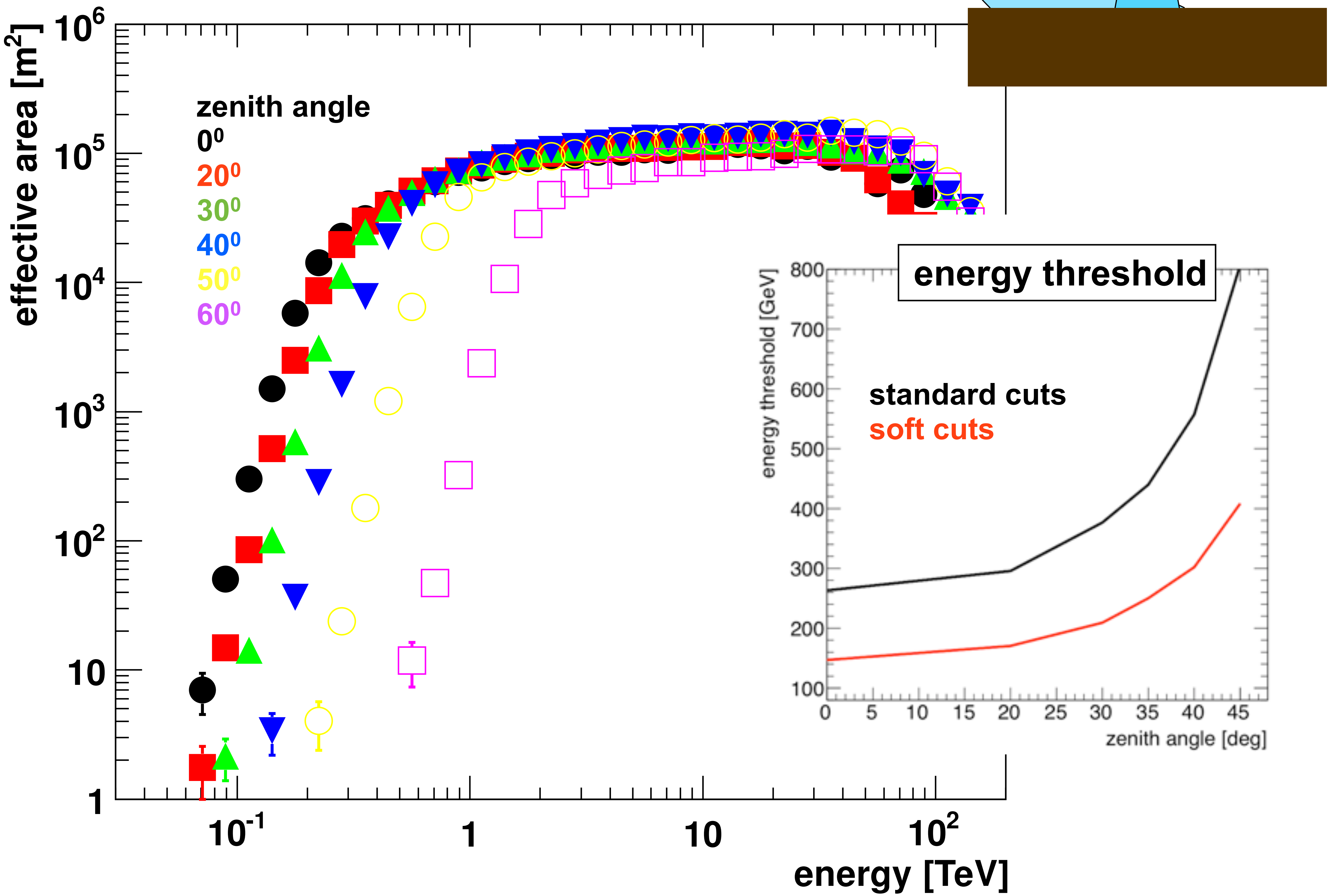

Detectability of a source

criteria for detectability of a source during an exposure time T

a minimum number n_0 (5...10) of gamma rays must be detected:

$$n_0 > R_\gamma T$$

the gamma-ray signal must be significant above the fluctuations in the background

$$\frac{T R_\gamma}{\sqrt{T \eta_{CR} R_{CR} \Omega}} > \sigma$$

significance

efficiency of analysis cuts (η_{CR})

background detection rate (R_{CR})

solid angle (Ω)

Li & Ma significances

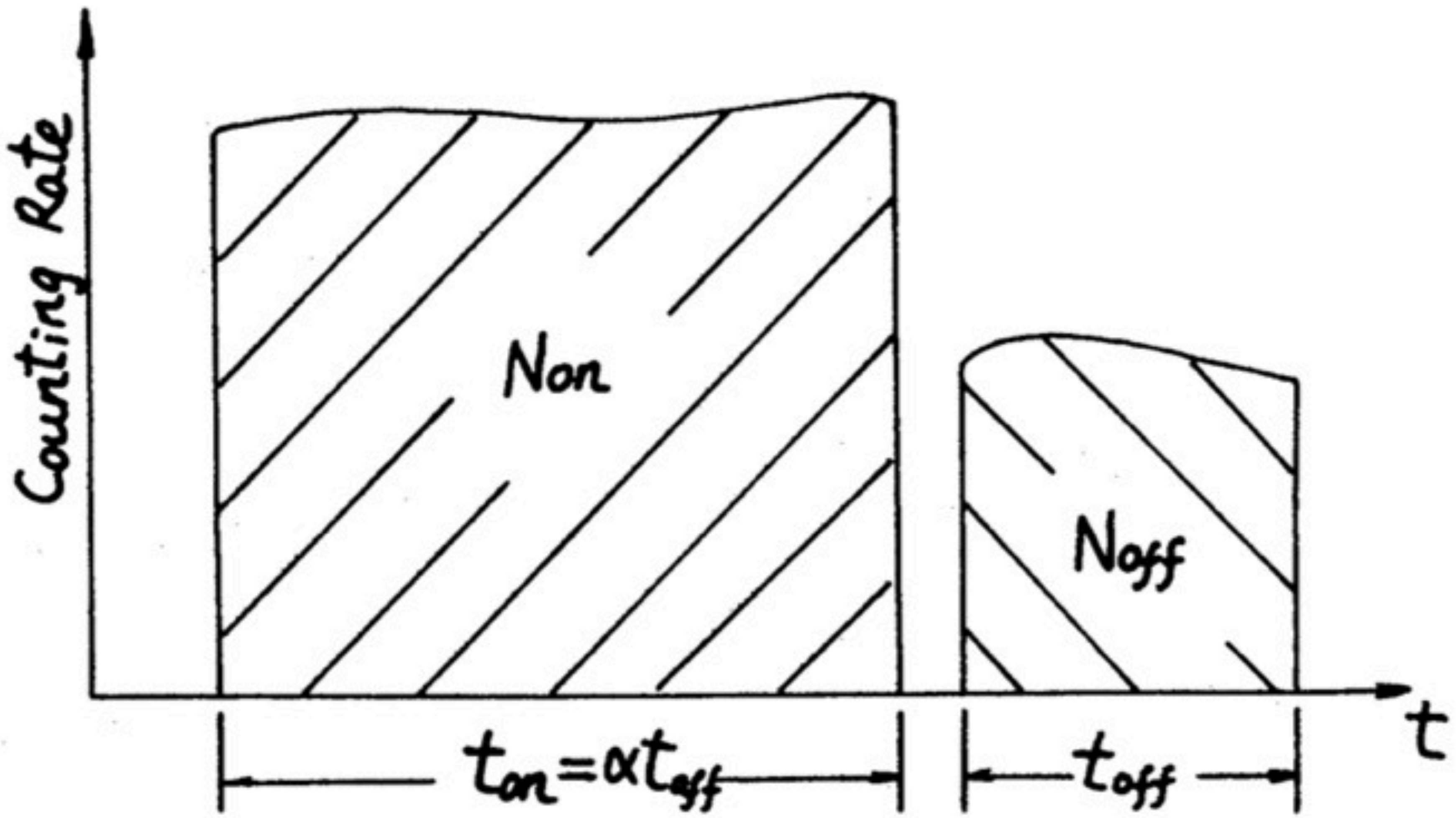

Likelihood ratio method after Li & Ma (1983):

$$S = \sqrt{-2\ln\lambda} = \sqrt{2}\left\{N_{\mathrm{on}}\ln\left[\frac{1+\alpha}{\alpha}\left(\frac{N_{\mathrm{on}}}{N_{\mathrm{on}}+N_{\mathrm{off}}}\right)\right] + N_{\mathrm{off}}\ln\left[(1+\alpha)\left(\frac{N_{\mathrm{off}}}{N_{\mathrm{on}}+N_{\mathrm{off}}}\right)\right]\right\}^{1/2} . \qquad (17)$$

Sensitivity

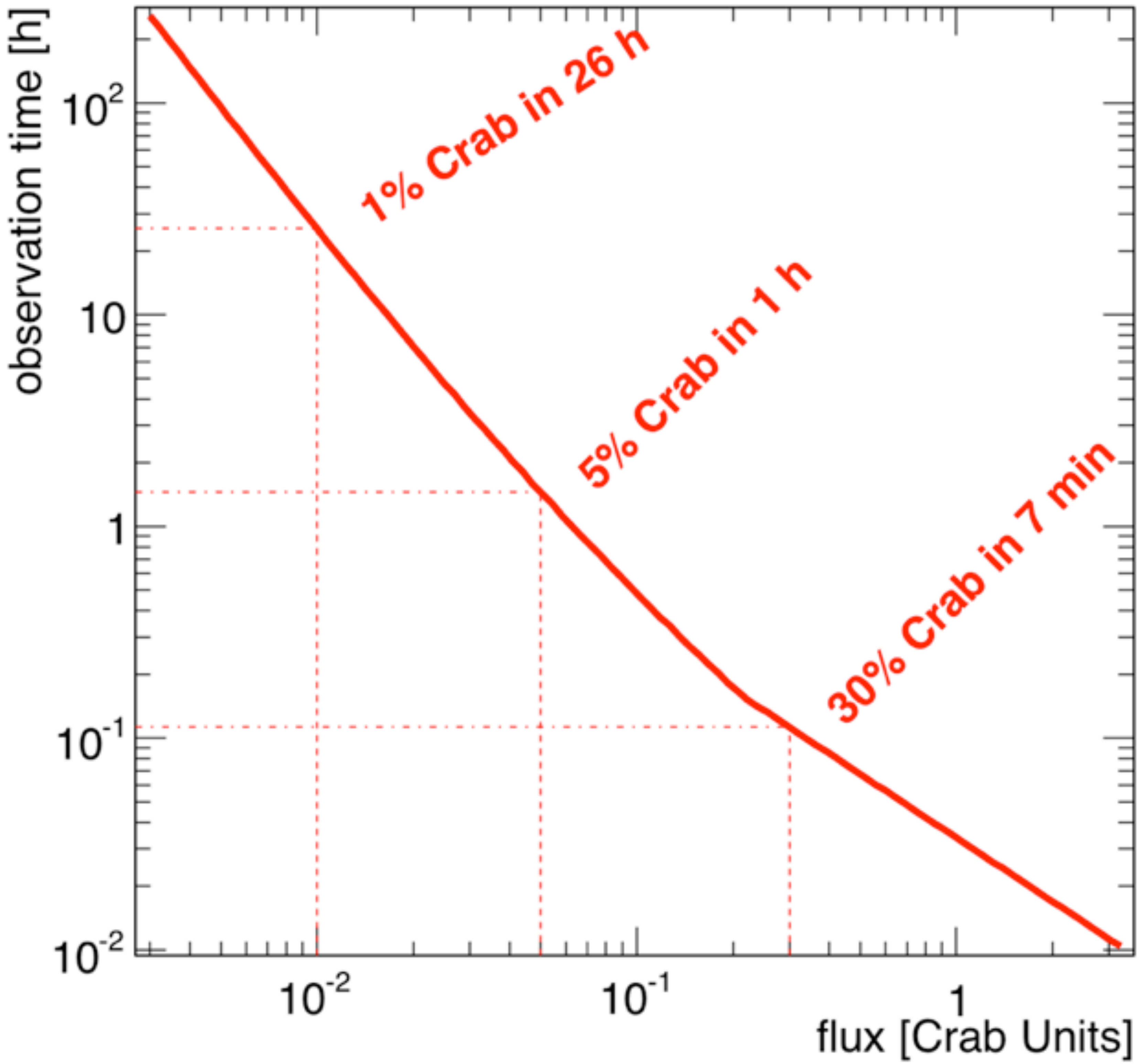

Next-generation instruments

Sensitivity Improvements

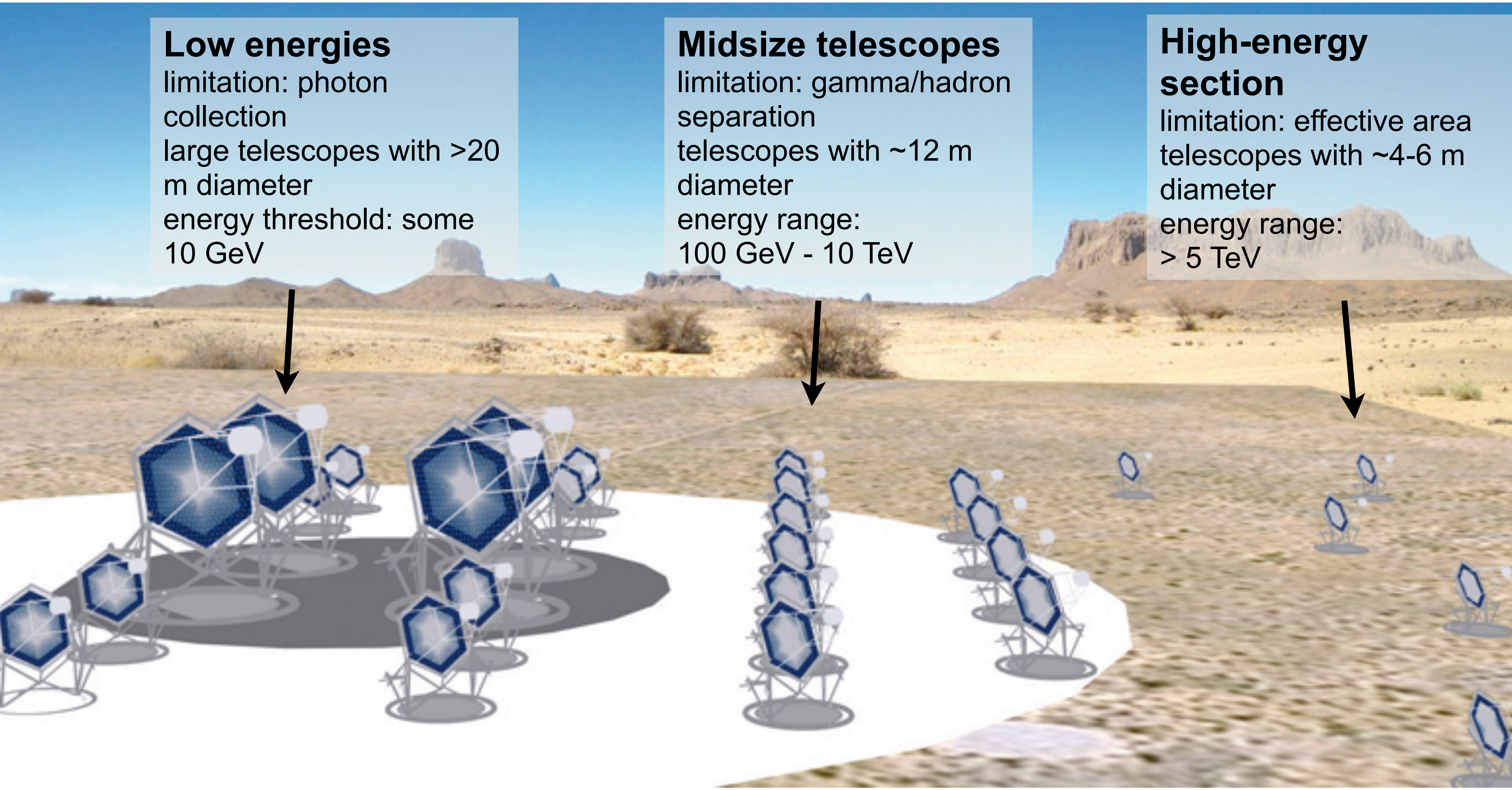

Sensitivity Improvements

Low energies
limitation: photon collection
large telescopes with >20 m diameter
energy threshold: some 10 GeV

Midsize telescopes
limitation: gamma/hadron separation
telescopes with ~12 m diameter
energy range:
100 GeV - 10 TeV

High-energy section
limitation: effective area
telescopes with ~4-6 m diameter
energy range:
> 5 TeV

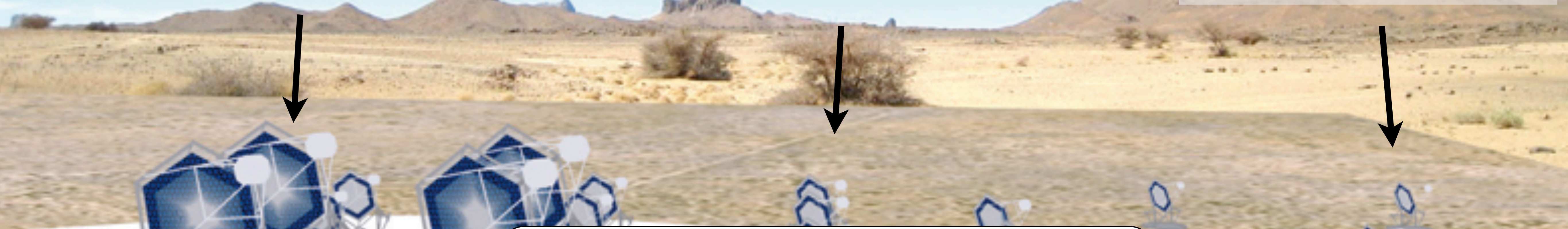

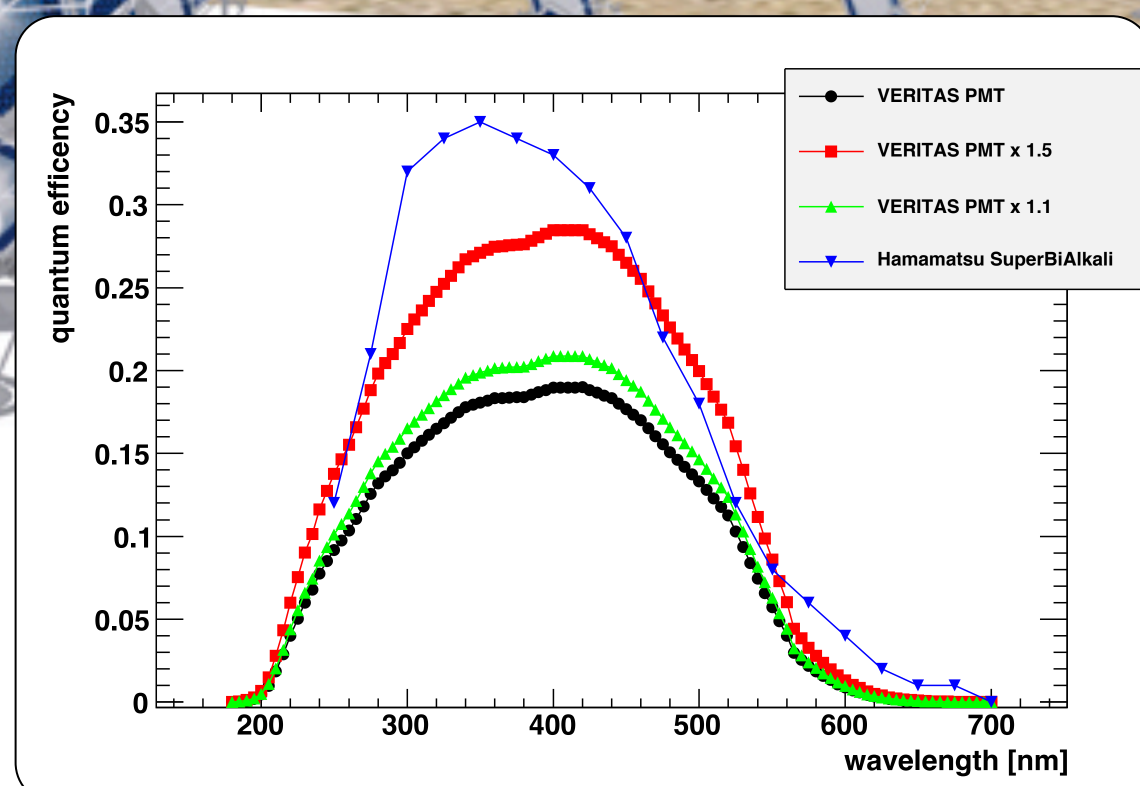

Schwarzschild-Couder Optics

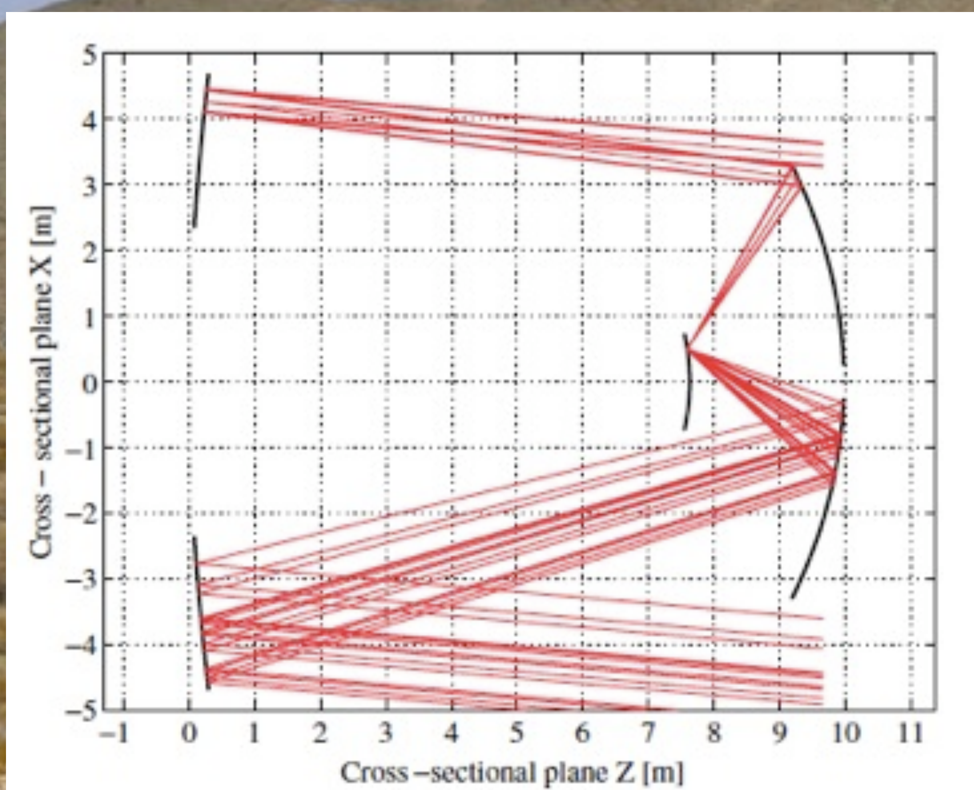

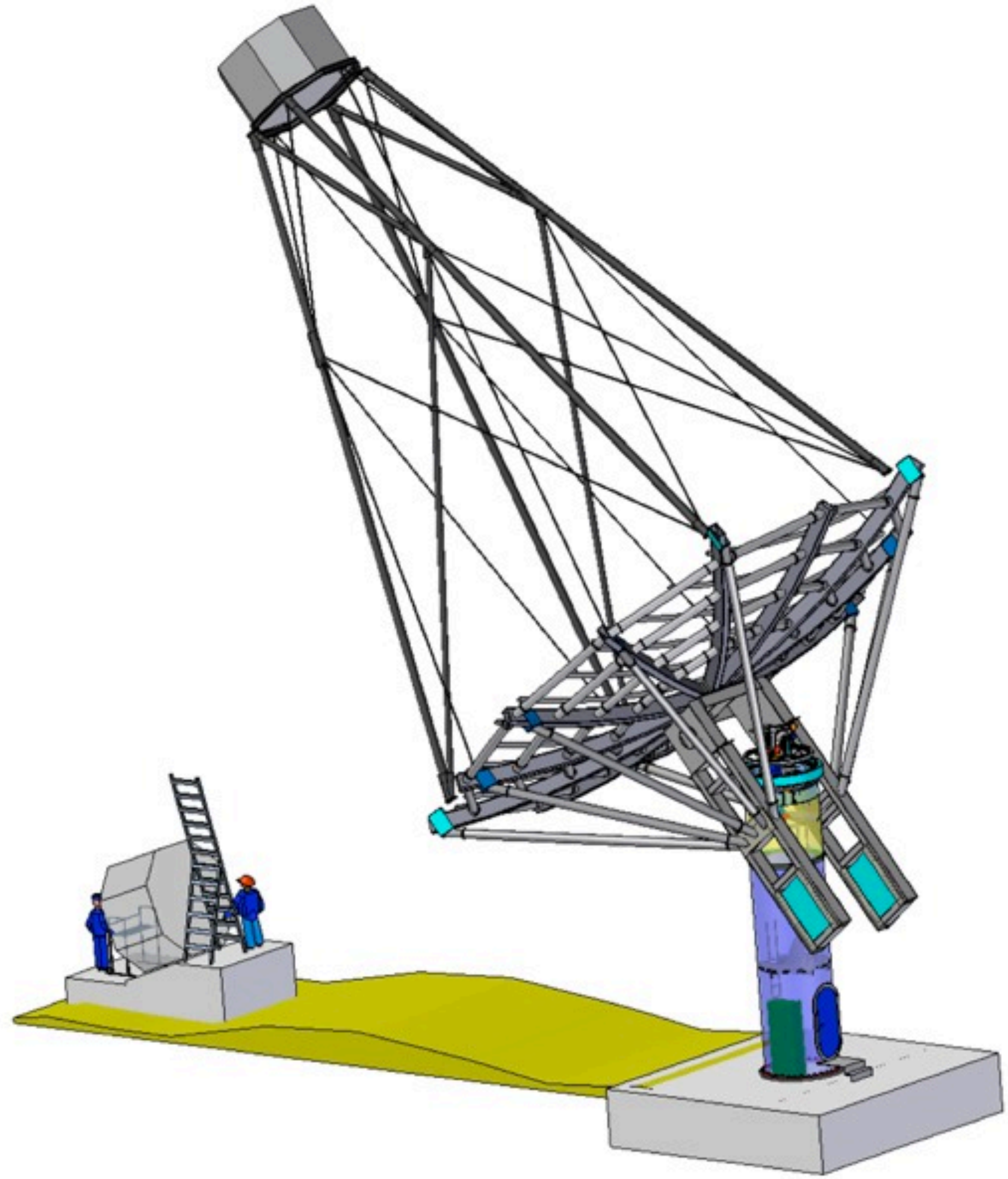

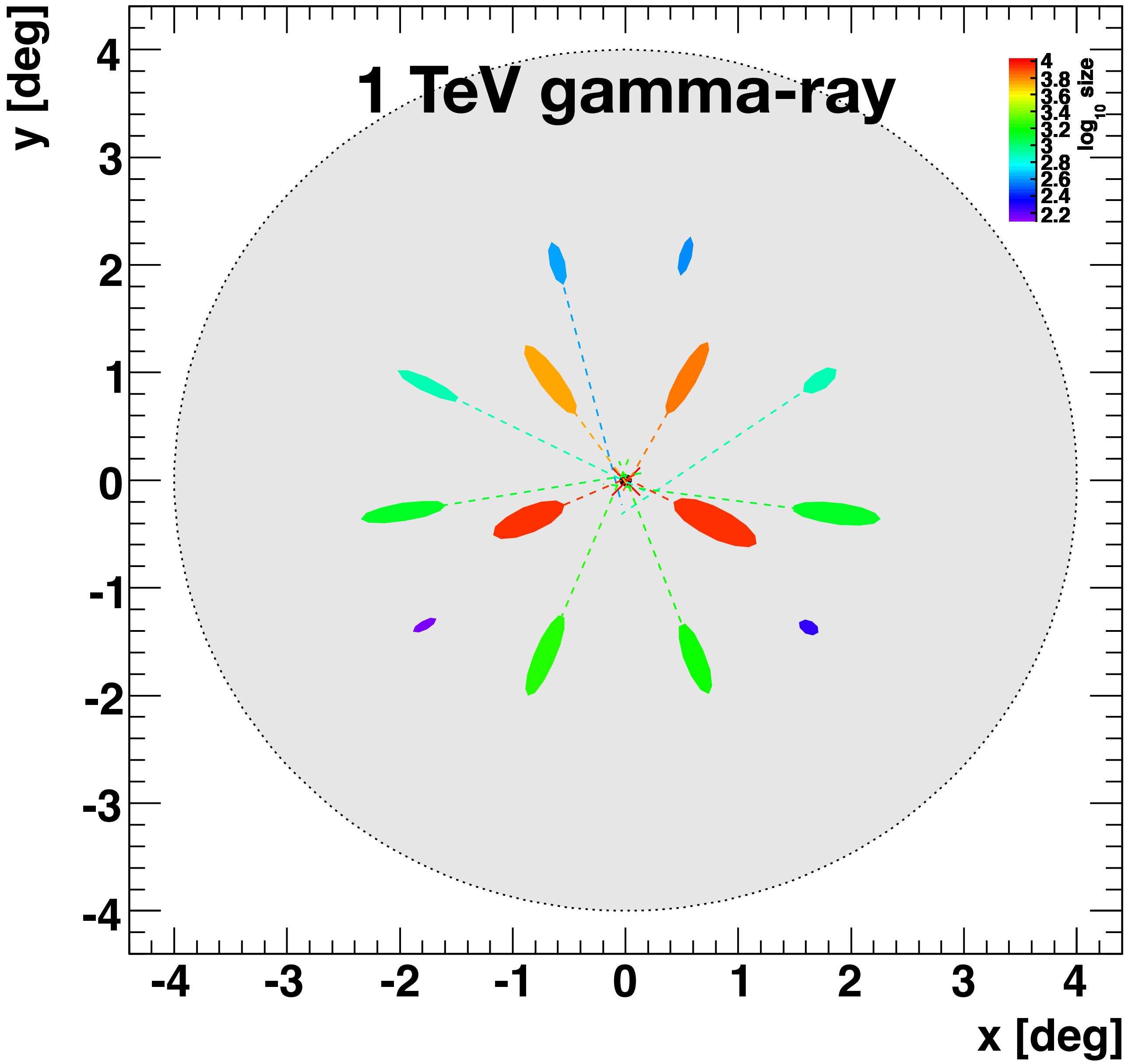
1 TeV gamma-ray
y [deg]
x [deg]
$\log_{10}$ size

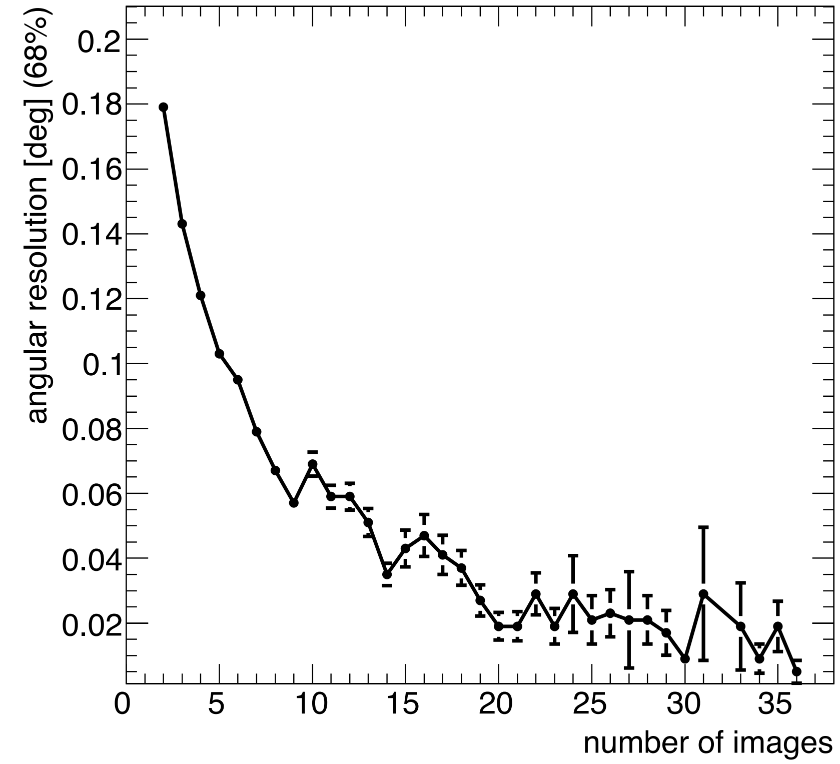
angular resolution [deg] (68%)
number of images

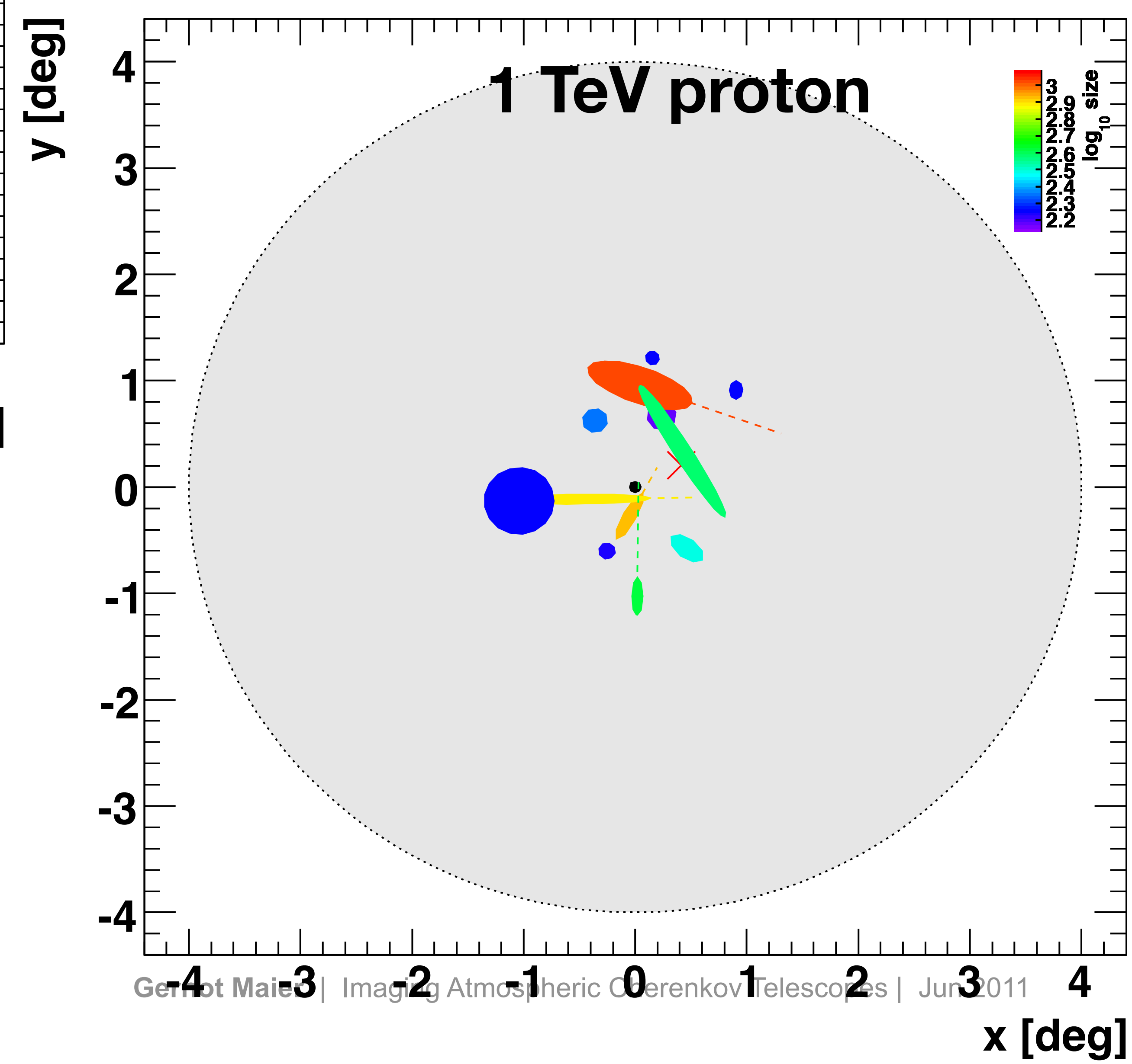
1 TeV proton
y [deg]
x [deg]
$\log_{10}$ size

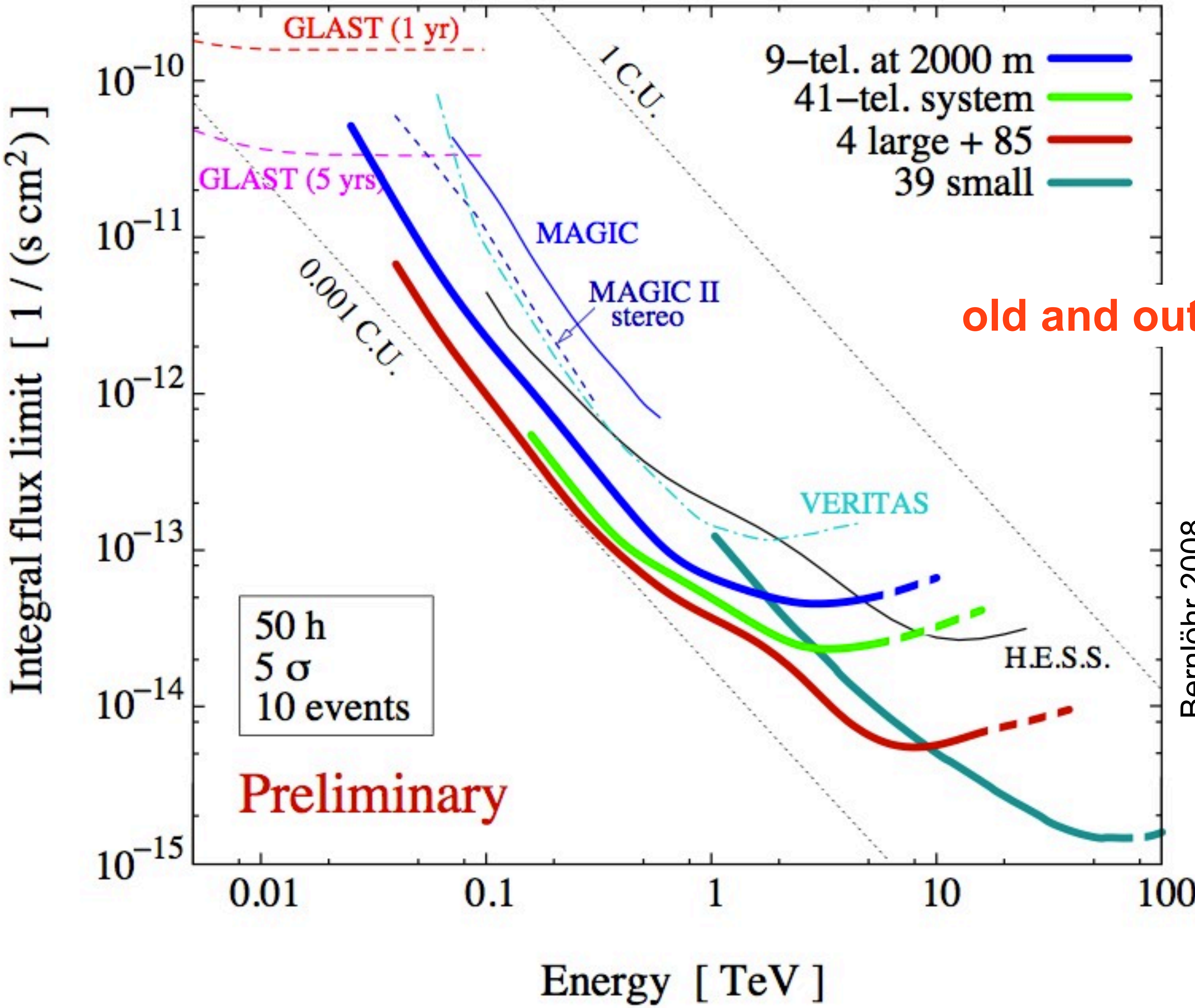

old and outdated

Bernlöhr 2008

CTA

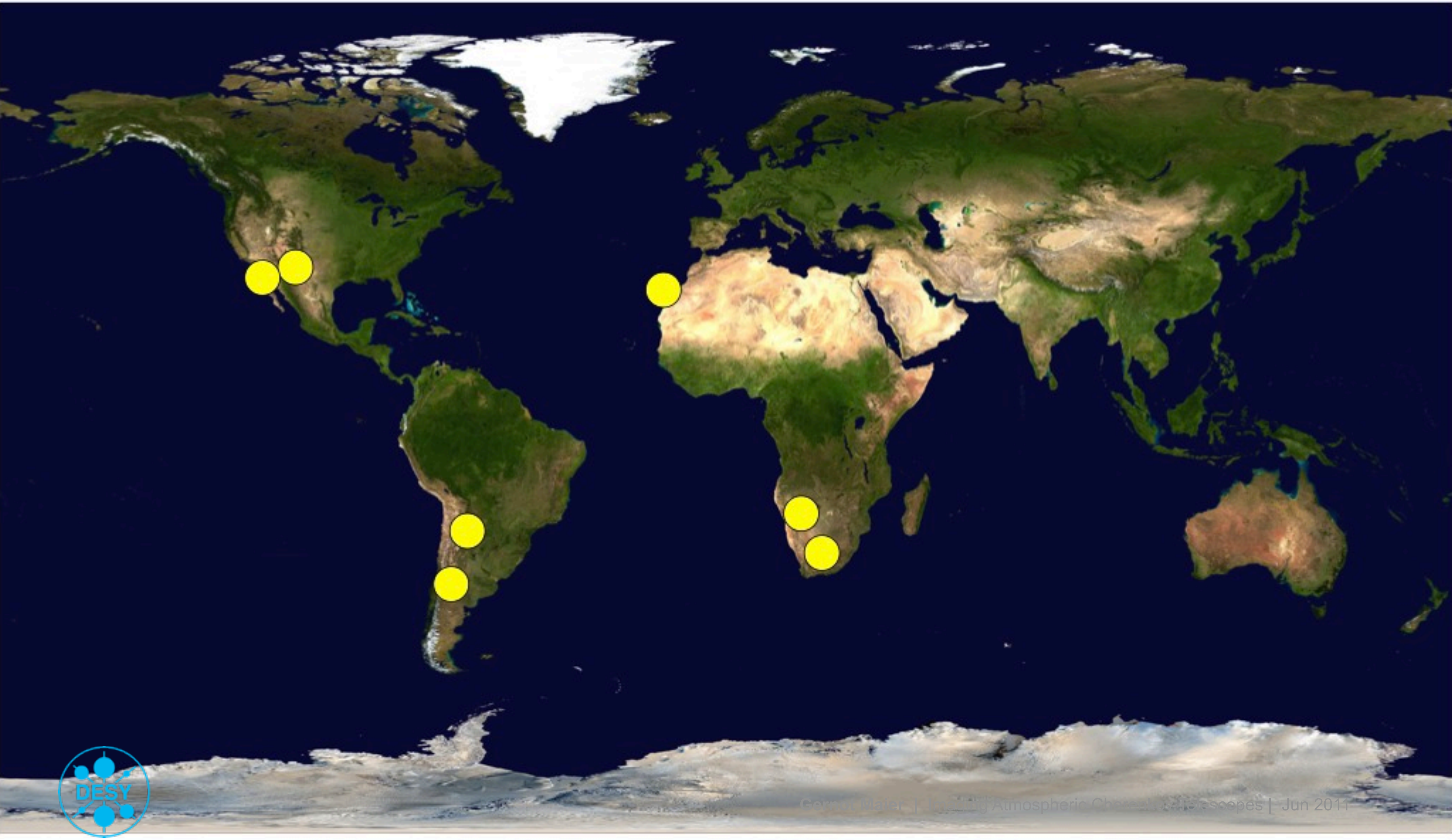

CTA

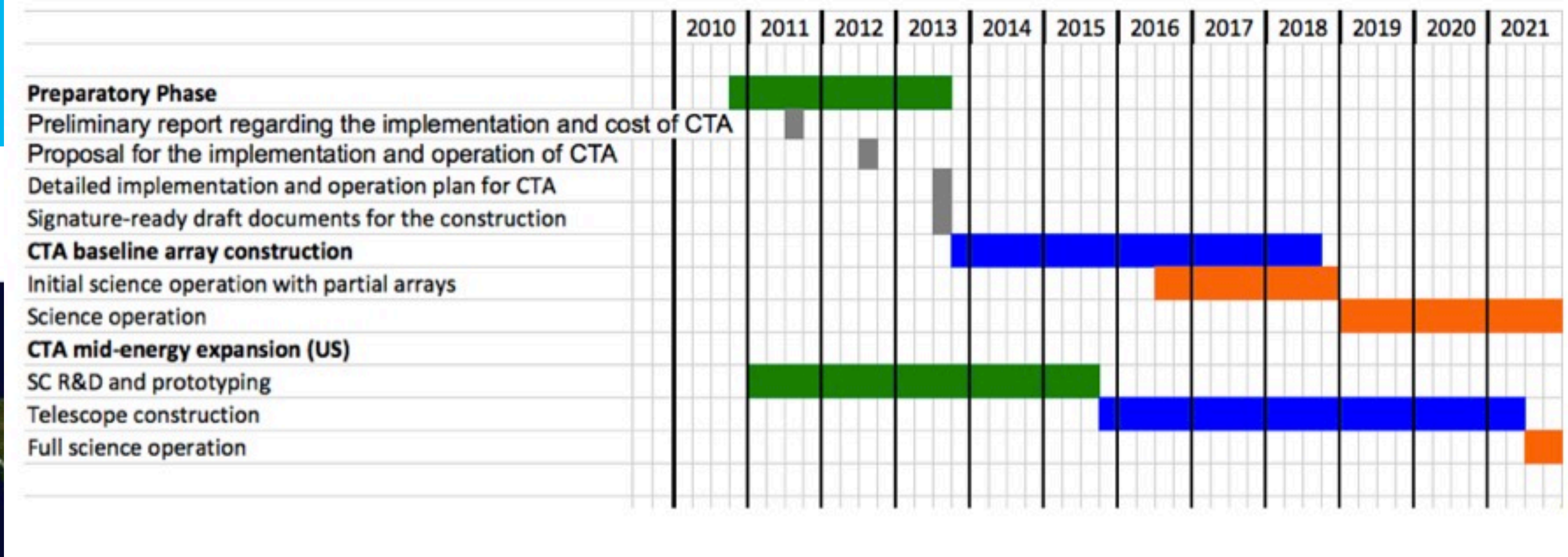
2010
2011
2012
2013
2014
2015
2016
2017
2018
2019
2020
2021
Preparatory Phase
Preliminary report regarding the implementation and cost of CTA
Proposal for the implementation and operation of CTA
Detailed implementation and operation plan for CTA
Signature-ready draft documents for the construction
CTA baseline array construction
Initial science operation with partial arrays
Science operation
CTA mid-energy expansion (US)
SC R&D and prototyping
Telescope construction
Full science operation

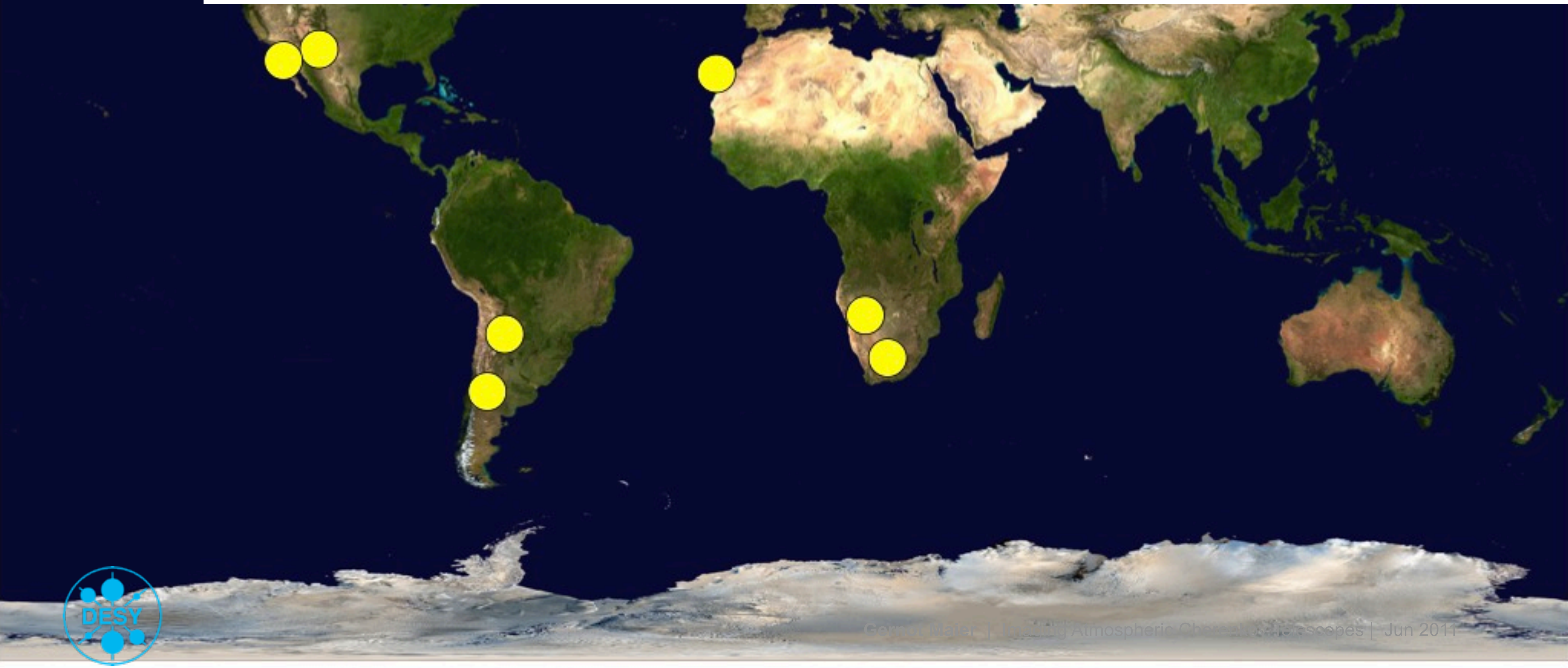

Literature

- Hillas, A.M. et al, ApJ 503, 744 (1998) (Crab Nebula detection)
- Weekes, T.: Very High Energy Gamma-Ray Astronomy (2003)
- Weekes, T., astro-ph/0811.1197
- Hinton, J., astro-ph/0803.1609
- Aharonian, F., Buckley, J., Kifune, T., Sinnis, G., Rep. Prog. Phys. 71 (2008) 096901